GROUND-WATER GEOCHEMISTRY OF THE ALBUQUERQUE-BELEN BASIN, CENTRAL NEW MEXICO

By Scott K. Anderholm

U.S. GEOLOGICAL SURVEY

Water-Resources Investigations Report 86-4094

Albuquerque, New Mexico

1988

DEPARTMENT OF THE INTERIOR

DONALD PAUL HODEL, Secretary

U.S. GEOLOGICAL SURVEY

Dallas L. Peck, Director

For additional information
write to:

District Chief
U.S. Geological Survey
Water Resources Division
Pinetree Office Park
4501 Indian School Rd. NE, Suite 200
Albuquerque, New Mexico 87110

Copies of this report can
be purchased from:

U.S. Geological Survey
Books and Open-File Reports
Federal Center, Building 810
Box 25425
Denver, Colorado 80225

CONTENTS

CONTENTS - Concluded

PLATES

[In pocket]

FIGURES

FIGURES - Concluded

TABLES

TABLES - Concluded

CONVERSION FACTORS

For use of readers who prefer to use metric units, conversion factors for terms used in this report are listed below:

Multiply inch-pound unit	By	To obtain metric (SI) units
mile	1.609	kilometer
acre	0.4047	hectare
foot	0.3048	meter
acre-foot per year	0.001233	cubic hectometer per year
foot per mile	0.1894	meter per kilometer
acre-foot	0.001233	cubic hectometer
inch	25.40	millimeter

Temperatures in degrees Fahrenheit (°F) or degrees Celsius (°C) can be converted as follows:

$$°F = 9/5\ (°C) + 32$$

$$°C = 5/9\ (°F - 32)$$

Sea level: In this report "sea level" refers to the National Geodetic Vertical Datum of 1929 (NGVD of 1929)--a geodetic datum derived from a general adjustment of the first-order level nets of both the United States States and Canada, formerly called "Sea Level Datum of 1929."

GROUND-WATER GEOCHEMISTRY OF THE ALBUQUERQUE-BELEN BASIN, CENTRAL NEW MEXICO

By

Scott K. Anderholm

ABSTRACT

The Albuquerque-Belen Basin, located in central New Mexico, is dependent on ground and surface water for irrigation and municipal use. The geochemistry of ground water in the basin was studied as part of the Southwest Alluvial Basins Regional Aquifer-Systems Analysis. The purpose of this study was to define the areal distribution of different water qualities, use the distribution to help define the ground-water flow system, and identify processes resulting in differences in ground-water quality in the Albuquerque-Belen Basin.

The Albuquerque-Belen Basin contains as much as 18,000 feet of basin-fill sediments of the Santa Fe Group, which form the principal aquifer in the basin. The majority of ground-water inflow to the principal aquifer occurs as infiltration of surface water through river channels, infiltration of surface inflow from adjacent areas, infiltration of excess irrigation water, ground-water inflow from adjacent bedrock units, and ground-water inflow from the upgradient Santo Domingo Basin. In general, ground water flows from the margins of the basin toward the basin center and then southward to the adjacent Socorro Basin. The majority of ground-water outflow is evapotranspiration, ground-water pumpage, and ground-water outflow to the Socorro Basin.

The chemistry of inflow water to the aquifer has the largest effect on the distribution of different water qualities in the Albuquerque-Belen Basin. In the southeastern area of the basin, inflow is derived from Paleozoic and Mesozoic rocks that contain gypsum. Specific conductance ranges from about 1,000 to 1,200 microsiemens per centimeter at 25 °Celsius in this area of the basin, and calcium and sulfate generally are the dominant ions. On the eastern side of the basin, inflow is derived from Precambrian and Paleozoic rocks. Ground water in this area of the basin has a specific conductance usually less than 400 microsiemens per centimeter, and calcium and bicarbonate are the dominant ions. Along the southwestern margin of the basin, ground water enters the basin from adjacent Paleozoic rocks and from the infiltration of surface water from adjacent areas. These two waters mix in the aquifer. The inflow from adjacent bedrock units has a specific conductance generally greater than 20,000 microsiemens per centimeter. This water contains large concentrations of sodium and chloride. The mixing of this water and the infiltration of surface water from adjacent areas, which generally has a small specific conductance, result in ground water with a large range of specific conductance. Sodium and sulfate are the dominant ions in ground-water inflow from Cretaceous rocks along the western margin of the basin.

In the northern area of the Albuquerque-Belen Basin, ground-water inflow from the Jemez geothermal reservoir mixes with local recharge water and ground water in the aquifer. Large concentrations of silica and chloride generally are indicators of ground water from the Jemez geothermal reservoir.

In a large area west of Albuquerque, sodium is the dominant cation in ground water. In this area of the basin, the exchange of calcium and magnesium for sodium probably is a dominant process affecting ground-water quality. This is the same area of the basin that is underlain by relatively fine grained sediments as indicated by drillers' and geophysical logs.

Ground water in the Rio Grande valley is affected by the infiltration of excess irrigation water. Excess irrigation water generally has a larger specific conductance than other ground water in the Rio Grande valley, so the mixing of these waters results in shallow ground water with a generally larger specific conductance than the deeper ground water.

INTRODUCTION

In 1978, Congress appropriated funds for a comprehensive national ground-water investigation program called Regional Aquifer-Systems Analysis (RASA). This program was designed to study large areas of the country that are underlain by a regional aquifer system. A regional aquifer system as defined by this program consists of hydraulically connected aquifers that underlie large regions, usually parts of several States.

Twenty-nine regional aquifer systems were identified for study (Bennett, 1979, p. 38). Individual regional aquifer-system studies are scheduled to take 4 to 5 years. The RASA program is expected to last for 10 years, with several regional studies starting each year. Although each regional system is different, the overall objectives are to assemble hydrologic information and develop predictive tools for management of the Nation's ground water (Bennett, 1979, p. 38). In general, the predictive tools consist of some type of computer model that will simulate the ground-water systems.

The Southwest Alluvial Basins (SWAB) East RASA study began in fiscal year 1978. The SWAB area includes the alluvial basins along the Rio Grande from its headwaters in southern Colorado to western Texas and several closed alluvial basins in southwestern and central New Mexico (fig. 1). Twenty-two alluvial basins were identified in this study area. Because of the duration of the project and the large number of basins identified, not all basins were studied with the same amount of detail. The principal objectives of the SWAB-RASA study are: (1) To develop a computerized data base; (2) to study the ground-water flow systems and ground-water quality; and (3) to develop digital computer models of the ground-water flow systems in selected basins (Wilkins and others, 1980, p. 10).

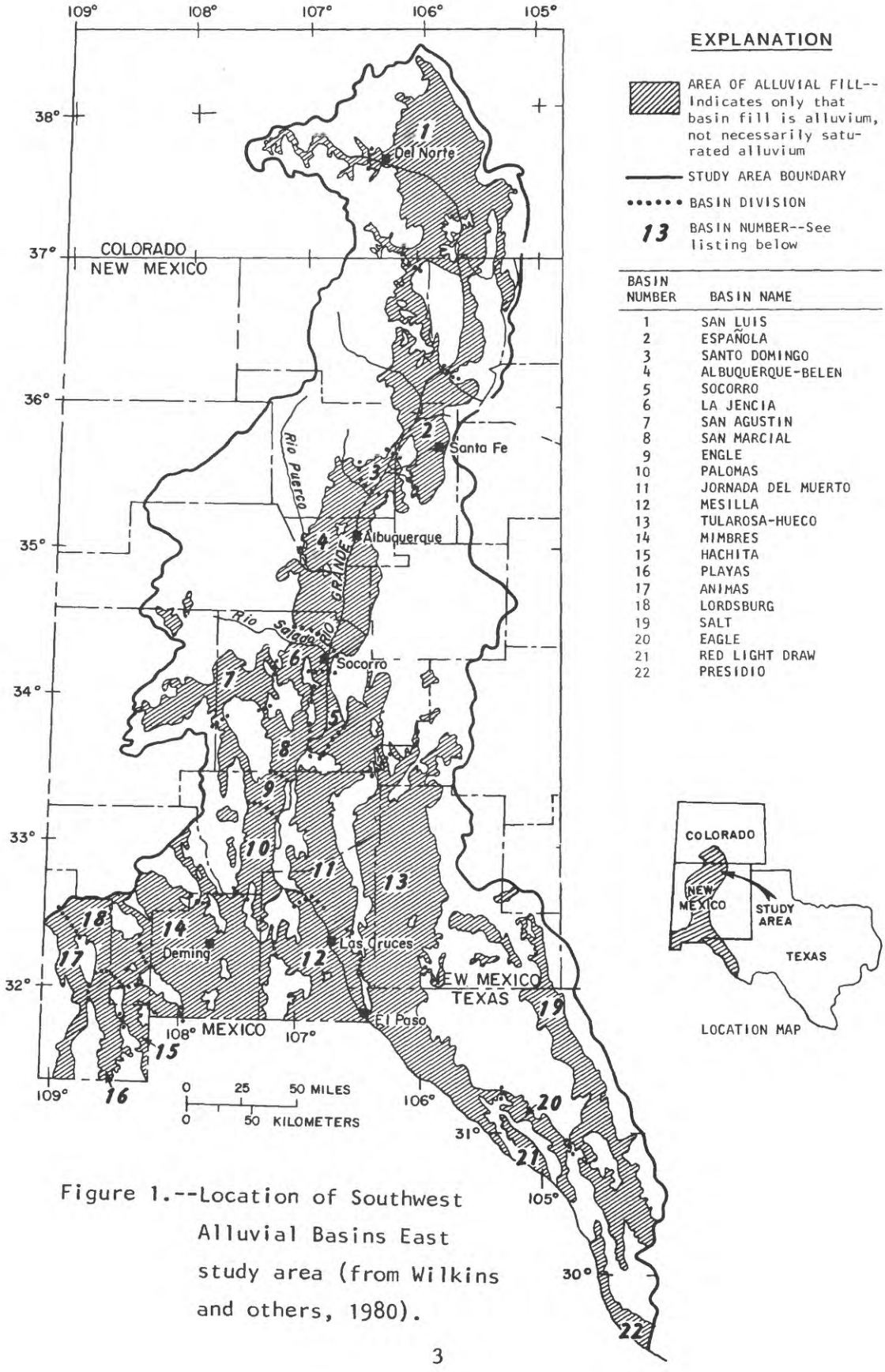

Figure 1.--Location of Southwest Alluvial Basins East study area (from Wilkins and others, 1980).

Acknowledgments

John Hawley and Richard Lozinsky of the New Mexico Bureau of Mines and Mineral Resources provided helpful comments on the section of the report concerning the Santa Fe Group. Field trips and discussions with John Hawley have greatly aided in the understanding of the stratigraphy of the Santa Fe Group.

Purpose and Scope

The purposes of this study were to define the areal distribution of different water qualities, use the distribution to help define the ground-water flow system, and identify the chemical processes that result in differences in ground-water quality in the Albuquerque-Belen Basin (fig. 1) in central New Mexico. This report documents the results of that part of the detailed study of the Albuquerque-Belen Basin pertaining to ground-water geochemistry.

Location

The Albuquerque-Belen Basin is in central New Mexico (basin 4 in fig. 1). The basin, one of many alluvial basins in the Rio Grande rift, is approximately 100 miles long and from 20 to 40 miles wide. The Rio Grande is the main drainage in the basin, and the Jemez River, Rio Puerco, and the Rio Salado are major tributaries to it (fig. 2). The Albuquerque-Belen Basin is hydraulically connected to the Santo Domingo Basin on the north and the Socorro Basin on the south by the Rio Grande and by ground-water flow through alluvial sediments.

The basin is bounded on the north by the Nacimiento uplift and the Jemez volcanic complex (fig. 2). The east boundary of the basin has the most topographic relief and consists of the Sandia, Manzanita, Manzano, and Los Pinos Mountains. The south border is formed partially by the Los Pinos Mountains, Joyita Hills, and the Ladron Mountains. The western boundary has little topographic relief and consists of the Lucero uplift and the Rio Puerco fault zone.

Albuquerque is the main population center in the basin, having a population of 331,767 in 1980 (U.S. Department of Commerce, 1981, p. 8). Bernalillo, Los Lunas, and Belen are other population centers in the basin (fig. 2).

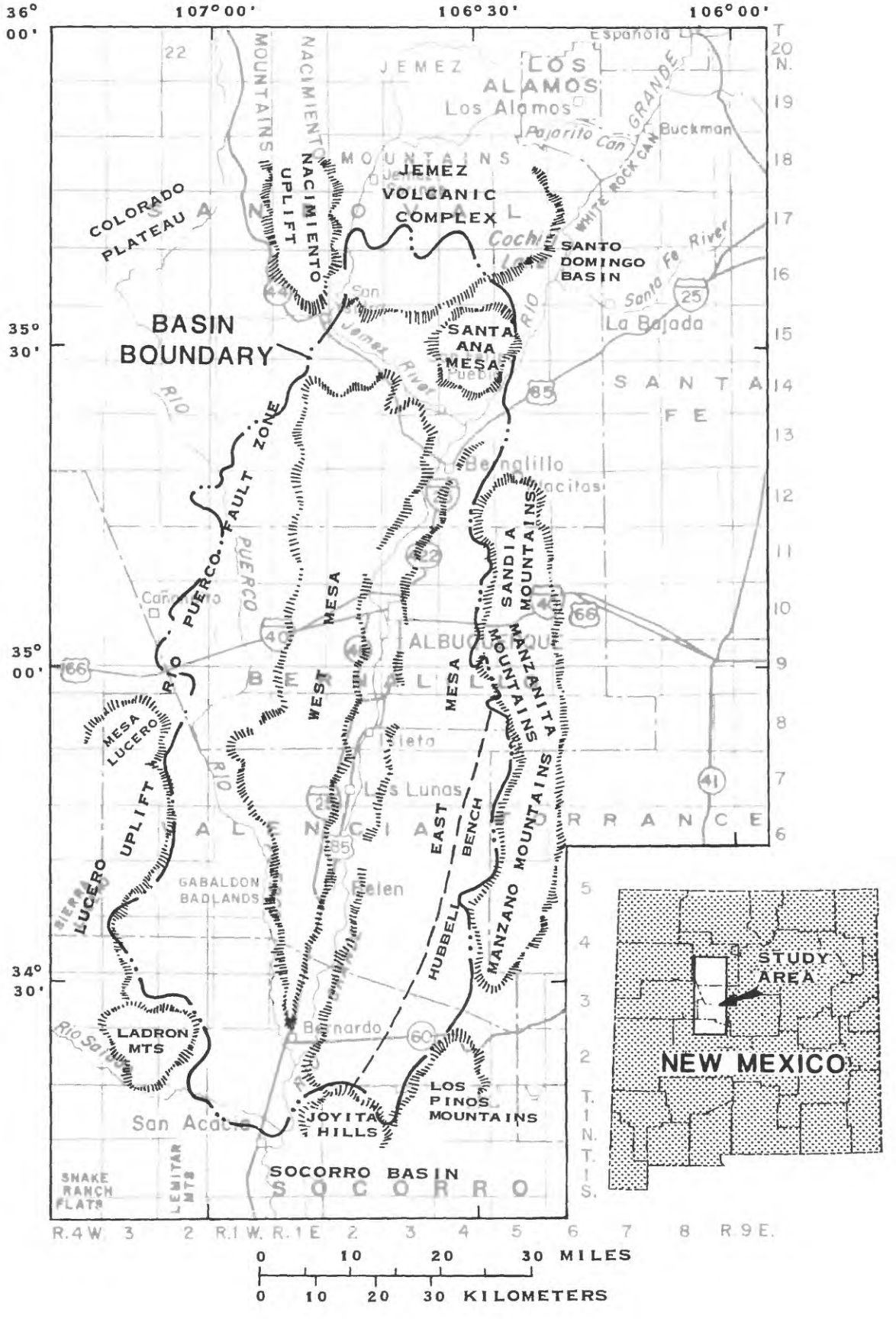

Figure 2.--Location of the Albuquerque-Belen Basin.

Climate

The climate of the Albuquerque-Belen Basin is semiarid. The mountainous areas adjacent to the basin generally receive more precipitation and the annual temperatures are much lower than in areas in the Rio Grande valley (table 1). The mean annual temperature at the Albuquerque airport weather station is 55.7 °Fahrenheit. July is the warmest month and January and December are the coolest months (Gabin and Lesperance, 1977). Approximately 45 percent of the precipitation is the result of thunderstorms that occur from late July to September (table 1). Winters are typified as being mild, sunny, and dry.

Previous Investigations

There have been many studies concerning the geology and hydrology of the Albuquerque-Belen Basin. The following discussion includes some of these studies.

Geology

Bryan (1909) first published a map of the Albuquerque area in 1909; later, Bryan and his students did considerable work on the stratigraphy of the Tertiary rocks in the Albuquerque-Belen Basin (Bryan and McCann, 1937; Bryan, 1938; Denny, 1940, 1941; Wright, 1946). V.C. Kelley conducted many studies on the geology of the Albuquerque area (Kelley and Wood, 1946; Kelley, 1952, 1974, 1977; Kelley and Northrop, 1977). The stratigraphy of the Santa Fe Group in the northern Albuquerque-Belen Basin was investigated by Galusha (1966) and Galusha and Blick (1971). Lambert (1968) described the Quaternary geology of the Albuquerque area. Smith, Bailey, and Ross (1970) published a map of the Jemez Mountains. A large part of the geology and structural geology sections in this report is condensed from Kelley (1977). Two New Mexico Geological Society Guidebooks (Northrop, 1961; Callender and others, 1982) contain articles concerning the geology of the Albuquerque-Belen Basin.

Hydrology

A comprehensive report on the ground-water conditions of the middle Rio Grande valley was presented by Theis (1938). The hydrology of northwestern Socorro County was described by Spiegel (1955), and the hydrology of Bernalillo and Sandoval Counties was described by Bjorklund and Maxwell (1961). Titus published reports on the hydrology of the Albuquerque-Belen Basin (1961) and of eastern Valencia County (1963). The effects of Albuquerque municipal pumpage on flow in the Rio Grande and the lowering of ground-water levels were analyzed in a report by Reeder, Bjorklund, and Dinwiddie (1967). Trainer (1974) investigated the hydrology of the southwestern Jemez Mountains. The hydrology of the Albuquerque area was discussed in a report by the U.S. Army Corps of Engineers (1979). Much of the data used in this report was published in Titus (1963) and Bjorklund and Maxwell (1961).

Table 1. Climatic data from four stations

[Precipitation in inches, temperature in degrees Fahrenheit]

Type of data	Jan.	Feb.	Mar.	Apr.	May	June	July	Aug.	Sept.	Oct.	Nov.	Dec.	Annual
Albuquerque airport station, Bernalillo County													
Latitude: 35°03'													
Longitude: 106°37'													
Altitude: 5,310 feet													
Precipitation:													
Years of record	94	95	94	95	96	94	95	93	95	95	96	92	89
Mean	0.37	0.34	0.42	0.53	0.56	0.70	1.44	1.42	0.94	0.84	0.43	0.45	8.61
Temperature:													
Years of record	83	83	83	83	83	83	83	83	83	83	83	83	83
Mean	34.5	39.5	46.3	54.8	63.8	77.7	85.6	75.2	68.3	56.7	43.9	35.1	55.7

Type of data	Jan.	Feb.	Mar.	Apr.	May	June	July	Aug.	Sept.	Oct.	Nov.	Dec.	Annual
Belen station, Valencia County													
Latitude: 34°40'													
Longitude: 106°46'													
Altitude: 4,800 feet													
Precipitation:													
Years of record	31	30	30	28	29	29	30	29	30	30	32	32	27
Mean	0.30	0.39	0.39	0.34	0.27	0.63	1.35	1.34	0.93	0.96	0.24	0.44	7.79
Temperature:													
Years of record	30	28	29	28	27	30	30	28	29	29	31	32	24
Mean	34.5	40.0	46.5	56.4	65.0	73.9	78.5	76.0	68.4	57.2	44.0	35.5	56.5

Table 1. Climatic data from four stations – Concluded

Type of data	Jan.	Feb.	Mar.	Apr.	May	June	July	Aug.	Sept.	Oct.	Nov.	Dec.	Annual
Bernardo station, Socorro County													
Latitude: 34°26'													
Longitude: 106°49'													
Altitude: 4,727 feet													
Precipitation:													
Years of record	13	13	13	14	14	14	14	14	14	14	14	14	13
Mean	0.15	0.30	0.24	0.18	0.28	0.35	1.24	1.72	1.33	1.08	0.22	0.36	7.50
Temperature:													
Years of record	13	13	13	13	14	14	14	14	14	14	14	13	11
Mean	32.7	37.3	45.5	52.7	61.2	68.7	75.1	72.3	65.0	54.5	44.3	33.8	53.5

Type of data	Jan.	Feb.	Mar.	Apr.	May	June	July	Aug.	Sept.	Oct.	Nov.	Dec.	Annual
Sandia Crest station, Bernalillo County													
Latitude: 35°13'													
Longitude: 106°27'													
Altitude: 10,675 feet													
Precipitation:													
Years of record	22	22	22	22	22	22	22	22	22	22	22	23	22
Mean	1.78	2.00	2.30	1.21	0.89	0.92	3.29	3.33	1.86	1.97	1.37	2.13	22.89
Temperature:													
Years of record	21	21	21	21	20	21	20	20	21	21	20	21	17
Mean	20.4	21.4	25.0	33.2	43.9	53.5	56.9	54.3	48.9	40.0	29.5	22.5	37.5

Well-Numbering System

The system of numbering wells in New Mexico is based on the common subdivision of public lands into sections (fig. 3). The well number, in addition to designating the well, locates its position to the nearest 10-acre tract in the land network. The number is divided by periods into four segments. The first segment denotes the township (T.) north (N.) or south (S.) of the New Mexico Base Line; the second segment denotes the range (R.) east (E.) or west (W.) of the New Mexico Principal Meridian; and the third segment denotes the section (sec.). The fourth segment consists of three digits that denote the 160-, 40-, or 10-acre tract, respectively, in which the well is located. For this purpose, the section is divided into four quarters, numbered 1, 2, 3, and 4, for the northwest, northeast, southwest, and southeast quarters, respectively. The first digit of the fourth segment gives the quarter section, which is a tract of 160 acres. Similarly, the 160-acre tract is divided into four 40-acre tracts denoted by the second digit and numbered in the same manner. Finally, the 40-acre tract is divided into four 10-acre tracts that are denoted by the third digit.

If a well cannot be located accurately within a 10-acre tract, a zero is used as the third digit, and if the well cannot be located accurately within a 40-acre tract, zeros are used for the second and third digits. If a well cannot be located more closely than the section, the fourth segment of the well number is omitted.

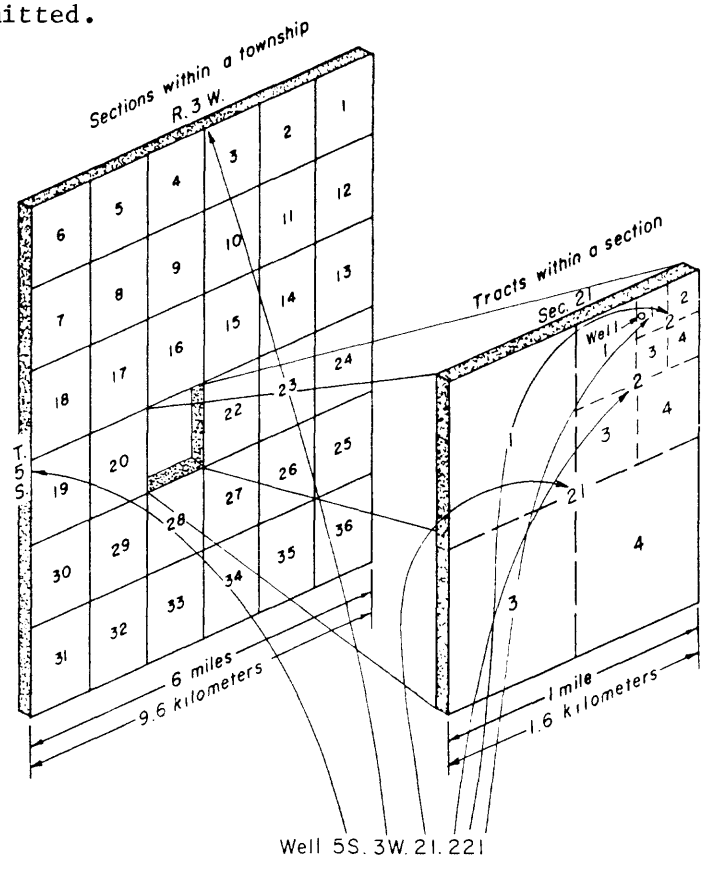

Figure 3.--Well-numbering system in New Mexico.

GEOLOGY

An understanding of the geology of the Albuquerque-Belen Basin and surrounding areas is important when determining water-quality types and their distribution and extent in the basin. Rocks from Precambrian to Holocene age are found in or surrounding the Albuquerque-Belen Basin (pl. 1). Each geologic unit is described in some detail in the following sections.

Precambrian Rocks

Precambrian rocks generally are exposed on the eastern side of the basin in the Sandia, Manzanita, Manzano, and Los Pinos Mountains (pl. 1). Precambrian rocks also are exposed in the Ladron Mountains in the southwest part of the basin. The Precambrian rocks consist of granite, gneiss, schist, quartzite, and greenstone (Kelley, 1977, p. 8).

Paleozoic Rocks

Mississippian and Pennsylvanian rocks border the Albuquerque-Belen Basin on all but the northern and northwestern sides (pl. 1). On the eastern side of the basin, these rocks cap the Sandia, Manzanita, Manzano, and Los Pinos Mountains. On the southern and southwestern sides of the basin, these rocks are exposed at the land surface or are in fault contact with the Santa Fe Group (Formation) of late Tertiary and Pleistocene age in the subsurface. The thickness of Mississippian rocks varies considerably. In many areas, Mississippian rocks are missing due to erosion or to not being deposited. In a measured section near Placitas, Mississippian rocks consist of a basal sandstone and conglomerate (6.6 feet thick), followed upward by stromatolitic dedolomite (33 feet thick) and limy mudstone and dolomite (34 feet thick) (Kelley and Northrop, 1975, p. 29).

Pennsylvanian rocks consist of the Sandia and Madera Formations. The Sandia Formation consists of sandstone, shale, limestone, and conglomerate, and averages approximately 150 feet thick (Kelley, 1977, p. 32). The Madera Formation forms large dip slopes around the eastern, southern, and southwestern sides of the Albuquerque-Belen Basin. The Madera Formation in the Sandia and Manzano Mountains is composed of a lower part dominated by gray marine limestone and an upper part of interbedded limestone, arkosic sandstone, conglomerate, and red shale. The thickness of the Madera Formation in the Sandia Mountains ranges from 1,300 to 1,400 feet (Kelley and Northrop, 1975, p. 34). In the Mesa Lucero area (fig. 2), the Madera Formation is composed of a lower dark-gray cherty limestone, a middle limestone with interbedded red shale and arkosic sandstone, and an upper interbedded red sandstone, red shale, conglomerate, and limestone (Kottlowski, 1961, p. 100). The thickness of the Madera Formation near Mesa Lucero is approximately 1,700 feet (Kottlowski, 1961, p. 100).

Permian rocks consist of the Abo Formation, Yeso Formation, Glorieta Sandstone, and San Andres Formation. The Abo Formation represents fluvial subareal deposition and consists of alternating reddish-brown mudstone and sandstone and minor conglomerate and limestone (Kelley and Northrop, 1975, p. 49-50). The thickness of the Abo Formation is approximately 700 to 900 feet in the Sandia Mountains (Kelley and Northrop, 1975, p. 50) and approximately 800 to 900 feet in the Mesa Lucero area (Baars, 1961, p. 115).

The Yeso Formation consists of gypsum, tan to brown sandstone, siltstone, limestone, and dolomite. Outcrops of the Yeso Formation are exposed in the southeastern and southern parts of the basin and on the southwestern side of the basin near the Ladron Mountains and Mesa Lucero. The presence of gypsum ($CaSO_4.2H_2O$) in this unit is important because gypsum is soluble and ground water that comes into contact with the Yeso Formation or associated sediment of the Yeso Formation tends to have large concentrations of calcium and sulfate. The Yeso Formation is approximately 500 feet thick in the Sandia Mountains (Kelley and Northrop, 1975, p. 51).

The Glorieta Sandstone and San Andres Formation undivided consists of the Glorieta Sandstone, composed of clean white sandstone, and the San Andres Formation, composed of limestone with minor interbedded sandstone and an overlying sandstone with interbedded limestone (Kelley and Northrop, 1975, p. 52). In the Sandia Mountains, the Glorieta and San Andres sequence is approximately 350 feet thick (Kelley and Northrop, 1975, p. 52); in the Mesa Lucero area, the formation is approximately 700 feet thick (Baars, 1961, p. 118).

Mesozoic Rocks

Triassic rocks consist of the Santa Rosa Formation and the Chinle Formation. The Santa Rosa Formation that crops out along the eastern margin of the basin consists of white to reddish-brown sandstone and minor conglomeratic lenses (Kelley and Northrop, 1975, p. 52). The Chinle Formation along the eastern side of the Albuquerque-Belen Basin consists predominantly of reddish-brown mudstone and interbedded thin sandstone stringers. On the western side of the basin, the Chinle Formation consists of a lower sandy facies and an upper red mudstone and shale and has a combined thickness of approximately 500 feet (Smith, 1961, p. 121-122).

Jurassic rocks are exposed near San Ysidro, Placitas, and Mesa Lucero (pl. 1). Jurassic rocks consist of the Entrada Sandstone, Todilto Formation, Summerville Formation, Bluff Sandstone, and Morrison Formation. The Entrada Sandstone is a buff to white sandstone that is approximately 100 feet thick (Kelley and Northrop, 1975, p. 54). The Todilto Formation consists of a lower flaggy limestone and an upper massive gypsum and has an approximate thickness of 180 feet (Kelley and Northrop, 1975, p. 55). The stratigraphic sequence of rocks between the Todilto and Morrison Formations is different on the eastern and western sides of the Albuquerque-Belen Basin. On the eastern side of the basin, the Todilto Formation is overlain by the Morrison Formation. The Morrison Formation consists of green to red mudstone and siltstone with interbedded white to orange sandstone (Kelley and Northrop, 1975, p. 56). On the western margin of the basin, the Todilto Formation is overlain by the

Summerville Formation and the Bluff Sandstone. The Summerville Formation consists of a lower brown mudstone and an upper light-brown sandstone and is approximately 120 feet thick (Moench and Schleep, 1967, p. 14). The overlying Bluff Sandstone consists of a well-sorted buff sandstone that is approximately 300 feet thick (Moench and Schleep, 1967, p. 15). On the western side of the basin, the Morrison Formation consists of a lower white sandstone and an upper red to green mudstone with interbedded white sandstone (Smith, 1961, p. 126-127).

Cretaceous rocks crop out along the northeastern and western sides of the Albuquerque-Belen Basin and consist of the Dakota Sandstone, Mancos Shale, and Mesaverde Formation. The Dakota Sandstone consists of white to buff sandstone and some black shale near the upper part of the unit (Kelley and Northrop, 1975, p. 58). The unit is approximately 120 feet thick on both the northeastern and western sides of the basin (Kelley, 1977, p. 9). The Mancos Shale is predominantly a black to green shale that is approximately 1,300 feet thick (Kelley and Northrop, 1975, p. 60). The Mesaverde Formation consists of interbedded mudstone, siltstone, sandstone, and coal. The Mesaverde Formation is approximately 3,500 feet thick in the northeastern part of the basin and 1,250 feet thick in the northwestern part of the basin (Kelley, 1977, p. 9).

Cenozoic Rocks including the Santa Fe Group (Formation)

The Galisteo Formation of early Tertiary age crops out in the northern part of the basin (pl. 1) and consists of interbedded sandstone and mudstone and some interbedded conglomerate (Lucas, 1982). The formation ranges from 1,000 to 4,000 feet in thickness (Kelley and Northrop, 1975, p. 66).

Outcrops of the Tertiary Baca Formation are found in the southern part of the Albuquerque-Belen Basin (pl. 1) and consist of interbedded sandstone, mudstone, and conglomerate. Lucas, Schoch, and Manning (1981, p. 965) showed that the Baca and Galisteo Formations were deposited at approximately the same time.

The Datil Formation of Oligocene age crops out in the southeastern part of the basin and is composed of rhyolitic to andesitic ash-flow tuffs and volcaniclastic conglomerate and sandstone as much as 2,000 feet thick. The Espinaso Formation of Stearns (1943) of Oligocene age crops out in the northern part of the Albuquerque-Belen Basin and consists of interbedded volcanic breccia and conglomerate approximately 1,400 feet thick (Kelley and Northrop, 1975, p. 67). The Galisteo Formation, Baca Formation, Datil Formation, and Espinaso Formation are pre-Santa Fe Group units that are associated with Laramide basins (early Tertiary) and volcanic centers (mid-Tertiary) that predate Rio Grande rift development.

Hayden (1869, p. 166) originally named rocks in the Rio Grande valley near Santa Fe the Santa Fe "marls." Darton (1922) was the first to use the term "Santa Fe Formation." Kirk Bryan and his students were first to study the Santa Fe Formation in detail and to work on the stratigraphic relations in the Santa Fe Formation in the Albuquerque-Belen Basin. Bryan and McCann (1937) named three informal members (the lower gray, middle red, and upper buff) within the Santa Fe Formation in the northwestern Albuquerque-Belen Basin. Bryan (1938) published a paper describing the chain of late Cenozoic basins that extend along the present Rio Grande drainage (Rio Grande depression) in New Mexico and southern Colorado. This work was important because many studies done on the Santa Fe Formation since that time have been based on Bryan's (1938) concept of what is now referred to as the Rio Grande rift (Chapin and Seager, 1975). Baldwin (1956) and Spiegel and Baldwin (1963) introduced the term Santa Fe Group and defined the Santa Fe Group to include sedimentary and volcanic rocks related to the Rio Grande trough. The upper limit was considered to include all but the terrace deposits and alluvium in present drainages. Since the term was introduced, the term has been used to describe Miocene to Quaternary basin-fill deposits in the Rio Grande rift.

Since the original work by Bryan and his students in 1937 and 1938, much work has been done in localized areas of the Albuquerque-Belen Basin (fig. 4). Hawley (1978, p. 238-239) presented correlation charts that are a compilation of names and ages of units along the Rio Grande rift. Lucas and Ingersoll (1981) presented an overview and extensive list of references dealing with the continental Cenozoic deposits of New Mexico.

Santa Fe Group terminology is complex in the Albuquerque-Belen Basin because of the large number of workers who have described the Santa Fe Group over the past century and the fact that most workers based their findings on outcrop geology (fig. 5). There are problems in laterally tracing units because of the lack of continuous outcrops and the large amount of faulting in the Rio Grande rift. Local structural highs present during deposition of the Santa Fe Group cause confusion because of the large changes in lithology or color of units in short distances. Older Santa Fe units were deposited in precursor basins whose boundaries may have been much different than the present basin. Kelley (1977, p. 10) probably best summed up the concept when he stated that the "...bulk of the sediment that has filled the subsiding trough does not have a direct relationship to late Pleistocene and Holocene land forms."

An attempt to relate the many units to the informal members originally described by Bryan and McCann (1937) will be made in the following discussion. This relation between units is not done because the author agrees or disagrees with any of the authors who have addressed the Santa Fe Group, but because a frame of reference is useful for this report. In the discussion, the term Santa Fe Group, more commonly used in the area, refers to the general description of the Santa Fe deposits. However, the map on plate 1 follows Kelley's (1977) usage of Santa Fe Formation and its members. The discussion starts with the oldest units in the Santa Fe Group and ends with the youngest units.

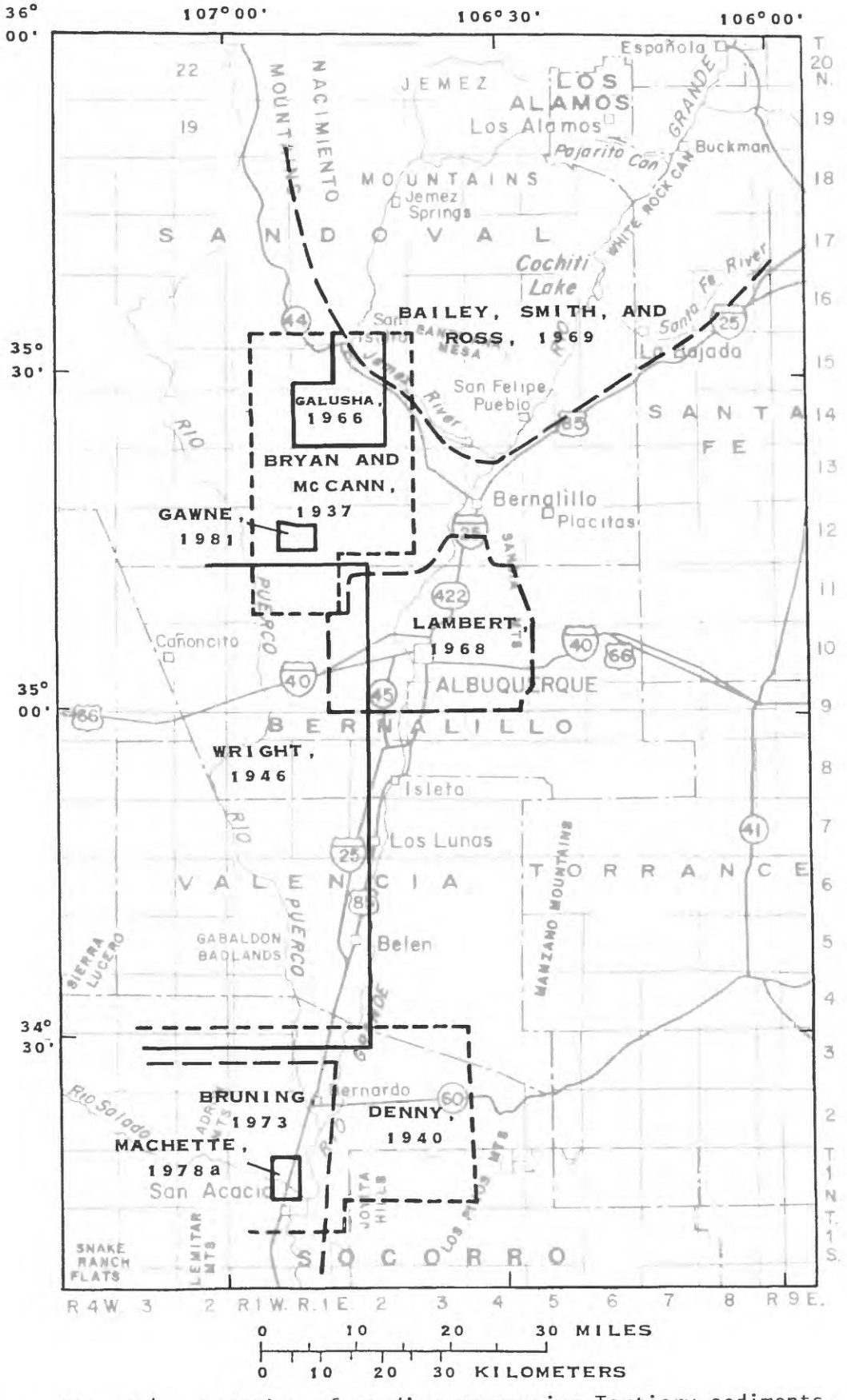

Figure 4.--Location of studies concerning Tertiary sediments.

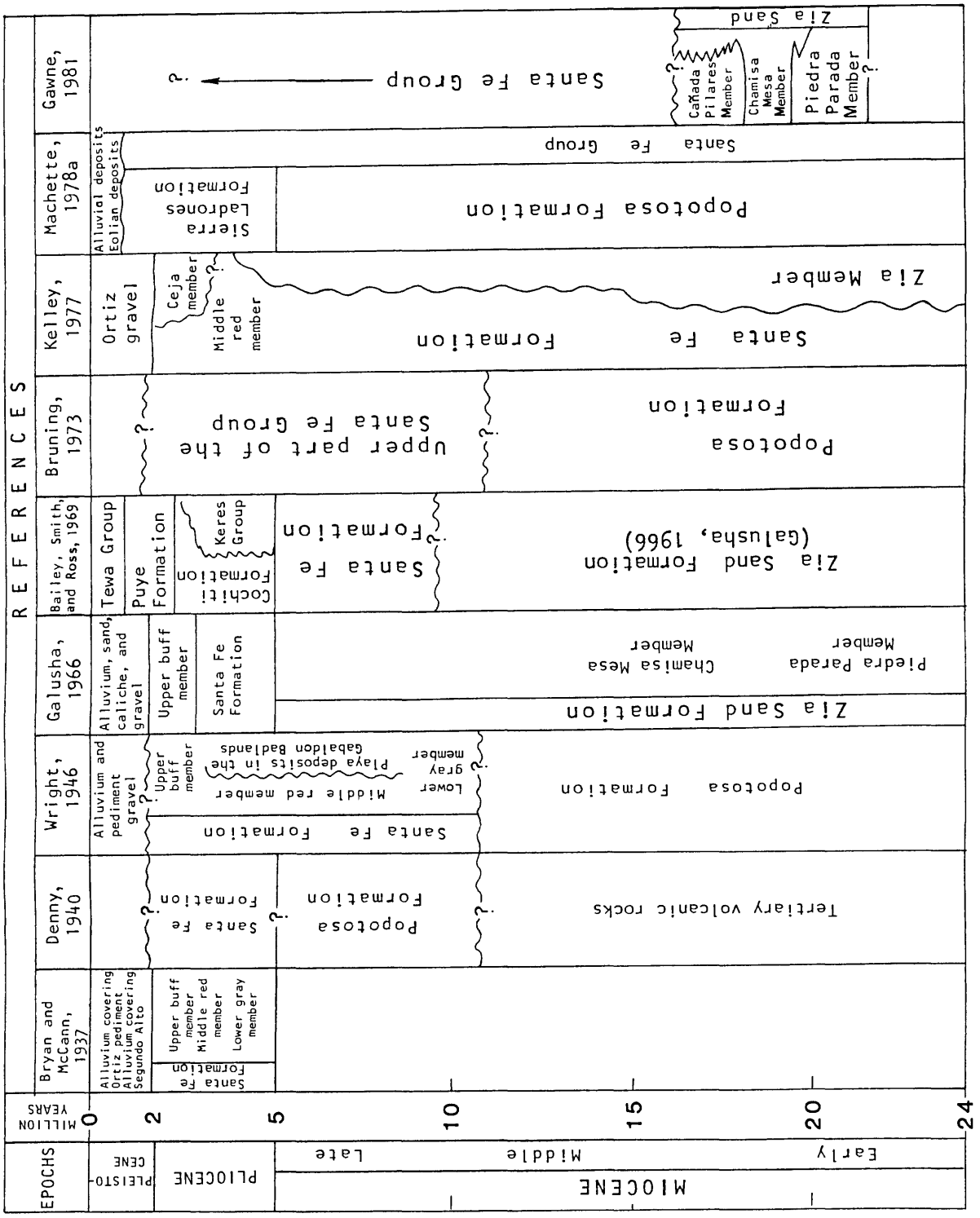

Figure 5.--Selected references on the nomenclature of the Santa Fe Group (Formation) and equivalent units.

Galusha (1966) first named the Zia Sand Formation for exposures in the northwestern part of the Albuquerque-Belen Basin (fig. 5). He subdivided the Zia Sand Formation into two members, the Piedra Parada Member and the Chamisa Mesa Member, both of Miocene age. Galusha (1966, p. 11) indicated that the Chamisa Mesa Member was described as the lower gray member of the Santa Fe Formation by Bryan and McCann (1937). Gawne (1981, p. 1,003) named a third upper member, the Cañada Pilares Member, in the unit she referred to as the Zia Sand. Tedford (1981, p. 1,014-15) showed that this unit is of Hemingfordian (early Miocene) age or about 16 to 20 million years old.

The Piedra Parada Member of the Zia Sand consists of a thin basal conglomerate that grades into a thick sequence of eolian sand. The overlying Chamisa Mesa Member is composed of eolian sand and some clay, silt, and limestone. In general, the Chamisa Mesa Member is finer grained than the Piedra Parada Member (Gawne, 1981). Gawne (1981, p. 1,003) reported that the Piedra Parada and Chamisa Mesa Members were deposited in a large dune field where water levels were close to land surface. The uppermost Cañada Pilares Member consists of red claystone and some interbedded sand. Gawne (1981, p. 1,003) reported that the Cañada Pilares Member was deposited as flood-plain and lacustrine deposits. In general, the sediments of the Zia Sand are oxidized and the grain size decreases upward. The total thickness of the Zia Sand in outcrop is approximately 1,000 feet (Galusha, 1966, p. 3; Gawne, 1981, p. 999). Galusha (1966, p. 4 and 11) mapped the beds above his Zia Sand Formation as the Santa Fe Formation (Santa Fe equivalent in measured section) and considered these beds to correspond to the middle red member of Bryan and McCann (1937). The lower part of the middle red member is included in the Cañada Pilares Member by Gawne (1981).

Wright (1946) mapped an area in the Albuquerque-Belen Basin from approximately T. 4 N. to T. 11 N. (fig. 4). Generally, this is south of the areas studied by Galusha (1966) (fig. 4). Wright (1946) did not find any outcrops of the lower gray member of the Santa Fe Formation as defined by Bryan and McCann (1937) (equivalent to the Chamisa Mesa Member (Galusha, 1966)) south of U.S. Highway 66 (Interstate Highway 40) (fig. 4). Wright (1946, p. 404) traced the middle red member (Bryan and McCann, 1937) southward to the Gabaldon Badlands. Wright (1946, p. 403-404) discussed a thick sequence of playa deposits in the badlands that interfingers with the middle red member and described the middle red member as consisting of pink and buff calcareous sandstone interbedded with red clay, silt, and gravel lenses. He also described approximately 4,100 feet of playa sediments in the Gabaldon Badlands that consist of tan, buff, and brown sand and brown to red gypsiferous silt and clay. Wright (1946, p. 410) suggested that these playa deposits are equivalent to the lower gray and middle red members of Bryan and McCann (1937).

Kelley (1977, p. 14) considered the middle red member to be the main body of the Santa Fe Formation and included the playa deposits of the Gabaldon Badlands in the main body of the Santa Fe Formation (fig. 5). Lozinsky (1986) showed that fossils collected from the middle third of the Gabaldon Badlands section represent a time span of 7 to 9 million years ago, which is much younger than the lower gray and middle red members of Bryan and McCann (1937). Lozinsky (1986) also found sediments at the top of the Gabaldon

Badlands section that were deposited by a large fluvial system, which probably indicates a change from closed-basin to through-flowing drainage.

Denny (1940) named the Popotosa Formation from outcrops on the east side of the Ladron Mountains (south of the Gabaldon Badlands). Osburn and Chapin (1983) described the Popotosa Formation as consisting of a lower mudflow facies and an upper playa facies near Socorro. The lower facies consists of well-indurated red conglomerate, and the upper facies consists of red to green claystone; however, these facies grade and intertongue with other facies and volcanic units. Machette (1978a) assigned the Popotosa Formation to the Santa Fe Group and indicated that the Popotosa is early to late Miocene (fig. 5).

The preceding discussion shows how much confusion exists concerning the terminology of the rocks in the Santa Fe Group. The concept that both the upper part of the Popotosa Formation and sediments in the Gabaldon Badlands have been described as playa sediments is significant. These rocks also are approximately the same age (fig. 5). These sediments (upper part of Popotosa and sediments in the Gabaldon Badlands) possibly may represent deposition in the same sedimentary basin.

Bailey, Smith, and Ross (1969, p. 8-9), in a study of the stratigraphy of the Jemez Mountains, named the Cochiti Formation of early through middle Pliocene age (now designated late Miocene and early Pliocene by the U.S. Geological Survey, based on a 5-million-year Pliocene-Miocene boundary). They placed the base of the Cochiti Formation at the top of the basalt of Chamisa Mesa, northeast of San Ysidro (the top of Gawne's (1981) Zia Sand is at the base of this basalt unit). An age date determined after the work of Bailey, Smith, and Ross (1969) was completed indicates that the basalt of Chamisa Mesa is approximately 10.5 million years old (Hawley, 1978, p. 239), and work by Gardner and others (1986, p. 1,766) indicates the Cochiti is middle to late Miocene age. The Cochiti Formation consists of a thick sequence of volcanic gravel and sand. Bailey, Smith, and Ross (1969) indicated that the formation becomes finer grained south of the Jemez Mountains and grades into coarse red sands that contain a larger proportion of granitic debris and a small proportion of volcanic material. It is possible that the lower part of the Cochiti Formation may represent deposition along the margins of the basin in which the Popotosa Formation and Gabaldon Badlands sediments may have been deposited. The Cochiti Formation may be about the same age as the playa sediments of the Gabaldon Badlands and the upper part of the Popotosa Formation (Gardner and others, 1986).

Lambert (1968) mapped and referred to sediments in the Albuquerque area equivalent to Bryan and McCann's (1937) upper buff member as the "upper buff formation." Lambert (1968, p. 74-75) described his upper buff formation as consisting of a lower part of mainly grayish-orange sands with some interbedded clay, mud, gravel, and mudstone and an upper part consisting of yellow to gray sandy-pebble gravel and pebble sand and minor interbedded clay, mud, and sand. Lambert (1968, p. 100, 102) believed that the lower part of his upper buff formation was deposited in the distal end of a piedmont slope and the adjoining basin floor and that the upper part of his upper buff formation was deposited on a piedmont alluvial plain by subparallel shifting streams. Lambert (1968, p. 104-106) did not find any axial-stream deposits

that could be traced into his upper buff formation but indicated that it was possible that axial-stream deposits (upper buff(?) gravel and upper buff(?) sand) in the Albuquerque area correlate with his upper buff formation.

Kelley (1977, p. 18-20) named and described the Ceja Member of the Santa Fe Formation, which is roughly equivalent to the upper buff formation of Lambert (1968) and the upper buff member of Bryan and McCann (1937) (fig. 5). Kelley (1977) noted that the Ceja Member thins and pinches out at approximately T. 8 N., R. 1 W.

Machette (1978a) named and described the Sierra Ladrones Formation of the Santa Fe Group of early Pliocene to middle Pleistocene age on the basis of outcrops in the southern Albuquerque-Belen Basin. The Sierra Ladrones Formation consists of light-brown to reddish-brown sandstone and conglomerate with minor interbedded silt, clay, and basalt. Machette (1978a) interpreted the Sierra Ladrones Formation as representing alluvial-fan, piedmont-slope, flood-plain, and axial-stream (ancestral Rio Grande) deposits.

The Sierra Ladrones Formation (Machette, 1978a) is broadly equivalent to the upper buff member and part of the middle red member of the Santa Fe Formation of Bryan and McCann (1937, fig. 5). Machette (1978b) mapped the units, which Kelley (1977) called the Ceja Member and Wright (1946) called the upper buff, as Sierra Ladrones from latitude 34° to latitude 35° North. The lower part of this unit may be equivalent to the uppermost part of the Cochiti Formation (Bailey and others, 1969) (fig. 5).

Although much confusion exists concerning the nomenclature of the upper part of the Santa Fe Group, the presence of generally coarse grained material in the upper buff member (Bryan and McCann, 1937) in contrast to the clay and fine-grained sediments of the middle red member is a characteristic upon which most investigators agree. The presence of axial-stream deposits in the Sierra Ladrones Formation and axial-stream deposits that Lambert (1968) tentatively correlated with his upper buff formation suggests that there may have been axial drainage in the Albuquerque-Belen Basin during deposition of the upper buff formation (Lambert, 1968) or Sierra Ladrones Formation. A study of geophysical logs of wells generally less than 2,000 feet deep in the Albuquerque area determined that there is a general change from coarse-grained material in the upper part of the logs to fine-grained material in the lower part of the logs. Lambert (1968, p. 97, fig. 2) also noticed this change in lithology and intepreted it to be the approximate contact between his upper buff formation and the Tertiary undivided alluvium (Bryan and McCann's (1937) middle red member). This change in lithology can be seen over a large area under the Llano de Albuquerque (fig. 6). This contact may represent a change from closed-basin to open-basin deposition.

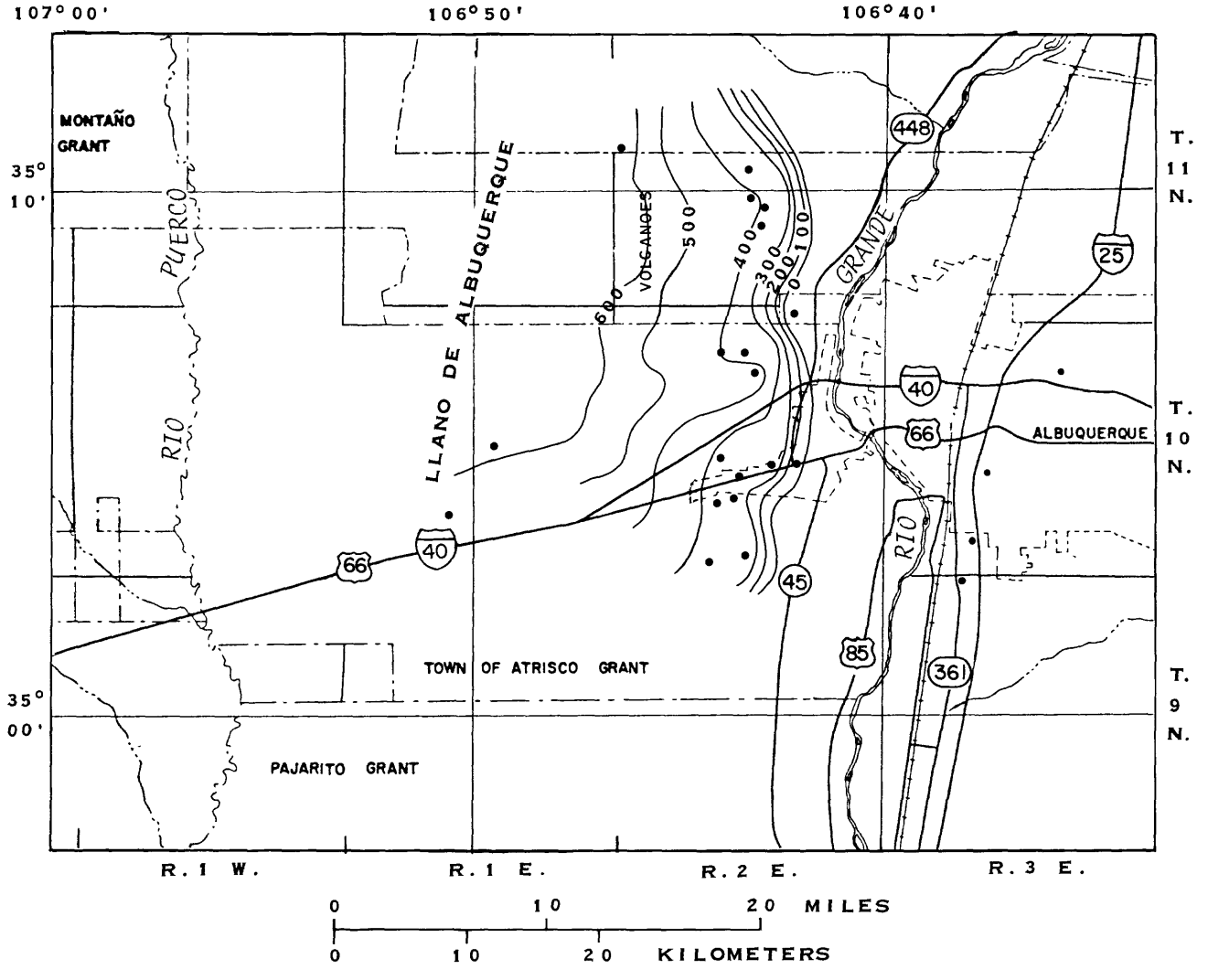

EXPLANATION

—600— LINE OF EQUAL THICKNESS OF FINE-GRAINED SEDIMENTS--Interval 100 feet

• DATA POINT

Figure 6.--Thickness of the fine-grained sediments west of Albuquerque.

Lambert (1968, p. 154) named and described, in ascending order, the "Los Duranes, Edith, and Menaul formations" (informal usage) on the basis of outcrops in the Albuquerque area and assigned the units to the Santa Fe Group. Lambert (1968, p. 161, 165, and 181) interpreted these formations as representing deposits of an axial river. The Los Duranes formation consists of alternating clay and mud layers with some interbedded pebbly sand and sandy gravel. The Edith formation consists of sandy-pebble to cobble gravel with some interbedded sand, mud, and clay. The Menaul formation consists of sandy-pebble gravel. Lambert (1968, p. 161, 163, and 181) interpreted the Edith and Menaul formations as representing axial-river deposits of late Pleistocene age. Lambert (1968, p. 154) indicated that the Los Duranes formation fills a broad valley that is eroded into his upper buff formation. He estimated that the formation is approximately 300 to 400 feet thick. The Edith and Menaul formations were interpreted to be deposits much like the Los Duranes, but not as thick and extensive as the Los Duranes (Lambert, 1968) (fig. 7). Lambert (1968, fig. 2) included the Los Duranes, Edith, and Menaul formations in the Santa Fe Group, but Hawley (1978, p. 238) indicated that these inset valley fills postdate the Santa Fe Group as defined by Spiegel and Baldwin (1963). Lambert (1968) also mapped upper Pleistocene to Holocene flood-plain alluvium in the present Rio Grande valley near Albuquerque. This alluvium consists mostly of sand and gravel and is approximately 120 to 130 feet thick (Lambert, 1968, p. 216). This lithology and thickness probably are similar in the present Rio Grande valley throughout the Albuquerque-Belen Basin.

Structural Geology

Callender and Zilinski (1976), Slack and Campbell (1976), and Kelley (1977) studied the structural geology of the Albuquerque-Belen Basin and adjacent areas. Much of the following discussion is from their publications.

The Albuquerque-Belen Basin is bounded by the Lucero uplift and Rio Puerco fault zone on the west side (fig. 2). The Lucero monocline (Lucero uplift) is a westward-tilted fault block of Paleozoic rocks. The boundary between the Lucero uplift and the Albuquerque-Belen Basin is the Comanche fault and the Santa Fe fault (pl. 1). The Comanche fault is a west-dipping reverse fault (Callender and Zilinski, 1976). In this area of the uplift, Pennsylvanian rocks are juxtaposed with Precambrian rocks; north of this area, Pennsylvanian rocks are juxtaposed with the Permian Yeso Formation.

The Santa Fe fault is east of the Comanche fault and generally trends north (pl. 1). The fault juxtaposes the Santa Fe Group with the Permian Yeso Formation or the Triassic Chinle Formation. Callender and Zilinski (1976, p. 57) estimated that the stratigraphic separation on the Santa Fe fault may be greater than 11,500 feet.

The Rio Puerco fault zone consists of a northeast-trending fault belt. Stratigraphic separation of the Rio Grande rift faults of the Rio Puerco fault zone, which are downthrown to the east, is as great as 3,300 feet (Slack and Campbell, 1976, p. 51). Generally, Mesozoic rocks are juxtaposed with the Santa Fe Group along faults related to the Rio Grande rift.

AGE	GROUP AND FORMATION[1]	
Holocene	Post-Santa Fe deposits	Flood-plain alluvium, eolian sand, and lacustrine deposits
Late Pleistocene	Santa Fe Group	"Menaul formation" "Edith formation"
Late(?) Pleistocene		"Los Duranes formation"
Late to early Pleistocene		Old piedmont-slope alluvium
Early Pleistocene to late Pliocene		Upper buff(?) gravel Upper buff(?) sand Upper buff formation
Middle (?) to early Pliocene		Middle red formation

Modified from Lambert (1968, table 5)
[1] Names are informal

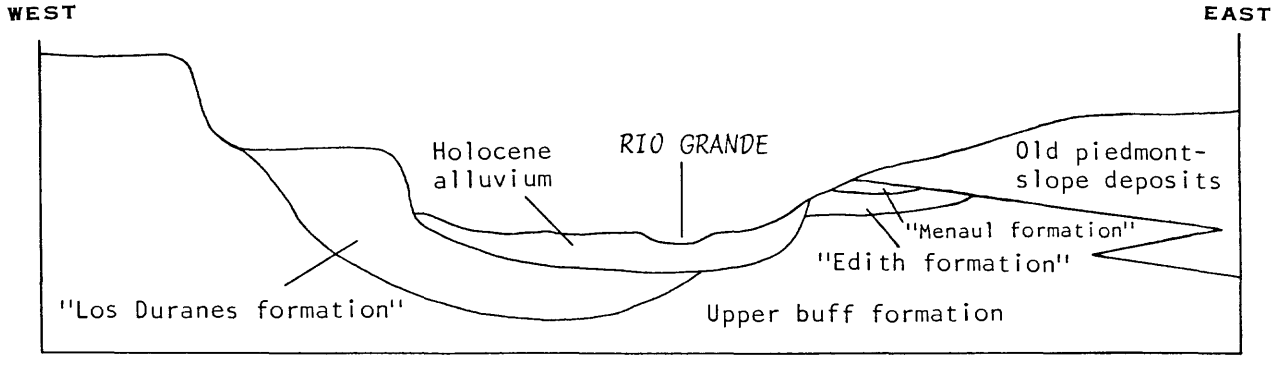

Modified from Lambert (1968, fig. 2)

Figure 7.--Schematic geologic section indicating relations between the upper part of the Santa Fe Group and overlying Holocene deposits.

Structural features on the northern boundary of the basin consist of the southern end of the Nacimiento uplift and the Jemez volcanic complex (fig. 2). The Nacimiento uplift is a Laramide uplift. Paleozoic sedimentary rocks dip eastward off the Nacimiento uplift under the Jemez volcanic complex. The Jemez volcanic complex consists of a large pile of Pliocene to Quaternary volcanic rocks that straddle the Rio Grande rift and the Nacimiento uplift (Woodward, 1982, p. 144).

The east border of the Albuquerque-Belen Basin consists of a north-trending fault-line scarp associated with the Sandia-Manzanita-Manzano Mountains and the Los Pinos Mountains (fig. 2). The Sandia-Manzanita-Manzano and Los Pinos Mountains consist of a west-facing core of Precambrian rocks and east-facing dip slopes of Paleozoic rocks. The Hubbell Bench trends parallel to the west-facing fault-line scarp of the Sandia-Manzanita-Manzano and Los Pinos Mountains (fig. 2 and pl. 1). The Hubbell Bench is 2 to 6 miles wide and 55 miles long (Kelley, 1982, p. 159). Rocks from Precambrian to the upper Tertiary Santa Fe Group are exposed along the bench (pl. 1). This bench has a significant effect on the ground-water flow system on the eastern side of the Albuquerque-Belen Basin.

The southern boundary of the Albuquerque-Belen Basin consists of the Los Pinos Mountains, Joyita Hills, and the Ladron Mountains (fig. 2). The Joyita Hills consist of outcrops of Precambrian, Paleozoic, and Mesozoic rocks with low topographic relief. Kelley (1982, p. 160) indicated that the Joyita Hills are the southernmost extent of the Hubbell Bench. The Ladron Mountains consist of Precambrian rocks with a west-facing dip slope of Paleozoic rocks. Sediments of the Santa Fe Group have been disturbed by uplift of the Ladron Mountains. Kelley (1977, p. 38) described the Ladron Precambrian mass as "...like a giant rivet driven up from below tacking down the southwest corner of the basin with the border."

There are many faults within the Albuquerque-Belen Basin, but the faults are difficult to recognize because of the unconsolidated nature of the Santa Fe Group and the undeformed sediments that cover many of them. The floor of the Rio Grande rift has considerable structural relief, as evidenced by the few deep oil-test wells and seismic work (Brown and others, 1980). The dip of the sediments (Santa Fe Group) in outcrop areas generally is less than 5°. The calculated thickness (based on gravity data) of the Santa Fe Group (Birch, 1980) is presented in figure 8.

Some major structural features in the basin are in the Ziana anticline, Belen fault, Monte Largo embayment, Apache graben, Sand Hill fault, and the large number of faults near Santa Ana Mesa (pl. 1). A more detailed discussion of the structure in the Albuquerque-Belen Basin may be found in Kelley (1977) and Brown and others (1980).

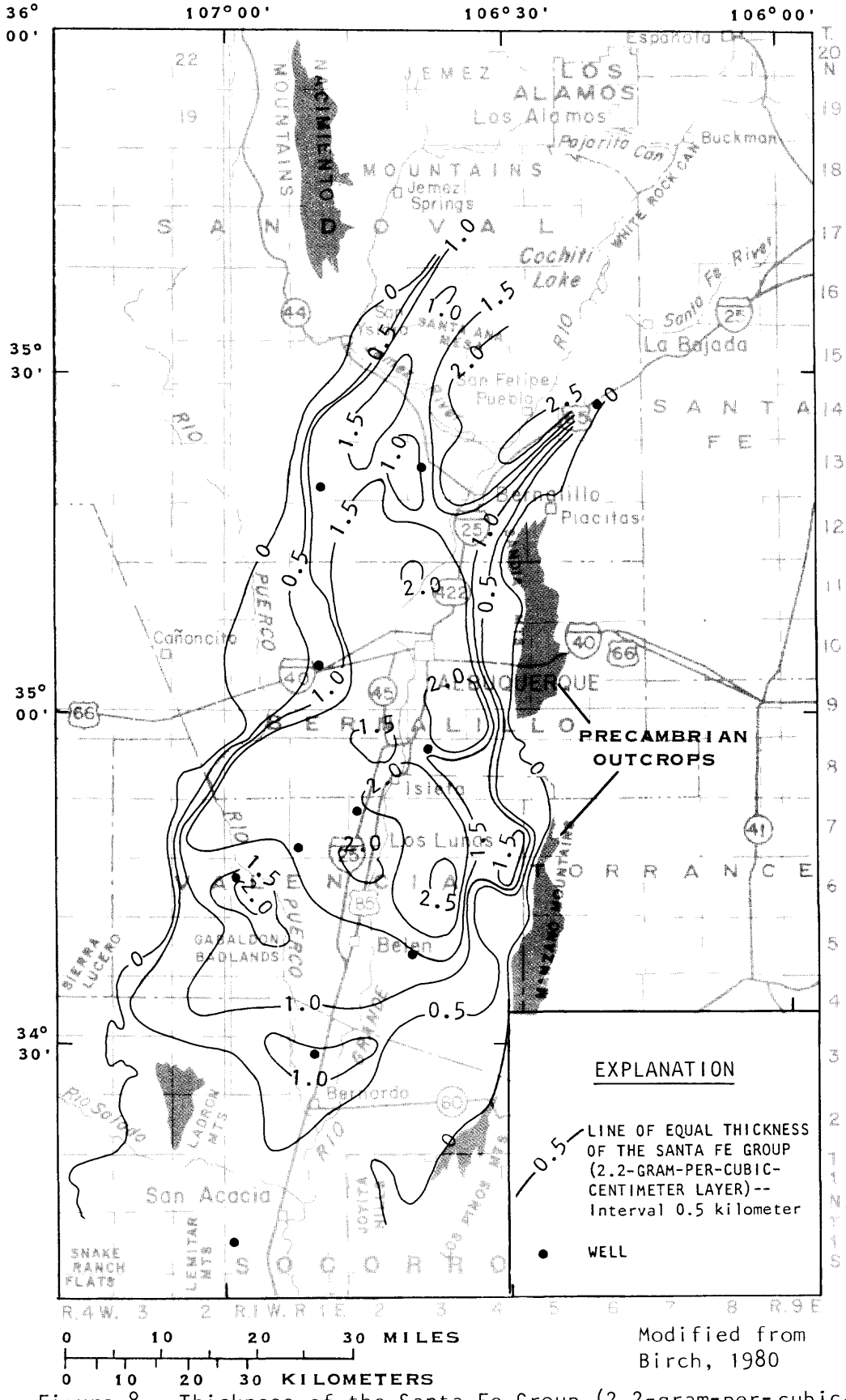

Figure 8.--Thickness of the Santa Fe Group (2.2-gram-per-cubic-centimeter layer).

GROUND-WATER FLOW SYSTEM

The Albuquerque-Belen Basin contains as much as 18,000 feet of basin-fill Tertiary and Quaternary Santa Fe Group to Holocene sediments. These sediments are considered to be the alluvial-basin aquifer, hereafter referred to as the aquifer. There is continuous recharge of ground water to and discharge of ground water from the aquifer, as indicated by the potentiometric-contour map (fig. 9).

Recharge

Recharge can have a significant effect on ground-water quality. In localized areas where there are large variations in ground-water quality, recharge commonly is a factor causing this variation.

Recharge to the aquifer in the Albuquerque-Belen Basin is due to six main processes (fig. 10):

1. Infiltration of surface water through river channels.
2. Infiltration of surface-water inflow from adjacent areas.
3. Direct recharge of precipitation.
4. Ground-water inflow from adjacent bedrock units.
5. Ground-water inflow from the Santo Domingo Basin.
6. Infiltration of excess irrigation water.

Infiltration of surface water through river channels is an important type of recharge to the aquifer. The Rio Grande is the main through-flowing drainage in the Albuquerque-Belen Basin. Since the 1930's, riverside drains along both sides of the river have controlled ground-water levels near the river. These drains maintain the water level below the level of the bottom of the river channel, thus the river loses water. Part of this lost water is recovered in the riverside drains, some of this water is used by vegetation along the river bank, and some recharges the aquifer. The quantity of this ground-water recharge was not calculated in this study because of the complex interaction between the riverside drains and the Rio Grande and because of the large errors inherent in evapotranspiration calculations.

The Jemez River, Rio Puerco, and Rio Salado are major drainages where channel infiltration is significant (fig. 10). J.D. Dewey (U.S. Geological Survey, written commun., 1980) calculated the recharge to the aquifer due to infiltration of surface water through river channels to be approximately 25,000 acre-feet per year for the Jemez River, 10,300 acre-feet per year for the Rio Puerco, and 13,000 acre-feet per year for the Rio Salado.

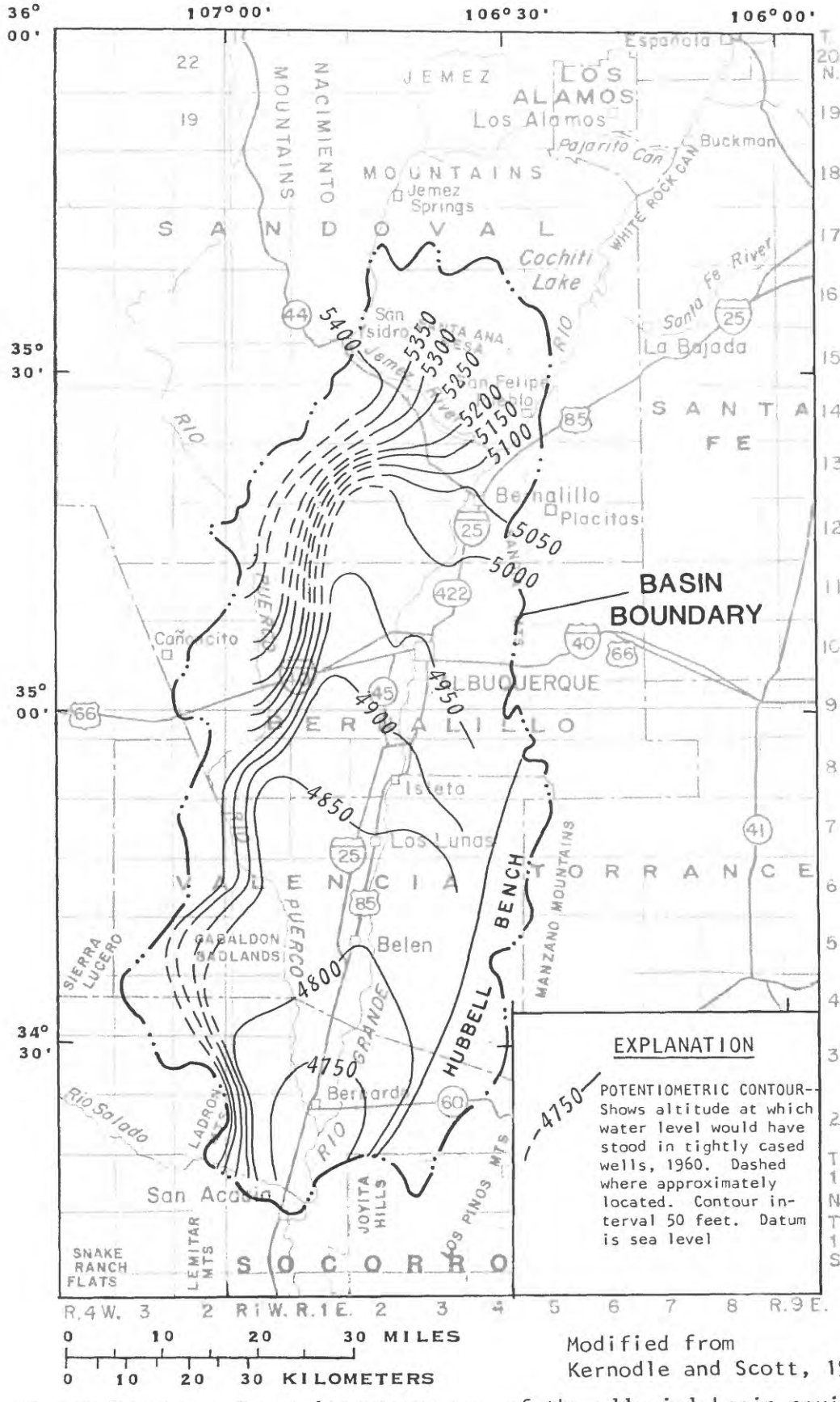

Modified from Kernodle and Scott, 1985

Figure 9.--Potentiometric-contour map of the alluvial-basin aquifer.

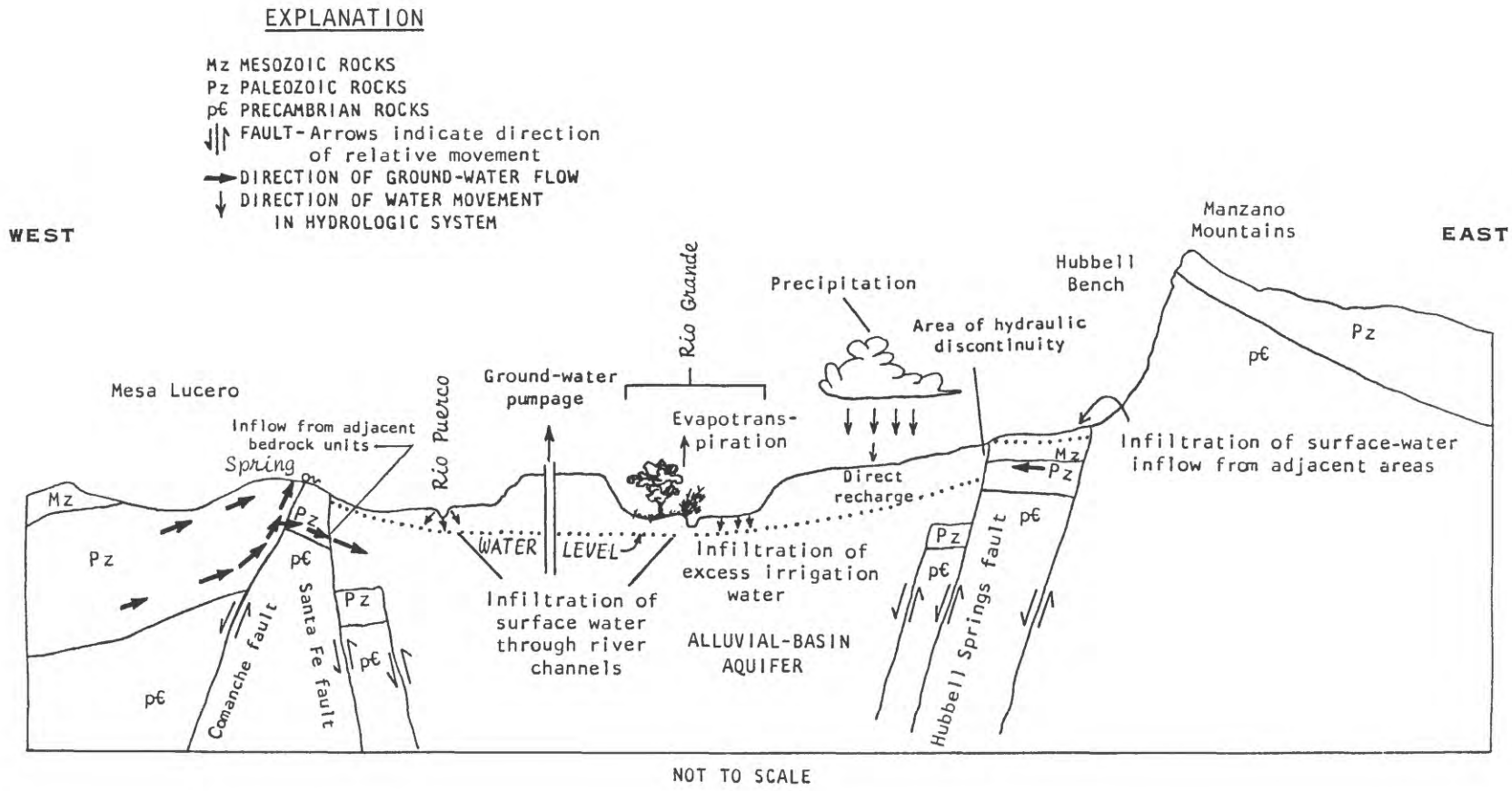

Figure 10.--Schematic geohydrologic section illustrating the hydrologic system.

Surface-water inflow from areas adjacent to the basin generally infiltrates and recharges the aquifer. Many areas bordering the basin are underlain by relatively impermeable rock, and flash floods from precipitation are common in these areas. The beds of ephemeral-stream channels in the basin consist of coarse-grained sediment, and water infiltrates rapidly through the channel beds after the channel enters the basin. The increase in infiltration after the channel enters the basin is demonstrated by a rapid decrease in channel width and depth after the channel enters the basin. Most ephemeral-stream channels do not have any clearly defined banks and beds that are continuous from the basin margins to the Rio Grande valley.

The calculated recharge to the aquifer along the basin margins and from the major drainages within the basin is summarized in figure 11. The total calculated recharge to the aquifer is approximately 128,700 acre-feet per year.

Direct recharge of precipitation or infiltration of precipitation within the basin also is a process resulting in recharge to the aquifer. A well-developed caliche is found in many areas of the basin. No direct recharge of precipitation is expected to occur through this caliche. In areas where sand dunes and permeable sediments are exposed, some direct recharge of precipitation probably occurs. Because of the minimal annual precipitation and the occurrence of most precipitation during the summer months when potential evapotranspiration is greatest, the quantity of direct recharge probably is small compared to the other recharge to the aquifer.

Inflow of ground water from adjacent bedrock units also recharges the aquifer. On the east side of the basin, the aquifer is in fault contact with Precambrian, Paleozoic, and Mesozoic rocks (fig. 10 and pl. 1). There are several springs along the fault between the Hubbell Bench and the main body of the aquifer. These springs indicate that ground water flows into the aquifer from the Paleozoic and Mesozoic rocks along the Hubbell Bench. The volume of flow probably is not large because of the small recharge area. On the west side of the basin, the aquifer also is in fault contact with Precambrian, Paleozoic, and Mesozoic rocks (fig. 10 and pl. 1). South of T. 8 N., the aquifer is in fault contact with Paleozoic rocks, and many springs and travertine deposits exist along the fault. In this area, recharge to the aquifer occurs due to inflow of ground water from the Paleozoic rocks. North of T. 8 N., the aquifer is in fault contact with Mesozoic rocks at the surface. A very thick section of permeable sediments is in fault contact with the aquifer north of T. 8 N. Very few hydrologic data exist for this area; thus, the direction or magnitude of ground-water inflow to or outflow from the aquifer can only be estimated. The presence of springs near Cañoncito and San Ysidro indicates the possibility of inflow of ground water to the aquifer along the entire western side of the Albuquerque-Belen Basin.

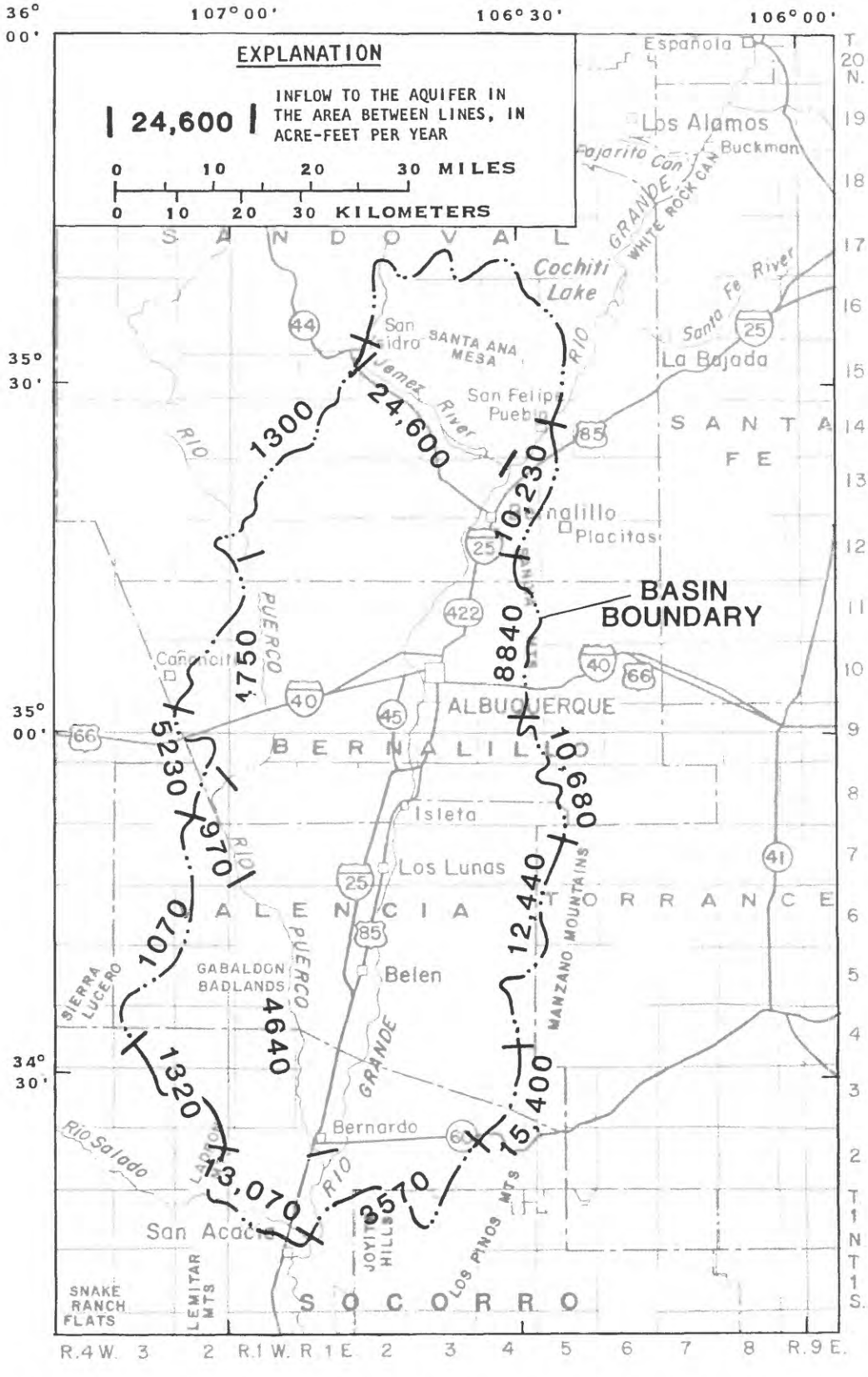

Figure 11.--Calculated recharge to the aquifer along the basin margins and major drainages.

At the north end of the Albuquerque-Belen Basin, the aquifer is in contact with Tertiary sediments and volcanic deposits. The hydraulic connection between the Jemez volcanic complex and the Albuquerque-Belen Basin is unknown. A water-level map by Titus (1961, p. 187) indicates that there is recharge or ground-water flow into the aquifer from the Jemez area. Trainer (1974, p. 344) suggested that ground water enters the aquifer from the Jemez area along Cañon de San Diego (pl. 1).

Potentiometric gradients indicate that ground water is recharging or entering the aquifer from the Santo Domingo Basin (figs. 1 and 9). This volume of ground-water recharge or inflow cannot be calculated because the cross-sectional area, permeability, and potentiometric gradients are not known. Along the southeast margin of the basin, the aquifer is in contact with Paleozoic limestone, sandstone, and shale. Spiegel (1955, p. 60) indicated that ground water flows from the Paleozoic rocks into the aquifer.

Recharge to the aquifer also occurs due to infiltration of excess irrigation water. Ground-water levels are maintained in the Rio Grande valley by a system of drains. These drains are constructed such that irrigation water that recharges the aquifer will not cause a permanent rise in water levels and waterlog fields but will flow to the drains. In areas where ground-water pumpage has lowered water levels below drain levels, excess irrigation water will recharge the aquifer.

Ground-Water Flow in the Aquifer

The potentiometric-contour map indicates that, in general, ground water flows from the basin margins toward the basin center and then southward in the Albuquerque-Belen Basin (fig. 9). The southward gradient near the Rio Grande is approximately the same as the gradient of the Rio Grande (5 feet per mile). Steep hydraulic gradients along the west margin of the basin are seen in the potentiometric-contour map (fig. 9). In many areas on the east side of the basin, there are hydraulic discontinuities, areas with large differences in water levels in short horizontal distances (fig. 10). These hydraulic discontinuities are due to structural benches along the basin margins. The Precambrian, Paleozoic, and Mesozoic rocks are not as permeable as the aquifer, thus water levels are much higher in areas where these rocks are close to the surface. The ground water maintains a steep gradient down to the water level in the main body of the aquifer after crossing the fault on the east side of the basin; this fault separates the main body of the aquifer and the relatively impermeable rocks that are overlain by a thin layer of the aquifer (fig. 10).

In the northern part of the basin, ground water flows southeastward parallel to the Jemez River (fig. 9). The gradients in this area are large compared to those near the center of the basin. Titus (1961, p. 186-189) was first to document a ground-water trough that is parallel to the Rio Grande (fig. 9). He noted that the axis of the trough coincides with the Rio Grande south of Belen but that north of Belen the axis of the trough is west of the Rio Grande. Ground water flows in the aquifer from the margins of the basin toward the trough. Titus (1961, p. 188) suggested that the trough is due to a

greater thickness of the aquifer (Santa Fe Group) or the greater permeability of the aquifer in this area than in other areas of the basin.

On a local scale, ground-water flow is dominated by the river, riverside drains, laterals, and drains (fig. 12) in the irrigated part of the Rio Grande valley. In general, the fields are sloped so that applied irrigation water will flow across the fields and into the drains. The farmers generally control the rate that they apply water so that most of the water infiltrates the fields and little or no applied water flows across the fields and into the drains. Part of the applied water that infiltrates into the ground is evapotranspired by crops and part of the water recharges the aquifer, causing water levels to rise under the fields. This rise in water levels causes ground water to flow toward the drains and to discharge into the drains (fig. 12). Ground water that flows into the drains flushes salts that were deposited by evapotranspiration from the soils, thus preventing the soils from becoming too salty for agricultural purposes. Water levels under irrigated areas of the Rio Grande valley fluctuate during the year because of infiltration of the applied irrigation water. On a year-to-year basis, however, the water levels do not change because they are controlled by the elevation of the bottom of the drains (fig. 12). This indicates that there is no change in ground-water storage in the irrigated part of the Rio Grande valley and that recharge due to irrigation is equal to ground-water discharge to the drains. In areas where ground-water pumpage has caused water levels to be lowered in the irrigated part of the Rio Grande valley, discharge from the aquifer to the drains is reduced, and there is a net recharge to the aquifer from irrigation practices.

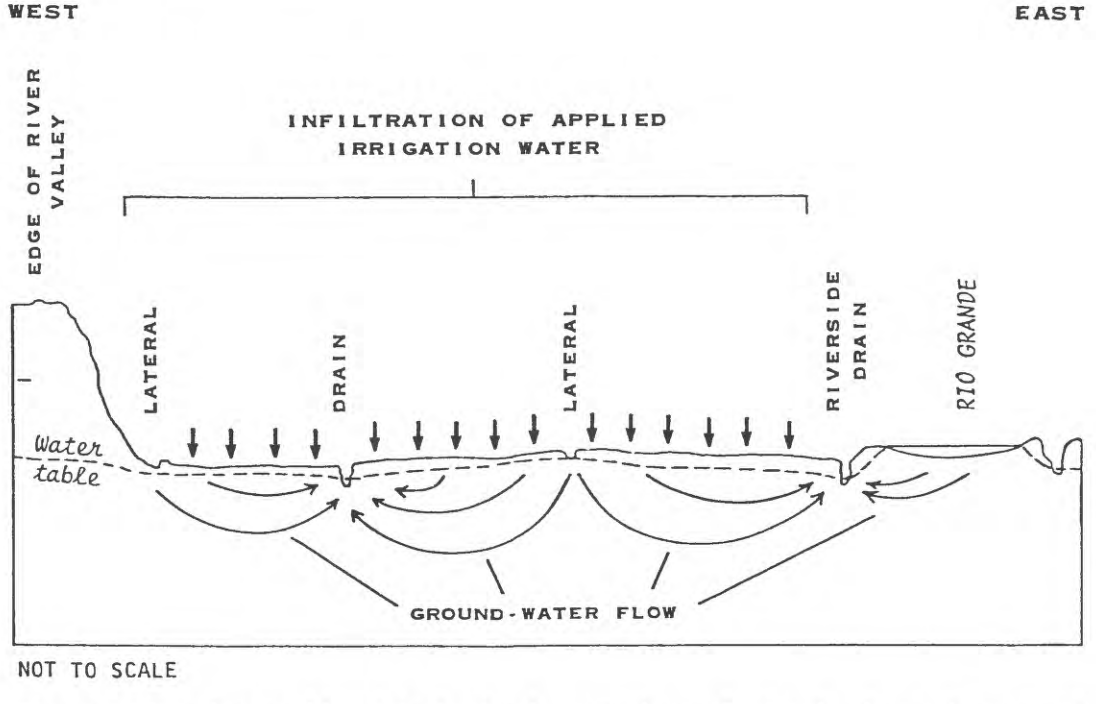

Figure 12.--Generalized hydrologic section of the irrigated part of the Rio Grande valley.

Discharge

Ground-water discharge from the aquifer is due to three main processes: (1) evapotranspiration, (2) ground-water outflow to the Socorro Basin, and (3) ground-water pumpage (fig. 10). Evapotranspiration probably is the major process of ground-water discharge from the Albuquerque-Belen Basin. The majority of evapotranspiration occurs in the Rio Grande valley. Although some evapotranspiration occurs along the Jemez River, Rio Puerco, and Rio Salado, the volume is negligible (J.D. Dewey, U.S. Geological Survey, written commun., 1980). J.D. Dewey (U.S. Geological Survey, written commun., 1980) estimated the evapotranspiration from the Rio Grande valley to be approximately 310,000 to 390,000 acre-feet per year.

The ground-water outflow from the Albuquerque-Belen Basin south to the Socorro Basin (fig. 1) cannot be calculated. The cross-sectional area, aquifer permeability, and potentiometric gradients are unknown.

Ground water is used for domestic, industrial, and stock-watering purposes and for irrigation when surface-water supplies are insufficient. The effect of pumpage for irrigation and stock watering on the ground-water flow system probably is negligible. Water pumped from storage for irrigation probably is replaced in following years by infiltration of excess irrigation water. The only areas where pumpage, primarily for domestic use, has a significant effect on the ground-water flow system is near Albuquerque, Belen, Bernalillo, and Los Lunas. The total ground-water production during 1977 for the area between Cochiti Lake and Bernardo was estimated to be 123,130 acre-feet (U.S. Army Corps of Engineers, 1979, p. 2-53). Most of this water was used by Albuquerque. Approximately one-half of the ground water pumped by Albuquerque is consumed, and approximately one-half is discharged into the Rio Grande as wastewater (James Smith, New Mexico State Engineer Office, oral commun., 1983).

SURFACE-WATER QUALITY

One of the main processes of recharge to the aquifer is infiltration of surface water through river channels. If the general water chemistry of this water is known, the way that it may affect the water chemistry in the aquifer may then be understood more clearly.

The four major river channels in the Albuquerque-Belen Basin are the Jemez River, the Rio Puerco, the Rio Salado, and the Rio Grande. Water-quality sampling stations have been established on each of these rivers (fig. 13). Mean, minimum, and maximum values of water-quality properties and constituents are listed for selected stations from September 1969 to August 1982 in table 2. The mean value for a given water-quality property or constituent was not calculated from the same number of measured values as other parameters. Generally, the specific-conductance and temperature data have the largest number of measurements at a particular station. The mean values are simple arithmetic averages of the measured values. Flow and time intervals were not weighted for the calculation. These mean, minimum, and maximum values are useful when comparing the general water quality of different stations.

The Jemez River enters the Albuquerque-Belen Basin near San Ysidro and flows into the Rio Grande near Bernalillo (fig. 13). Water in the Jemez River is derived mainly from the Jemez Mountains, and the river is perennial to approximately San Ysidro. Downstream from San Ysidro, the Jemez River is perennial only during years of greater-than-average precipitation.

The sampling station on the Jemez River is downstream from the Jemez Canyon Dam near Bernalillo (fig. 13). The mean specific conductance for the Jemez River at this station is 1,283 microsiemens (microsiemens per centimeter at 25 °Celsius). The standard deviation for specific conductance is 650 microsiemens, which is large relative to the mean and indicates that the chemistry of recharge water from the river varies considerably. Sodium is the dominant cation and sulfate and chloride are the dominant anions in water from the Jemez River (table 2).

The Rio Puerco enters the Albuquerque-Belen Basin on the northwestern side and flows approximately parallel to the basin border until it enters the Rio Grande near Bernardo (fig. 13). The mean specific conductance of water from the Rio Puerco near Bernardo is 2,047 microsiemens. The specific conductance ranges from 437 to 4,870 microsiemens, and the standard deviation is 821 microsiemens per centimeter (table 2). Calcium, sodium, and sulfate are the dominant ions in water from the Rio Puerco.

The Rio Salado enters the Albuquerque-Belen Basin near the southwest boundary and flows approximately parallel to the southern boundary until it enters the Rio Grande north of San Acacia (fig. 13). The specific conductance of water from the Rio Salado also varies considerably (table 2) and has a mean specific conductance of 1,670 microsiemens. Water from the Rio Salado contains large concentrations of dissolved sodium (mean of 204 milligrams per liter) and sulfate (mean of 432 milligrams per liter).

The large variation in the quality of water from the Rio Puerco and Rio Salado is caused by the rock type, distribution of rock type, and distribution of precipitation in each drainage basin. In many areas, gypsum-bearing rocks are exposed and are dissolved by precipitation. Runoff from these areas contains a relatively large dissolved-solids concentration. If precipitation occurs in an area where relatively impermeable and insoluble rocks crop out, the runoff would be expected to have a relatively small dissolved-solids concentration. A large volume of precipitation throughout the basin in a short time also may result in a large percentage of runoff and a relatively small dissolved-solids concentration. On the basis of the statistical data in table 2, the chemical characteristics of recharge water from the Rio Puerco and Rio Salado vary considerably.

Water-quality sampling stations on the Rio Grande are located at San Felipe, at Isleta, near Bernardo, and at San Acacia (fig. 13). The average specific conductance at San Felipe is 358 microsiemens, and the average specific conductance at San Acacia is 752 microsiemens. This increase in specific conductance is due to: (1) inflow of more mineralized water from the Jemez River, Rio Puerco, and Rio Salado; (2) return of excess irrigation water with increased salinity from the drainage canals; and (3) evapotranspiration that removes water and concentrates the salinity of shallow ground water.

Differences in the mean concentration of selected dissolved constituents between the stations on the Rio Grande at San Felipe and near Bernardo were calculated. These two stations have a large number of measurements with which to calculate the mean and are located on the Rio Grande close to the upstream and downstream margins of the basin (table 2 and fig. 13). The mean sodium concentration increased by 20.5 milligrams per liter and the mean calcium concentration increased by 12.7 milligrams per liter from San Felipe to near Bernardo (table 2). This represents approximately a twofold increase in the sodium concentration. The mean sulfate concentration increased by 35.1 milligrams per liter, the mean chloride concentration increased by 14.4 milligrams per liter, and the mean alkalinity concentration increased by 31.5 milligrams per liter (table 2). The mean chloride concentration near Bernardo is 3.3 times the mean chloride concentration at San Felipe (table 2).

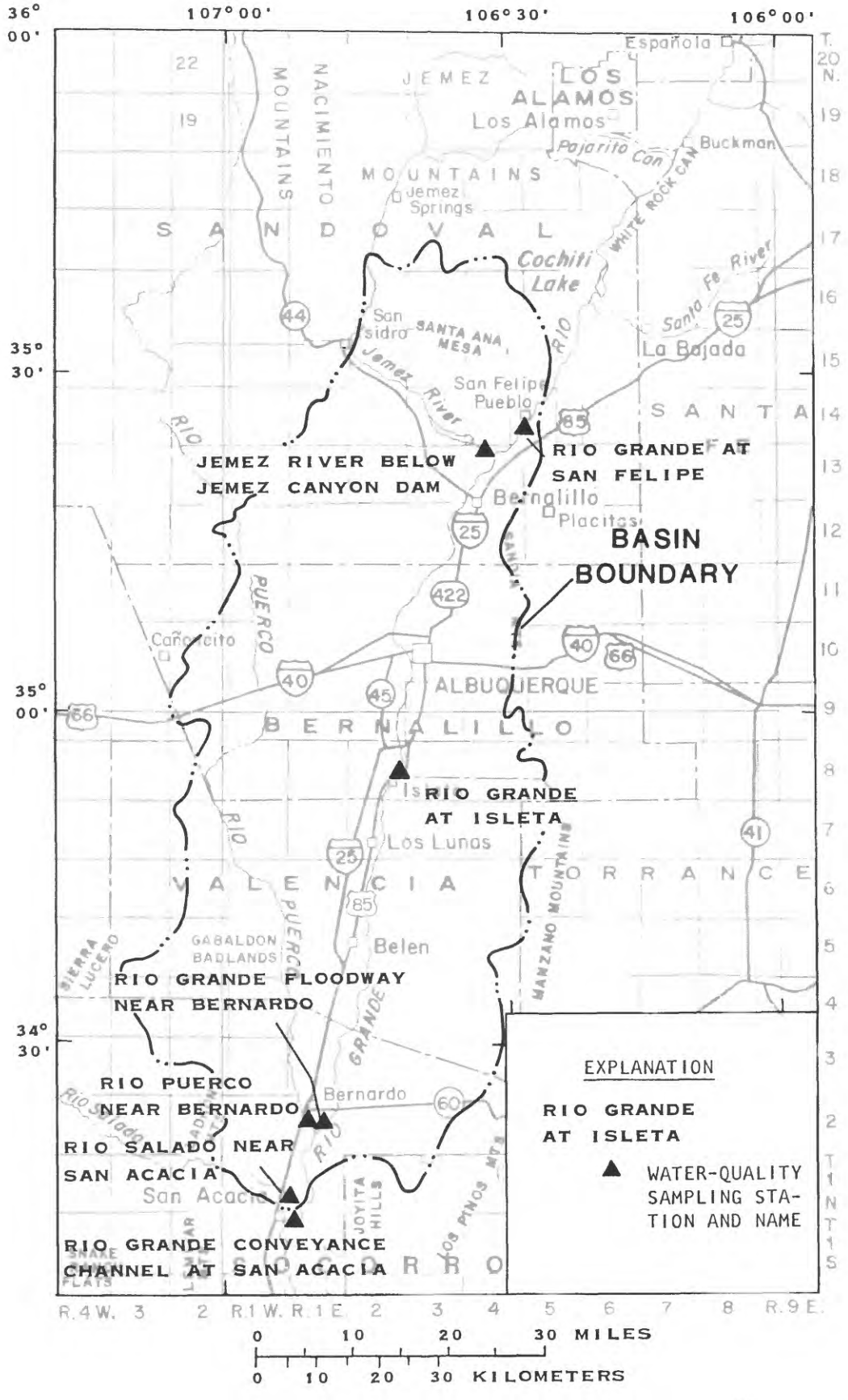

Figure 13.--Location of major rivers and water-quality sampling stations.

Table 2. Surface-water-quality data for selected sites, September 1969 to August 1982

[mg/L, milligrams per liter]

Type of data	Number of measurements	Mean	Standard deviation	Minimum	Maximum
08319000 Rio Grande at San Felipe, New Mexico					
Specific conductance (microsiemens per centimeter at 25 °Celsius)	85	357.6	65.4	173.0	510.0
Temperature (degrees Celsius)	121	11.8	6.4	.9	24.9
Calcium, dissolved (mg/L as Ca)	74	41.4	8.2	22.0	59.9
Magnesium, dissolved (mg/L as Mg)	74	7.2	1.5	3.5	10.0
Sodium, dissolved (mg/L as Na)	74	21.1	5.9	4.5	34.0
Sodium + potassium, dissolved (mg/L as Na)	8	19.3	4.1	12.0	26.0
Sulfate, dissolved (mg/L as SO_4)	74	63.7	18.9	27.0	110.0
Chloride, dissolved (mg/L as Cl)	75	6.2	2.0	2.3	13.0
Alkalinity, field (mg/L as $CaCO_3$)	65	105.9	22.7	57.0	142.0
Dissolved solids, residue at 180 °Celsius (mg/L)	63	228.5	46.9	125.0	320.9
Dissolved solids, sum of constituents (mg/L)	69	225.6	47.6	115.0	314.0
08329000 Jemez River below Jemez Canyon Dam, New Mexico					
Specific conductance (microsiemens per centimeter at 25 °Celsius)	210	1,283.2	650.5	174.0	4,700.0
Temperature (degrees Celsius)	226	11.3	7.8	.0	32.5
Calcium, dissolved (mg/L as Ca)	109	72.3	42.7	28.0	334.9
Magnesium, dissolved (mg/L as Mg)	109	9.8	5.4	2.7	35.9
Sodium, dissolved (mg/L as Na)	104	192.1	115.7	26.0	770.0
Sodium + potassium, dissolved (mg/L as Na)	15	215.4	88.7	46.0	380.0
Sulfate, dissolved (mg/L as SO_4)	108	215.5	199.5	27.0	1,500.0
Chloride, dissolved (mg/L as Cl)	128	178.1	102.7	19.0	610.0
Alkalinity, field (mg/L as $CaCO_3$)	105	196.2	65.0	70.0	417.0
Dissolved solids, residue at 180 °Celsius (mg/L)	11	661.5	384.8	214.0	1,290.0
Dissolved solids, sum of constituents (mg/L)	107	815.8	471.6	179.0	3,390.0

Table 2. Surface-water-quality data for selected sites, September 1969 to August 1982 - Continued

Type of data	Number of measurements	Mean	Standard deviation	Minimum	Maximum
08331000 Rio Grande at Isleta, New Mexico					
Specific conductance (microsiemens per centimeter at 25 °Celsius)	119	463.4	104.2	220.0	720.0
Temperature (degrees Celsius)	122	15.5	6.7	1.0	27.4
Calcium, dissolved (mg/L as Ca)	96	47.9	10.1	23.0	74.0
Magnesium, dissolved (mg/L as Mg)	96	7.7	1.5	4.0	11.0
Sodium, dissolved (mg/L as Na)	96	33.5	9.7	9.9	56.0
Sodium + potassium, dissolved (mg/L as Na)	11	29.2	9.3	13.0	41.0
Sulfate, dissolved (mg/L as SO_4)	96	80.0	23.0	27.0	160.0
Chloride, dissolved (mg/L as Cl)	96	17.2	6.6	3.1	34.0
Alkalinity, field (mg/L as $CaCO_3$)	87	121.5	23.5	62.0	183.0
Dissolved solids, residue at 180 °Celsius (mg/L)	87	291.5	65.3	132.0	429.0
Dissolved solids, sum of constituents (mg/L)	94	290.6	65.6	123.0	435.0
08332010 Rio Grande Floodway near Bernardo, New Mexico					
Specific conductance (microsiemens per centimeter at 25 °Celsius)	130	520.4	127.3	224.0	900.9
Temperature (degrees Celsius)	244	12.8	7.1	.0	31.0
Calcium, dissolved (mg/L as Ca)	119	54.1	15.8	.0	130.0
Magnesium, dissolved (mg/L as Mg)	119	8.7	2.2	.0	16.0
Sodium, dissolved (mg/L as Na)	109	41.6	14.2	.0	94.0
Sodium + potassium, dissolved (mg/L as Na)	23	40.4	13.3	20.0	73.9
Sulfate, dissolved (mg/L as SO_4)	120	98.8	39.5	34.0	310.0
Chloride, dissolved (mg/L as Cl)	120	20.6	8.4	2.9	46.0
Alkalinity, field (mg/L as $CaCO_3$)	114	137.4	30.6	54.0	236.0
Dissolved solids, residue at 180 °Celsius (mg/L)	17	346.1	90.8	190.0	513.0
Dissolved solids, sum of constituents (mg/L)	119	338.6	90.9	112.0	589.9

Table 2. Surface-water-quality data for selected sites, September 1969 to August 1982 - Continued

Type of data	Number of measurements	Mean	Standard deviation	Minimum	Maximum
08353000 Rio Puerco near Bernardo, New Mexico					
Specific conductance (microsiemens per centimeter at 25 °Celsius	240	2,047.4	820.9	437.0	4,870.0
Temperature (degrees Celsius)	173	18.6	6.5	.0	30.9
Calcium, dissolved (mg/L as Ca)	234	176.0	83.6	27.0	47.0
Magnesium, dissolved (mg/L as Mg)	233	38.7	19.8	4.2	98.0
Sodium, dissolved (mg/L as Na)	201	254.6	125.1	41.0	780.0
Sodium + potassium, dissolved (mg/L as Na)	48	249.4	109.6	86.9	688.9
Sulfate, dissolved (mg/L as SO_4)	233	838.7	422.4	86.0	2,269.9
Chloride, dissolved (mg/L as Cl)	233	87.5	70.7	20.0	500.0
Alkalinity, field (mg/L as $CaCO_3$)	231	164.1	48.3	1.0	353.0
Dissolved solids, residue at 180 °Celsius (mg/L)	12	1,519.1	647.4	754.0	2,710.0
Dissolved solids, sum of constituents (mg/L)	231	1,512.8	680.5	258.0	3,779.9
08354000 Rio Salado near San Acacia, New Mexico					
Specific conductance (microsiemens per centimeter at 25 °Celsius	54	1,670.5	941.3	275.0	5,230.0
Temperature (degrees Celsius)	88	22.7	5.1	10.9	31.9
Calcium, dissolved (mg/L as Ca)	53	138.9	63.2	19.0	370.0
Magnesium, dissolved (mg/L as Mg)	53	30.2	16.6	3.2	88.0
Sodium, dissolved (mg/L as Na)	46	203.8	153.8	29.0	860.0
Sodium + potassium, dissolved (mg/L as Na)	7	165.9	116.8	47.9	380.0
Sulfate, dissolved (mg/L as SO_4)	51	431.7	258.8	35.0	1,500.0
Chloride, dissolved (mg/L as Cl)	52	158.0	196.2	17.9	1,000.0
Alkalinity, field (mg/L as $CaCO_3$)	51	231.3	79.9	91.0	428.0
Dissolved solids, residue at 180 °Celsius (mg/L)	5	1,130.2	709.8	127.0	1,970.0
Dissolved solids, sum of constituents (mg/L)	49	1,102.2	639.9	171.0	3,430.0

Table 2. Surface-water-quality data for selected sites, September 1969 to August 1982 - Concluded

Type of data	Number of measurements	Mean	Standard deviation	Minimum	Maximum
08354800 Rio Grande Conveyance Channel at San Acacia, New Mexico					
Specific conductance (microsiemens per centimeter at 25 °Celsius)	75	751.5	421.1	256.0	3,209.9
Temperature (degrees Celsius)	301	15.7	7.4	.0	28.9
Calcium, dissolved (mg/L as Ca)	5	125.9	148.9	53.0	391.9
Magnesium, dissolved (mg/L as Mg)	5	20.5	22.7	8.9	60.9
Sodium, dissolved (mg/L as Na)	5	107.5	113.4	44.0	308.9
Sodium + potassium, dissolved (mg/L as Na)	0	—	—	—	—
Sulfate, dissolved (mg/L as SO_4)	4	117.5	29.8	90.0	160.0
Chloride, dissolved (mg/L as Cl)	4	29.2	9.5	19.0	42.0
Alkalinity, field (mg/L as $CaCO_3$)	1	177.0	—	177.0	177.0
Dissolved solids, residue at 180 °Celsius (mg/L)	1	2,699.9	—	2,699.9	2,699.9
Dissolved solids, sum of constituents (mg/L)	4	400.0	85.5	331.0	525.0

GROUND-WATER GEOCHEMISTRY

One purpose of this study was to define the areal distribution of different water qualities. An examination of the available chemical analyses of ground water indicated that there is a paucity of trace-metal data and that most major-ion data are from wells completed in the upper 400 feet of the aquifer. Because of the small amount of data, the water-quality part of the study was limited to the major dissolved ions in the upper part of the aquifer; no attempt was made to examine the distribution of trace metals. Changes in ground-water chemistry with time also were not examined because of a lack of data.

When this study began, very few ground-water-quality data and well-completion data were stored in the U.S. Geological Survey Water-Data Storage and Retrieval System (WATSTORE), a system of computer files containing hydrologic data. The water-quality file for surface water and ground water and the ground-water site-inventory (GWSI) file are parts of that system. The first step of this study was to enter previously collected data into the WATSTORE system. An initial examination of the distribution of data in the updated WATSTORE file indicated that more data needed to be collected in some areas. Therefore, in the summer of 1980, data were collected where possible in areas where few data were available, and the new data were added to the WATSTORE system. All data for the Albuquerque-Belen Basin were retrieved and stored in a computer file.

In most areas, the density of data was sparse, and all available water-quality data from any site were used. For areas with dense data, the data were sorted, and representative analyses were selected. The sorting of this data involved a step-by-step process to use only the most complete and accurate data (fig. 14). The data were first plotted on a map to examine data density. The second step consisted of checking to see if a particular sample had been analyzed for major ions (is analysis complete?). If the analysis was complete, the anion-cation balance was checked. The analysis was eliminated if the balance had an error of 5 percent or greater. The next step was to examine the well-completion data; wells that did not have any completion data were eliminated. Wells that sampled very deep parts of the aquifer (deep exploratory oil-test wells) and wells that sampled shallow parts of the aquifer known to be affected by irrigation practices were eliminated because samples from these wells are not representative of the general water quality of the area. Multiple analyses (well sampled at several different times) were examined for any significant changes in water chemistry with time. If there were significant changes, only the first sample analyzed was used and all other samples were eliminated. Changes in water chemistry may indicate some type of stress on the system, and the purpose of this study was to examine relatively unstressed distributions of water quality. If there were still many analyses for an area, a representative analysis was selected.

After the data set was sorted and the density of wells was considered to be adequate, the data were plotted on maps. These areal plots were used to examine patterns in water chemistry.

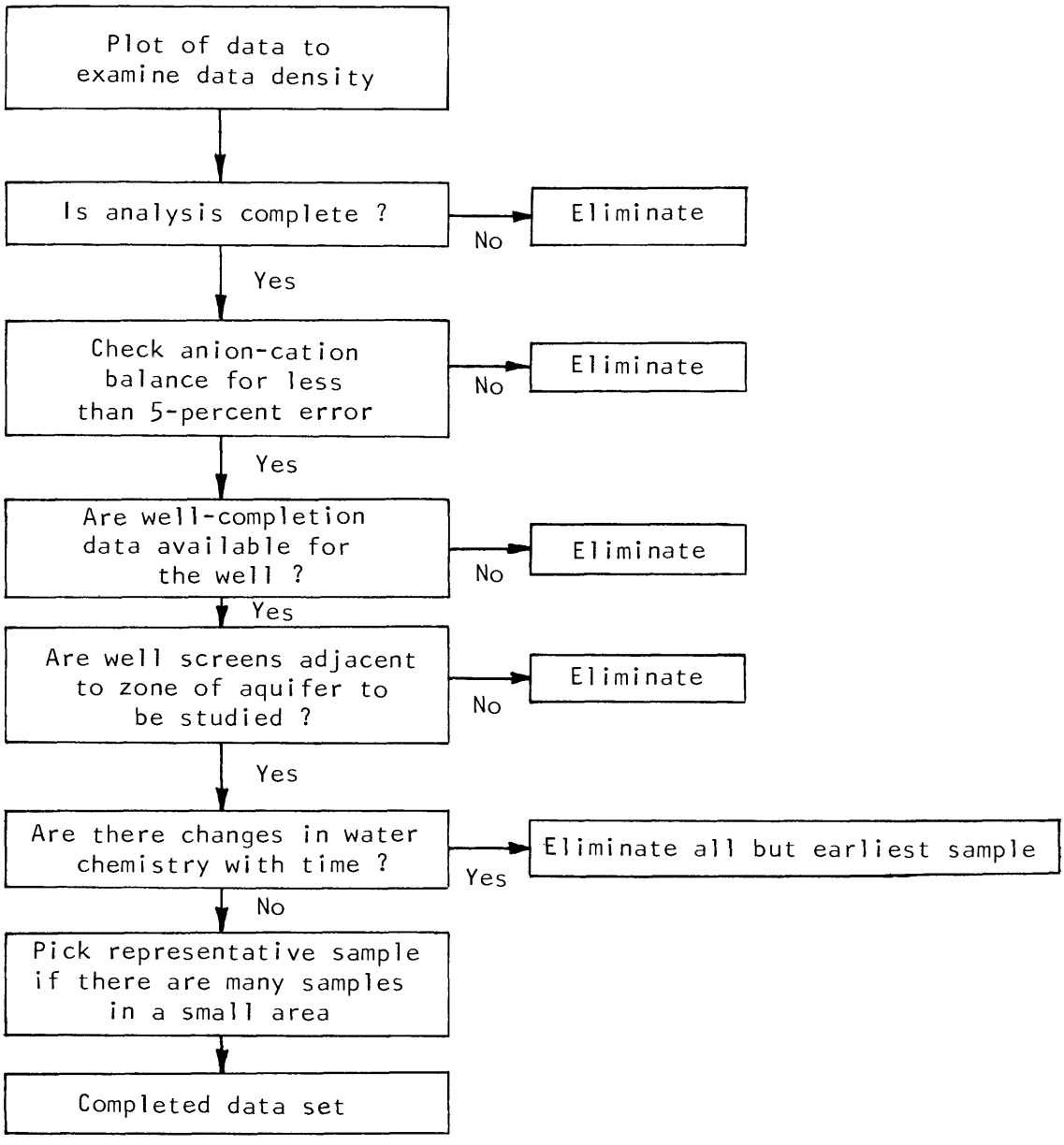

Figure 14.--Flow chart showing the method used to sort the water-quality data set for areas with a high density of data.

This study of the geochemistry of ground water in the Albuquerque-Belen Basin involved the use of many different methods of evaluating and interpreting the data. The methods that were the most helpful and beneficial are described below.

Piper diagrams (Piper, 1944) are useful aids when examining the differences in water quality of many samples. One water analysis is represented by three points on a Piper diagram (fig. 15). The point in the left triangle represents the percentage of the total milliequivalents per liter (meq/l) of the major cations: sodium plus potassium, magnesium, and calcium. The right triangle represents the percentage of the total milliequivalents per liter of the major anions: bicarbonate plus carbonate, chloride, and sulfate. The diamond-shaped field is used to represent the overall composition of the water with respect to ion concentration. The point in the diamond-shaped field is at the intersection of the rays projected from the points in the cation and anion triangular fields (fig. 15). For water that has a density approximately equal to 1 gram per cubic centimeter, the concentration, in milliequivalents per liter, of a specific ion is calculated with the following equation:

$$\text{meq/l} = \frac{\text{concentration of ion in milligrams per liter x valence of ion}}{\text{molecular weight of ion}} \quad (1)$$

The percentage of total milliequivalents per liter of a particular anion is calculated with the following equation:

$$\text{percentage of total meq/l of anions} = \frac{\text{meq/l of the particular anion x 100}}{\text{total meq/l of anions}} \quad (2)$$

The same equation is used for the cations with the substitution of the particular cation and the total milliequivalents per liter of cations. The calculation of the milliequivalent percentages and the plot of the analysis are demonstrated by the example in figure 15. In the discussion of water quality, any reference to percentage is with respect to the Piper diagram; thus, the percentage is percentage of total milliequivalents per liter of the major cations or anions.

The Piper diagram is useful but limited when comparing water with large differences in dissolved solids. This is due to the calculation of percentages of total milliequivalents per liter, which has the effect of normalizing the relative concentrations. For example, a water with a dissolved-solids concentration of 500 milligrams per liter and a water with a dissolved-solids concentration of 30,000 milligrams per liter will plot as the same point on a Piper diagram if they both have the same ionic-percentage composition.

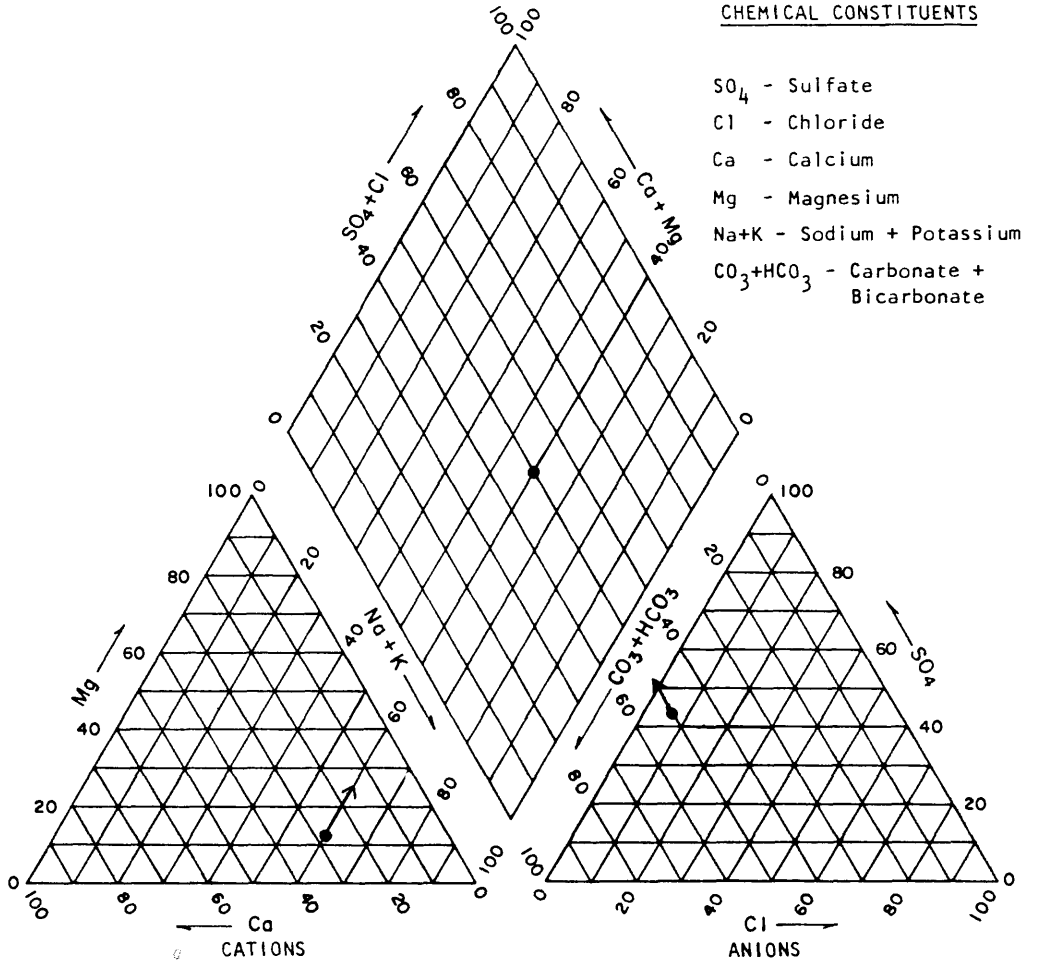

PERCENTAGE OF TOTAL IONS, IN MILLIEQUIVALENTS PER LITER

DISSOLVED ION	CONCENTRATION (milligrams per liter)	CONCENTRATION (milliequivalents per liter)	PERCENT CATION OR ANIONS
Calcium	27	1.35	28
Magnesium	7	.57	12
Sodium plus potassium	66	2.87	60
Chloride	12	.34	7
Sulfate	96	2.0	43
Carbonate	0	.0	
Bicarbonate	140	2.3	50

Total milliequivalents per liter for cations = 4.79

Total milliequivalents per liter for anions = 4.64

Figure 15.--Sample Piper diagram and example of calculations used to plot a data point on the diagram.

A computer program called WATEQF (Plummer and others, 1978) is used in the discussion of water quality to examine the saturation state of the ground water with respect to specific minerals. WATEQF models the thermodynamic speciation of inorganic ions in solution for a given water analysis. WATEQF (Plummer and others, 1978) also calculates the saturation index (SI) for minerals with the following equation:

$$SI = \log \left(\frac{\text{ion-activity product for the mineral-water reaction}}{\text{equilibrium constant of a particular mineral}} \right) \quad (3)$$

If the SI is greater than 0, the water is supersaturated with respect to the particular mineral. If the SI is less than 0, the water is subsaturated with respect to the particular mineral.

The chemical composition of ground water in the aquifer generally does not increase in dissolved constituents downgradient or down a flow line. In many areas, there are large differences in the chemical composition of ground water in a relatively short distance. Ground water downgradient from several of the basin margins has less dissolved constituents than ground water near the basin margins. The general lack of a pattern in ground-water chemistry down a flow line or a well-defined evolution of ground water in the aquifer may indicate that recharge has a dominant effect on the chemical composition of ground water. Because the ground-water system is not a closed system, mass-balance calculations between individual wells were not appropriate. As an alternative to mass-balance calculations between individual wells, some water-quality data were examined assuming that all dissolved species were derived from chemical weathering of minerals in the aquifer or adjacent areas. Garrels and MacKenzie (1971, p. 135-173) discussed this method and called it a "material balance." This method is useful when examining water-quality data because the relative contributions of dissolved constituents through chemical processes that result in a specific water chemistry can easily be examined. The method also is useful to test if the chemical processes proposed adequately describe the chemical nature of the ground water.

The chemical processes used in the material-balance model need to be consistent with the mineralogy of the aquifer and surrounding areas. WATEQF (Plummer and others, 1978) and other chemical-speciation programs can be used to examine chemical-equilibrium relations between the ground water and specific minerals in the aquifer system.

On the basis of geology and examination of results of many WATEQF (Plummer and others, 1978) runs, six major chemical processes were used to explain the chemical evolution of water in the Albuquerque-Belen Basin. These processes are as follows: dissolution or precipitation of calcite; dissolution of dolomite; dissolution or precipitation of halite; dissolution of gypsum; alteration of plagioclase to calcium montmorillonite; and cation exchange (calcium exchanged for sodium on clay minerals). These processes probably are not the only processes that affect the chemical composition of ground water in the Albuquerque-Belen Basin, but they probably are the major processes that can be represented in the model. The reasoning used to arrive at these processes is discussed after the description of the material-balance model.

The material-balance model was used to examine water analyses and to define the most dominant chemical processes. This model examines the sodium, calcium, magnesium, bicarbonate, sulfate, chloride, and silica ions. The model is based on the assumption that precipitation, a major source of recharge, virtually is distilled water that reacts with minerals, resulting in the ground-water chemistry observed in the aquifer. The model stepwise removes (subtracts) dissolved species from water corresponding to the ratios determined by the assumed reactions and in effect calculates the number of mmoles (millimoles) of each mineral dissolved to replicate a specific water analysis.

A simple flow chart of the material-balance model and a sample calculation are presented in figure 16. The model first calculates the concentration, in mmoles, of each dissolved constituent. Chloride is removed from the water, assuming a sodium to chloride ratio of 1:1 representing the dissolution of halite. Generally, there is a net excess of dissolved sodium after chloride is removed. Magnesium and a part of the calcium and bicarbonate are removed next. This step represents dissolution of dolomite with a magnesium to calcium to bicarbonate ratio of 1:1:4. Sulfate and some calcium are removed next from the solution. This reaction represents the dissolution of gypsum with a sulfate to calcium ratio of 1:1 for this reaction. The alteration of plagioclase feldspar to calcium montmorillonite is the next reaction modeled. All of the silica is removed from solution in this step, along with part of the sodium, calcium, and bicarbonate. The sodium to calcium to silica to bicarbonate ratio for this reaction is 0.85:0.38:0.61:1.62. Bicarbonate is the next constituent removed from solution. If the calculated bicarbonate concentration at this step is positive, bicarbonate is removed along with part of the calcium to represent the dissolution of calcite. If the calculated concentration of bicarbonate is negative, it is assumed that calcite has precipitated from solution at some point in the evolution of the water because it is not possible to have a negative concentration. If this is the case, the negative concentration of bicarbonate calculated by the model is added to the solution to zero the bicarbonate concentration. Calcium is added to the solution to represent the calcite precipitation at a calcium to bicarbonate ratio of 1:2.

At this point in the model calculations, all of the chloride, magnesium, sulfate, silica, and bicarbonate have been removed from a particular water analysis (fig. 16). The remaining constituents in the water are sodium and generally a negative concentration of calcium. The next reaction modeled is cation exchange, whereby one calcium ion is removed from solution (exchanged to a clay surface) and two sodium ions are released into solution. To model this reaction, the calculated calcium concentration, which generally is negative at this point in the model, is added to the calculated sodium concentration. The resulting value is referred to as the excess (fig. 16). A positive value represents excess sodium unaccounted for in the water. A negative value represents an excess of calcium in the system. Because magnesium, bicarbonate, and sulfate are "zeroed" out at the expense of calcium, the input or output to the system of these constituents, at a ratio different than the assumed ratios by any mechanism other than the mechanisms used in the model, will result in an excess.

FLOW CHART

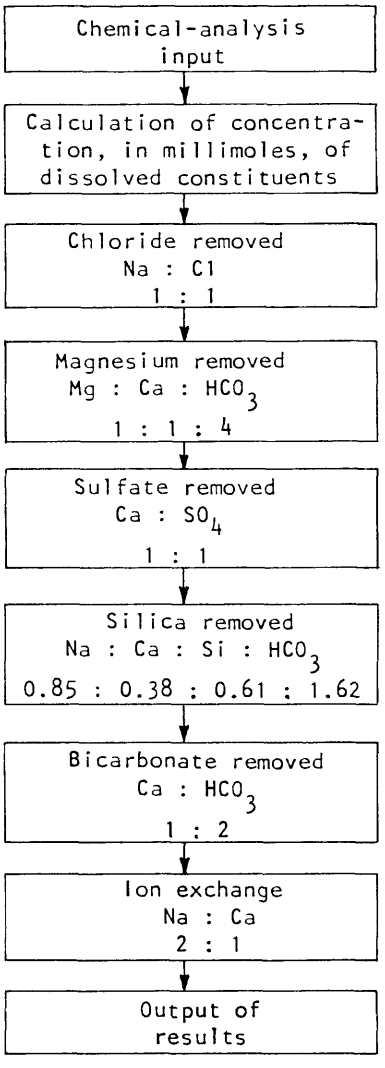

RESULTS OF SAMPLE CALCULATION

Constituent	Initial concentration (millimoles)	Chloride removed (millimoles)	Magnesium removed (millimoles)	Sulfate removed (millimoles)	Silica removed (millimoles)	Bicarbonate removed (millimoles)	Ion exchange (millimoles)
Sodium (Na)	1.48	1.25	1.25	1.25	0.51	0.51	0.03
Chloride (Cl)	.23	0	0	0	0	0	0
Magnesium (Mg)	.25	.25	0	0	0	0	0
Calcium (Ca)	.57	.57	.33	−.20	−.54	−.24	0
Bicarbonate (HCO_3)	1.80	1.80	.82	.82	.60	0	0
Sulfate (SO_4)	.53	.53	.53	0	0	0	0
Silica (Si)	.53	.53	.53	.53	0	0	0

Figure 16.--Flow chart of material-balance model and results of sample calculation.

The assumptions that the dissolution of calcite, dolomite, and gypsum and the precipitation of calcite are major geochemical processes occurring in the basin are based on physical evidence and chemical-speciation calculations. Many of the sediments in the Albuquerque-Belen Basin have calcite cement, and beds of gypsum also occur in the sediments. The presence of limestone, dolomite, and gypsum beds in rocks bordering the aquifer suggests that calcite, dolomite, and gypsum are disseminated in the principal reservoir because the sediment matrix of the aquifer was in part derived from these rocks. The presence of calcite, dolomite, and gypsum in samples from the aquifer was documented by whole-rock X-ray analysis (Anderholm, 1985). Chemical-speciation calculations using WATEQF (Plummer and others, 1978) indicate that, in many cases, ground water is in equilibrium with calcite or dolomite or both and, in some cases, in equilibrium with gypsum. The chemical-speciation calculations do not prove that the dissolution or precipitation of these minerals is occurring, but the calculations, in conjunction with documentation that these minerals are present in the aquifer, strongly suggest that these chemical processes are occurring.

The material-balance-model step of removing sodium and chloride assuming dissolution of halite may not be a true representation of the chemical processes occurring because large deposits of halite are not found near or within the basin. Chloride concentrations in ground water probably result from solution of fluid inclusions in igneous rocks or mineral grains, dissolution of disseminated halite in marine sedimentary deposits in areas adjacent to the basin, and infiltration of surface water from runoff due to precipitation. The sodium to chloride ratio for precipitation in the study area is approximately 1:1. The assumption of halite dissolution was used in the model for simplicity because of the 1:1 ratio of sodium to chloride in the mineral halite. This does not, however, imply that all chloride in a particular water is the result of the dissolution of halite.

There probably are many silicate mineral-alteration reactions occurring in the basin. The silica concentrations generally increase from the basin margins toward the basin center and usually are less than 40 milligrams per liter (fig. 17). Plagioclase and orthoclase were the most abundant silicate minerals detected by whole-rock X-ray analysis of samples from the aquifer (Anderholm, 1985). Calcium montmorillonite was the most abundant clay mineral detected by X-ray analysis of the clay fraction of samples from the aquifer (Anderholm, 1985). Potassium was not included in the material-balance model because of the large number of samples that were not analyzed for potassium and because of the small potassium concentrations in ground water. The alteration of orthoclase to kaolinite was not included in the material-balance model because dissolved potassium is a product of this reaction and potassium was not included in the model.

The alteration of plagioclase to calcium montmorillonite was assumed to be the only source of dissolved silica in the material-balance model. The composition of the plagioclase used in the model is not based on any analytical data of plagioclase compositions in the Albuquerque-Belen Basin, but is the plagioclase composition used by Garrels and MacKenzie (1967) in their material-balance analysis of spring water from the Sierra Nevada.

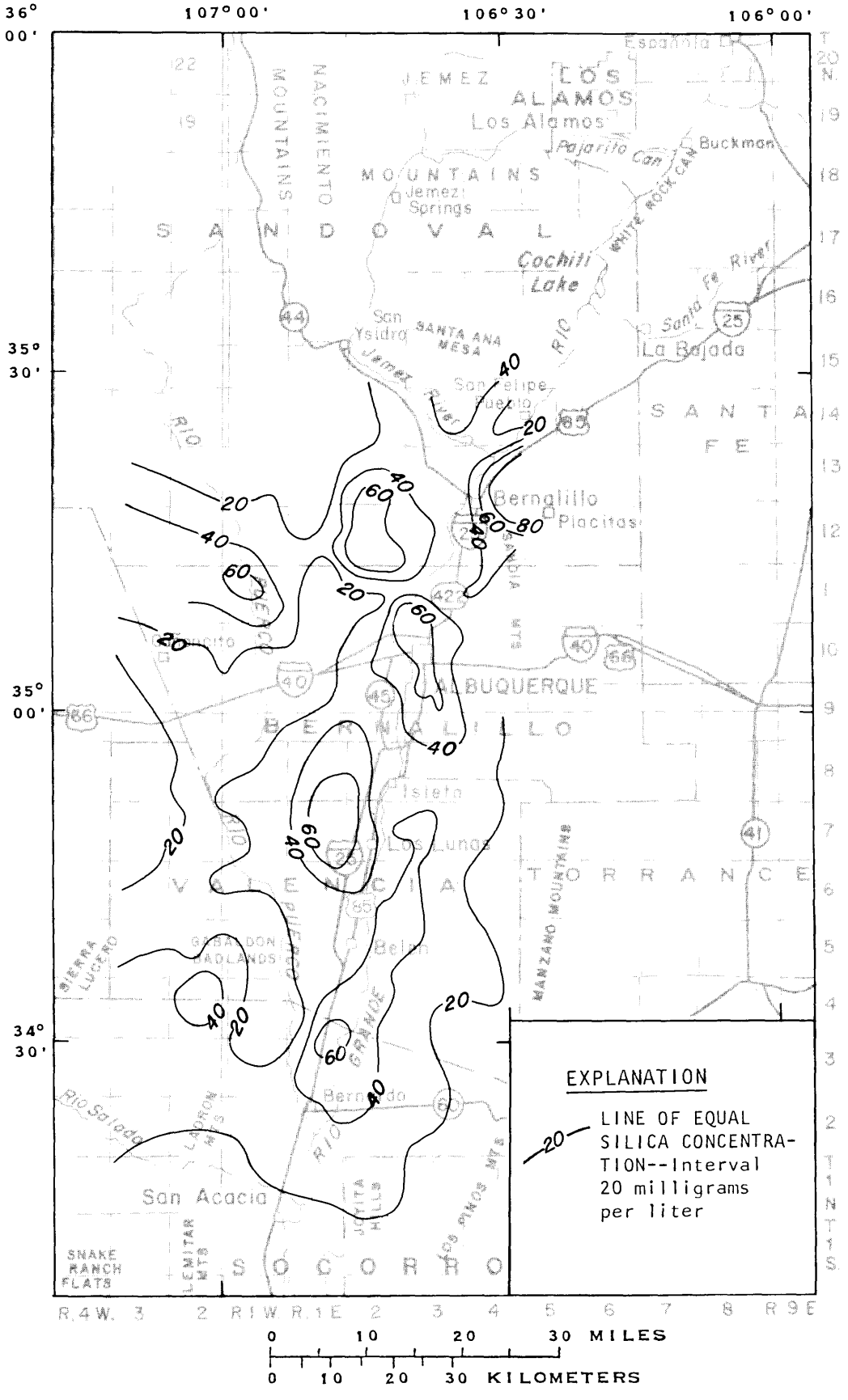

Figure 17.--Silica concentrations in ground water.

The alteration of volcanic glass may be another source of dissolved silica in the Albuquerque-Belen Basin. A large part of the aquifer material probably is derived from volcanic rocks that contain volcanic glass. No attempt was made to include the alteration of volcanic glass in the material-balance model. In cases where there is a calculated, seemingly anomalous concentration of dissolved constituents after the removal of silica in the model, the alteration of volcanic glass may be a significant reaction.

The sediments in the aquifer generally are composed of a mixture of sand, silt, and clay. The presence of clay with generally large ion-exchange capacities was documented by X-ray defraction of samples from the aquifer (Anderholm, 1985).

Other chemical processes may be taking place in the system with the same ratios as those proposed in the model. The model results, however, would not change. For example, the weathering of albite to kaolinite can be written:

$$2NaAlSi_3O_8 + 2CO_2 + 11H_2O = Al_2Si_2O_5(OH)_4 + 2Na^+ + 2HCO_3^- + 4H_4SiO4 \quad (4)$$

This reaction would input sodium and bicarbonate into the system. If the water affected by this reaction were modeled, an abundance of sodium after the removal of chloride would result. There would be a negative concentration of calcium when bicarbonate was removed. But because the ratio of sodium to bicarbonate for the feldspar reaction is 2:2, the calcium bicarbonate (calcite) reaction ratio is 1:2, and the ion-exchange reaction of sodium to calcium is 2:1. This reaction is completely masked in the model. Errors also would result if the calcium to magnesium ratio in dolomites that dissolve were not 1:1 and if the ratio of calcium to sodium in the plagioclase-alteration reaction were not the same as plagioclase in the aquifer.

The Albuquerque-Belen Basin was divided into four areas to aid in the discussion of the ground-water quality. The divisions were based on the geology, ground-water flow system, and ground-water quality or chemical processes of an area.

The discussion of each area begins with a description of the boundaries and the flow system in the area. This is followed by a discussion of the chemical nature of the recharge water to the area and the general chemical nature of ground water. In some cases, the chemical nature of ground water in an area is complex and the available data are sparse. Because of the complex nature of the geochemistry in some areas, processes affecting quality of water from individual wells are discussed. Where similar processes affect large parts of an area (groups of wells), the water quality is discussed on a regional scale. When processes are discussed that affect water from an individual well, estimates cannot be made as to the extent of the area affected by these processes.

Southeastern Area

The southeastern area is bounded on the east and south by the Los Pinos Mountains and the Joyita Hills (pl. 2). The Joyita Hills and part of the Los Pinos Mountains consist of Paleozoic and Mesozoic rocks (pl. 1). The Paleozoic rocks contain gypsum; thus, much of the water entering the basin from these areas may have been in contact with gypsum-bearing rocks. Gypsum also probably would be found in sediments of the aquifer in this area. The northern boundary of the area is the approximate northern extent of ground water in the aquifer that is affected by the chemistry of recharge water from Abo Arroyo (pl. 2). Recharge water from Abo Arroyo is derived from Paleozoic and Mesozoic rocks, whereas recharge water north of Abo Arroyo is derived mainly from Precambrian rocks. The western boundary of this area is the Rio Grande.

Major recharge to the southeastern area occurs as infiltration of surface-water and ground-water inflow from the adjacent areas. Ground water in this area flows northwestward and westward toward the Rio Grande (Spiegel, 1955, pl. 2).

Recharge

Wells 1N.2E.15.223 and 3N.4E.28.244 are near the southeastern basin boundary adjacent to Paleozoic and Mesozoic rocks. Calcium and sulfate are the dominant ions in water from the wells (table 3). The chemical composition of water from these wells is similar and probably represents the general chemical composition of recharge water from Paleozoic and Mesozoic terrane. The material-balance model indicates that there is a negative concentration of bicarbonate after the magnesium is removed from the analysis and that the sulfate concentrations are relatively large (table 4). The negative concentration of bicarbonate probably indicates that calcite has precipitated from the ground water, which probably is caused by the dissolution of gypsum. As gypsum dissolves, the calcium concentration increases, causing calcite saturation and precipitation of calcite. The calcite that has precipitated, as calculated by the material-balance model, is equal to one-half the bicarbonate after removal of silica (table 4). A negative value in the column "Bicarbonate after silica removal" indicates calcite precipitation, and a positive value indicates calcite dissolution.

Well 2N.3E.28.221 is near the basin boundary but adjacent to Precambrian rocks. Water from this well also represents recharge water, but this water has a smaller specific conductance and a larger percentage of bicarbonate than does the other recharge water (fig. 18 and table 3). The differences in specific conductance and percentage of bicarbonate in recharge water are due to the rock type in the area from which the water is derived. Water derived from Precambrian terrane does not come into contact with the same proportion of soluble minerals as water derived from the Paleozoic and Mesozoic terrane; thus, recharge water from Precambrian terrane generally has a smaller value of specific conductance than does recharge water from Paleozoic and Mesozoic terrane. The model indicates that water from well 1N.2E.15.223 and well 3N.4E.28.244 dissolved 5.42 and 8.65 mmoles of gypsum, respectively, whereas water from well 2N.3E.28.221 dissolved only 0.61 mmole of gypsum (table 4, under sulfate).

Ground Water Downgradient from Recharge Areas

The majority of ground water downgradient from the recharge areas has a specific conductance of approximately 1,100 microsiemens; sulfate is the dominant anion, and the percentage of calcium plus magnesium is greater than 65 (table 3 and fig. 18). The specific conductance of ground water downgradient from the recharge area is smaller than the specific conductance of ground water in the recharge area, which is derived from Paleozoic and Mesozoic rocks (table 3). This may indicate that recharge derived from Paleozoic and Mesozoic rocks mixes with other recharge that has a relatively small specific conductance. Examination of the material-balance-model results indicates that, in general, there is a negative concentration of bicarbonate after removal of silica (table 4). This may mean that calcite has precipitated from the water, which may be caused by increases in the calcium concentration resulting from dissolution of gypsum. Gypsum dissolution is a significant reaction in the evolution of ground water in this area, as evidenced by the relatively large sulfate concentrations in the material-balance-model results (table 4). The material-balance-model results also indicate that ion exchange is an important process in the evolution of ground water in this area, as indicated by the negative calcium concentration after the removal of silica (table 4).

Mixture of Upward-Moving Ground Water and Local Ground Water

The chloride concentration of water from well 3N.2E.33.222 is 1,100 milligrams per liter, which is very large for this area (table 3). This well is close to a rift-zone boundary fault (southern extension of Hubbell Springs fault (pl. 1). The chloride concentration in water from two other wells in this area, 3N.2E.31.431 and 3N.2E.27.123, also is relatively large compared to that in other ground water in the southeastern area (fig. 19 and table 3). Well 3N.2E.31.431 is downgradient from well 3N.2E.33.222 (fig. 19). Well 3N.2E.27.123 is northeast of well 3N.2E.33.222 and approximately the same distance downgradient from the rift-zone boundary faults (fig. 19). The large chloride concentration in water from these wells probably is due to the mixing of ground water with large chloride concentrations moving upward along the rift-zone boundary faults and ground water moving downgradient from the recharge area. The upward movement of ground water with large chloride concentrations probably is localized because water from other wells east of the rift-zone boundary faults does not have chloride concentrations as large as that of water from well 3N.2E.33.222 (fig. 19). The volume of ground water with large chloride concentrations moving upward along the rift-zone boundary faults also probably is small because of the large decrease in chloride concentration in water from wells 3N.2E.33.222 and 3N.2E.31.431 (fig. 19).

Ground water in the southeastern area generally has a common chemical evolution. The material-balance model indicates that in all but one case, when silica is removed, there is a deficit of bicarbonate. This may be due to precipitation of calcite while gypsum dissolves (table 4). The conceptual chemical evolution of ground water in the southeastern area is as follows: (1) dissolution of dolomite and calcite, (2) dissolution of gypsum and the precipitation of calcite due to the common ion effect, and (3) continual ion exchange. Water from wells 1N.2E.15.223 and 3N.4E.28.244, which probably represents water that has just entered the aquifer, has negative concentrations of bicarbonate after removal of silica. This indicates that dissolution of calcite and dolomite probably does not occur in the aquifer and that these minerals are precipitated within the aquifer as cementing materials.

Conclusions

The available data indicate that the quality of ground-water recharge along the Los Pinos Mountains and Joyita Hills is of two types. One type contains a large percentage of calcium and sulfate. The other type generally has a small specific conductance; bicarbonate is the dominant anion and no cation is dominant.

The specific conductance of water in the aquifer in the southeastern area generally is in the range of 1,000 to 1,200 microsiemens, and calcium and sulfate generally are the dominant ions. Some ion exchange occurs in the area, which is indicated by the large range in the percentage of calcium in the ground water. There seems to be some upward-moving ground water with a large chloride concentration near the rift-zone boundary faults. The extent and volume of upward-moving water probably are not large, as evidenced by the lack of a large plume of ground water with large chloride concentrations.

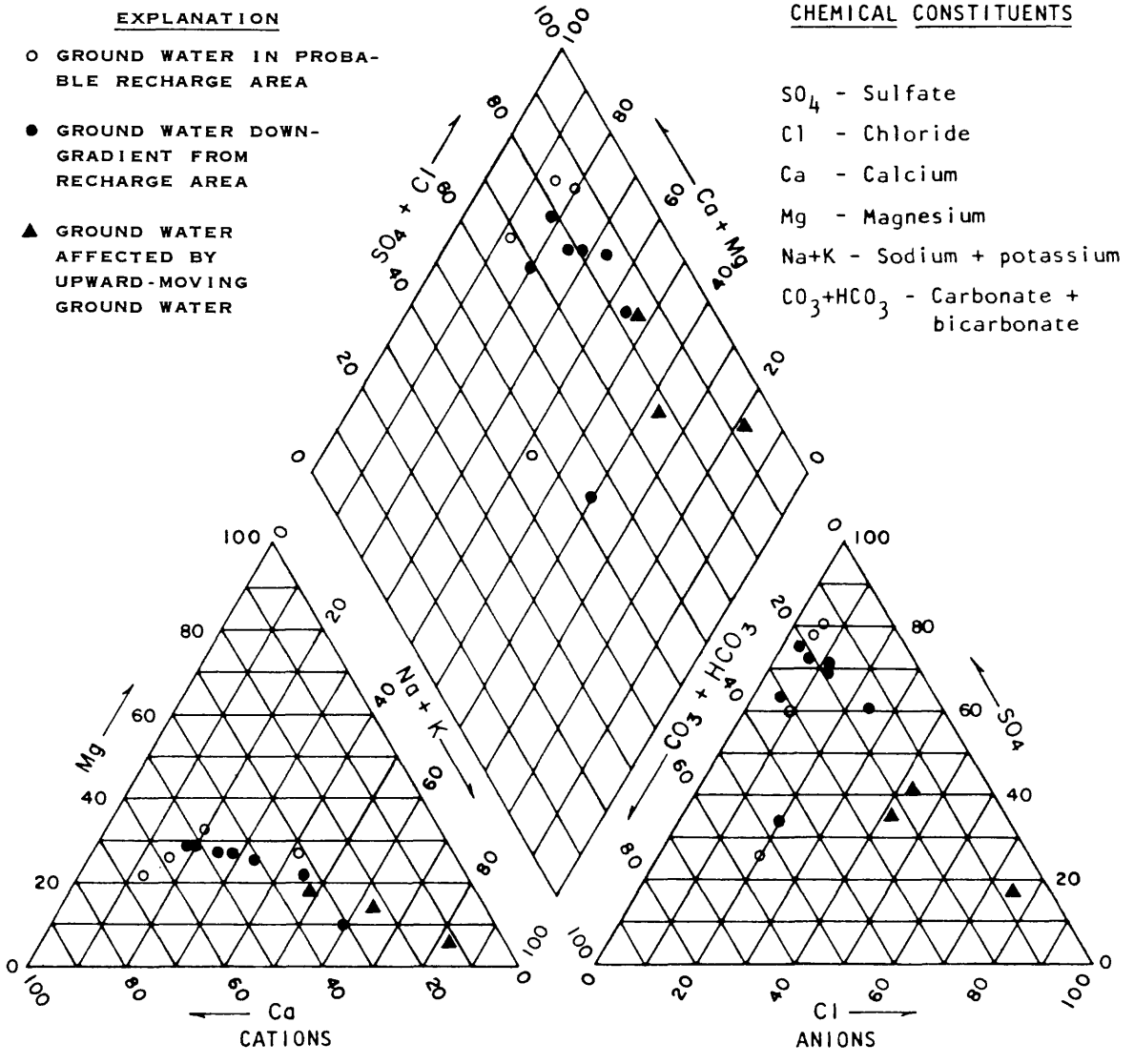

Figure 18.--Piper diagram of selected water analyses in the southeastern area.

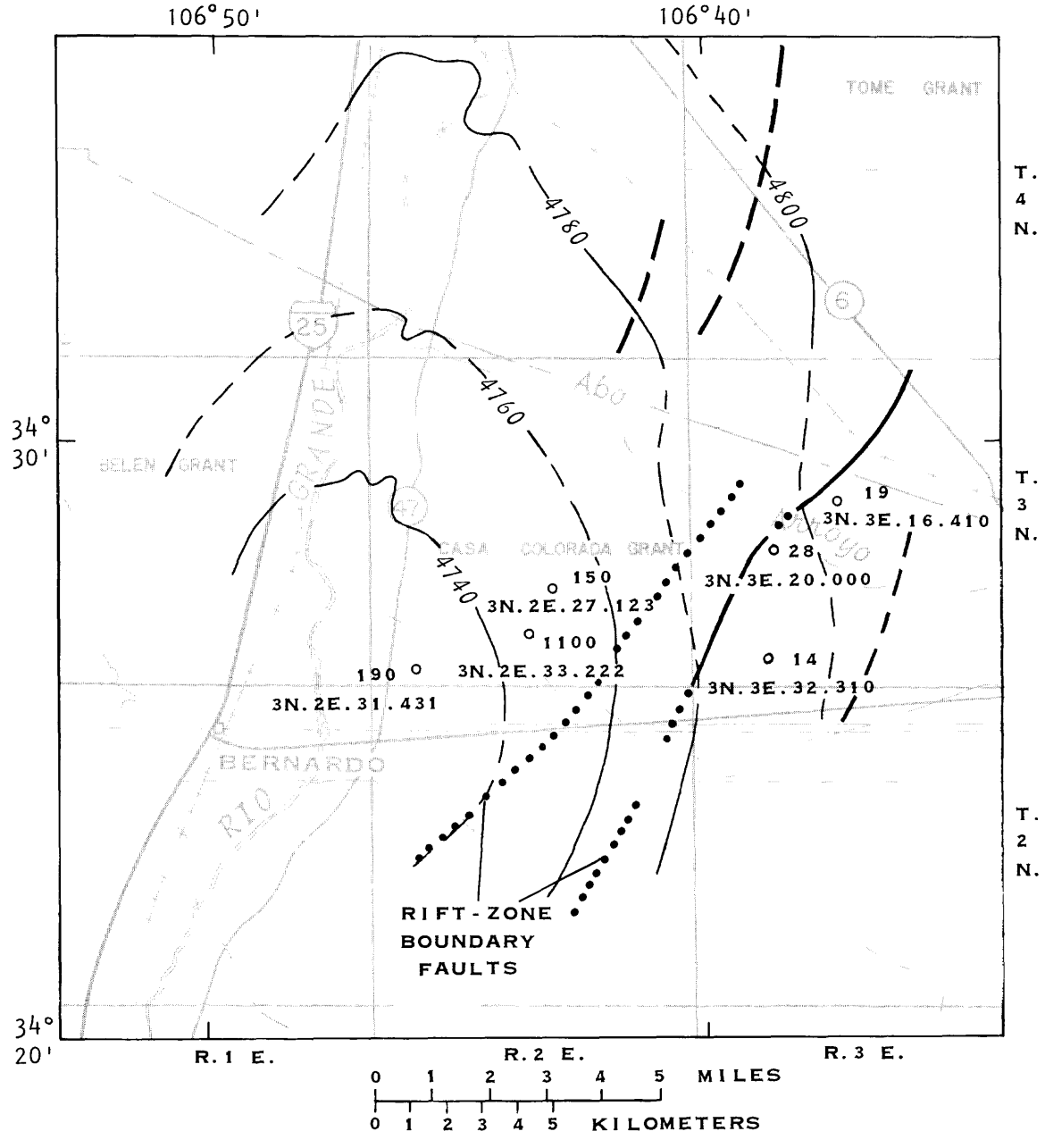

EXPLANATION

FAULT--Dashed where approximately located, dotted where concealed. From Kelley, 1977

4740 — POTENTIOMETRIC CONTOUR--Shows altitude at which water level would have stood in tightly cased wells, 1949-50. Dashed where approximately located. Contour interval 20 feet. Datum is sea level. From Spiegel, 1955

o 190
3N.2E.31.431 — WELL--Upper number is concentration of chloride, in milligrams per liter. Lower number is well number

Figure 19.--Location of wells in the southeastern area that have water with large chloride concentrations.

Table 3. Ground-water-quality data for selected sites in the southeastern area

[Well depth, asterisk (*) indicates water level, in feet below land surface; ft, feet; °C, degrees Celsius; mg/L, milligrams per liter]

Location	Date sampled	Well depth (ft)	Temperature (°C)	Specific conductance (microsiemens per centimeter at 25 °C)	pH	Calcium (mg/L)	Magnesium (mg/L)	Sodium (mg/L)	Sodium plus potassium (mg/L as sodium)	Potassium (mg/L)	Bicarbonate (mg/L)	Carbonate (mg/L)	Sulfate (mg/L)	Chloride (mg/L)	Fluoride (mg/L)	Silica (mg/L)	Dissolved solids (mg/L)
							Recharge water										
1N.2E.15.223	1-24-50	—	18.0	1,360	—	180	49.0	—	53	—	140	0	520	24	0.5	24	—
3N.4E.28.244	5-30-80	192	15.5	1,550	7.3	200	82.0	96	—	2.0	180	0	830	45	.8	16	—
2N.3E.28.221	5- 4-76	—	—	466	7.9	30	16.0	45	—	3.0	158	0	59	34	2.3	17	—
							Mixture of upward-moving ground water and local ground water										
3N.2E.31.431	6-11-80	135	22.5	1,150	8.3	84	27.0	120	—	27.0	120	0	240	190	1.4	56	—
3N.2E.33.222	5-30-80	320	17.5	3,400	7.6	98	31.0	770	—	9.0	180	0	330	1,100	2.9	30	—
3N.2E.27.123	5-30-80	380	17.0	975	7.9	48	17.0	140	—	22.0	140	0	170	150	1.7	44	—
							Ground water downgradient from recharge areas										
1N.1E. 2.113	1-25-50	116 *	19.5	677	—	90	18.0	20	27	—	130	0	200	23	0.3	28	—
2N.2E.30.34	1-25-50	270 *	20.3	1,130	—	77	32.0	—	120	—	120	0	390	42	2.0	24	—
2N.1E.23.323	1-25-50	27 *	—	1,070	—	88	35.0	—	84	—	99	0	310	94	1.0	27	—
2N.2E.17.000	12- 1-49	—	—	1,040	—	100	38.0	—	74	—	130	0	380	48	—	—	—
3N.3E.32.310	8-20-49	388	20.7	1,080	7.8	110	40.0	65	—	3.0	150	0	420	14	.9	27	—
3N.3E.20.000	12- 1-49	380	—	1,100	—	130	45.0	—	52	—	160	0	440	28	—	—	—
3N.2E.19.200	5-13-65	65	—	433	7.6	26	5.0	57	—	—	119	0	67	29	1.0	44	288
3N.3E.16.410	12- 1-49	400	19.0	834	—	94	33.0	—	42	—	170	0	280	19	—	—	—

Table 4. Material-balance-model results for selected ground-water analyses in the southeastern area

Location	Sodium (Na^+) (milli-moles)	Chloride (Cl^-) (milli-moles)	Magnesium (Mg^{2+}) (milli-moles)	Calcium (Ca^{2+}) (milli-moles)	Bicarbonate (HCO_3^-) (milli-moles)	Sulfate (SO_4^-) (milli-moles)	Silica (Si) (milli-moles)	Sodium (Na+) after chloride removal (milli-moles)	Calcium (Ca^{2+}) after magnesium removal (milli-moles)	Bicarbonate (HCO_3) after magnesium removal (milli-moles)	Calcium (Ca^{2+}) after sulfate removal (milli-moles)	Calcium (Ca^{2+}) after silica removal (milli-moles)	Bicarbonate (HCO_3) after silica removal (milli-moles)	Sodium (Na^+) after silica removal (milli-moles)	Calcium (Ca^{2+}) after bicarbonate removal (milli-(moles)	Excess sodium (Na^+) (milli-moles)
Recharge water																
1N.2E.15.223	2.31	0.68	2.02	4.49	2.30	5.42	0.40	1.63	2.48	-5.77	-2.94	-3.19	-6.83	1.07	0.22	0.76
3N.4E.28.244	4.18	1.27	3.37	4.99	2.95	8.65	.27	2.91	1.62	-10.54	-7.03	-7.20	-11.25	2.5	-1.57	-.30
2N.3E.28.221	1.96	.96	.66	.75	2.59	.61	.28	1.00	.09	-.04	-.52	-.70	-.79	.60	-.30	-.00
Ground water downgradient from recharge areas																
1N.1E. 2.113	0.87	0.65	0.74	2.25	2.13	2.08	0.47	0.22	1.51	-0.83	-0.58	-0.87	-2.07	-0.43	0.17	-0.05
2N.2E.30.34	5.22	1.18	1.32	1.92	1.97	4.06	.40	4.03	.60	-3.30	-3.46	-3.71	-4.36	3.48	-1.53	.21
2N.1E.23.323	3.65	2.65	1.44	2.20	1.62	3.23	.45	1.00	.76	-4.14	-2.47	-2.75	-5.33	.38	-.09	.10
3N.3E.32.310	2.83	.39	1.65	2.74	2.46	4.38	.45	2.43	1.10	-4.12	-3.28	-3.56	-5.32	1.81	-.90	.01
3N.2E.19.200	2.48	.82	.21	.65	1.95	.70	.73	1.66	.44	1.13	-.25	-.71	-.82	.64	-.30	.02
Mixture of upward-moving ground water and local ground water																
3N.2E.31.431	5.22	5.36	1.11	2.10	1.97	2.50	0.93	-0.14	0.99	-2.48	-1.51	-2.10	-4.95	-1.44	0.38	-0.34
3N.2E.33.222	33.49	31.03	1.28	2.45	2.95	3.44	.50	2.46	1.17	-2.15	-2.27	-2.58	-3.48	1.77	-.84	.04
3N.2E.27.123	6.09	4.23	.70	1.20	2.30	1.77	.73	1.86	.50	-.50	-1.27	-1.73	-2.45	.84	-.50	-.09

Eastern Area

This area is bounded on the east by the Precambrian core of the Manzano Mountains and on the west by the east side of the ground-water trough (pl. 2). The Hubbell Bench on the east side is a structural bench of Paleozoic, Mesozoic, and Tertiary rocks bounded by the Manzano Mountains on the east and the main body of the aquifer on the west. The northern area boundary (pl. 2) is north of Los Lunas and is based on a slight difference in specific conductance north and south of the boundary; north of this boundary, the specific conductance of ground water generally is larger than the specific conductance south of the boundary. This difference in specific conductance probably is due to a difference in rock type with which recharge water to the basin has come into contact. The southern boundary is the northern boundary of the southeastern area as discussed in the previous section.

Surface-water inflow from the Precambrian terrane of the Manzano Mountains recharges the aquifer along the eastern side of the Hubbell Bench. This water moves westward on the Hubbell Bench, which consists of an uplifted block of Paleozoic, Mesozoic, and Tertiary rocks covered by a thin layer of the aquifer. A hydraulic discontinuity exists along the Hubbell Spring fault where ground water perched on the Hubbell Bench moves downward into a thick section of the aquifer. After the water enters this thick section of the aquifer, it moves westward or southwestward toward the ground-water trough or the Rio Grande (fig. 9).

Ground Water on the Hubbell Bench

Surface-water inflow, derived from Precambrian rocks, that infiltrates and recharges the aquifer is not expected to contain large concentrations of dissolved constituents because of the general lack of readily soluble minerals associated with the Precambrian rocks and the short time the water is in contact with the Precambrian rocks. Water that infiltrates between the Precambrian rocks of the Manzano Mountains and the Hubbell Spring fault (pl. 1) may come into contact with Paleozoic, Mesozoic, and Tertiary rocks that are close to land surface on the Hubbell Bench before moving downgradient to the main body of the aquifer west of the Hubbell Bench. The chemical quality of ground water that comes into contact with the Paleozoic, Mesozoic, and Tertiary rocks on the Hubbell Bench may vary considerably depending upon the rock types that the water has contacted. Chemical analyses of water samples indicate that the dominant cation is calcium, the dominant anion is bicarbonate, and that the water has a small specific conductance (table 5 and fig. 20). This may indicate that the residence time of water in contact with the Paleozoic, Mesozoic, and Tertiary rocks along the bench is short or that the water sampled does not come into contact with the Paleozoic, Mesozoic, and Tertiary rocks that contain gypsum and other soluble minerals. Chemical-speciation calculations indicate that in all but one case the water on the Hubbell Bench is supersaturated with respect to calcite (table 6). In general, the water was determined to be undersaturated with respect to dolomite and gypsum (table 6). The results of the material-balance model do not show that calcite is precipitating from ground water on the Hubbell Bench,

but instead show that calcite has dissolved (table 7). This is not inconsistent with the chemical-speciation calculations because the model results represent only the total mass of a particular reaction. For example, if 10 mmoles of calcite have dissolved in a particular ground water and the ground water then dissolves gypsum, resulting in the precipitation of 3 mmoles of calcite, the model would calculate that 7 mmoles of calcite have dissolved.

Results of the material-balance model indicate that the alteration of plagioclase to calcium montmorillonite is a relatively insignificant reaction and that dissolutions of calcite, dolomite, and gypsum are relatively significant reactions in the evolution of ground water on the Hubbell Bench (table 7). Sodium is the dominant cation in water from well 5N.4E.29.142 (table 5). This well is on the Hubbell Bench and the water may come into contact with clay that has a large cation-exchange capacity, thus removing calcium ions from solution.

Ground Water East of the Rio Grande Valley and West of the Hubbell Bench

Ground water east of the Rio Grande valley and west of the Hubbell Bench generally has a specific conductance of less than 400 microsiemens. This small specific conductance may indicate that the component of ground-water inflow from the east that has come into contact with Paleozoic and Mesozoic rocks is small or that the water does not come into contact with rocks that contain readily soluble minerals. Calcium and bicarbonate are the dominant ions in ground water in this area (fig. 20). In general, ground water is supersaturated with respect to calcite and undersaturated with respect to gypsum (table 6). Examination of the material-balance-model results indicates that bicarbonate generally is negative after silica is removed (table 7), an indication that more calcite has precipitated than has dissolved.

A negative bicarbonate would result after the removal of silica if the alteration of plagioclase to calcium montmorillonite reaction was not the only source of dissolved silica. The negative sodium after the removal of silica also indicates that the plagioclase-alteration reaction may not be the only reaction that results in dissolved silica (table 7). The silica concentrations generally are larger in ground water west of the Hubbell Bench (tables 5 and 7) compared to silica concentrations in ground water from the Hubbell Bench, indicating that reactions that result in dissolved silica do occur as ground water moves downgradient from the Hubbell Bench. Results of the material-balance model seem to indicate that other reactions resulting in dissolved silica occur in this area. Water from wells 4N.2E.35.214, 4N.3E.26.144, and 4N.3E.18.220 seems to be affected by ion-exchange processes. This is evidenced on the Piper diagram by the three points from the area west of the Hubbell Bench and east of the Rio Grande valley that have greater than 40 percent sodium (fig. 20) and in the results of the material-balance model by the relatively large negative values of calcium after bicarbonate is removed (table 7).

Water from well 8N.3E.32.412 has a specific conductance and a sulfate concentration larger than most other water sampled east of the Rio Grande valley (table 5). This well is located in Hells Canyon Wash, which is one of the few arroyos that has a well-defined channel from the mountain front to the river valley. Surface water that infiltrates along this arroyo may have large concentrations of dissolved solids due to evaporation. Water from well 8N.3E.32.412 may represent infiltrating surface water concentrated by evaporation, water that has come into contact with gypsum-bearing rocks along the Hubbell Bench, water that has dissolved minerals associated with the mining activity along the arroyo, or a mixture of these waters.

Ground Water in the Rio Grande Valley

The water sampled from wells located within the Rio Grande valley, particularly those near irrigation canals and irrigated fields, indicates that irrigation affects ground-water quality to varying degrees (table 5 and fig. 19). In general, calcium is the dominant cation and sulfate the dominant anion (fig. 20). Sulfate varies from 18 to 65 percent in water from wells in the Rio Grande valley (fig. 20). Water from wells 7N.2E.13.441 and 7N.2E.11.210 has a large specific conductance in comparison to that in water from other wells in the river valley (table 5). Both of these wells are located close to drains and may yield water in which the dissolved solids may have been concentrated by evaporation as the result of irrigation practices. The quality of water in the drains indicates quality of water yielded by shallow wells near the drains. The specific conductance of drain water sampled near wells 7N.2E.13.441 and 7N.2E.11.210 is 900 and 1,200 microsiemens, respectively, which is less than the specific conductance of 2,170 and 1,620 microsiemens of water from these two wells, respectively. This implies that water from these wells is not as fresh as is the ground water near these drains. Water from well 7N.2E.13.441 is supersaturated with respect to calcite and dolomite (table 6). The material-balance-model results indicate that more calcite precipitated than dissolved in 6 out of 10 samples from wells in the Rio Grande valley (table 7). If calcite precipitated from solution during evaporation caused by irrigation practices, the ratio of bicarbonate to sulfate in the water would decrease or the percentage of sulfate in the water would increase. This may explain the large variation in the percentage of sulfate in ground water in the Rio Grande valley (fig. 20). The material-balance-model results also indicate that the amount of ion exchange generally is larger in the Rio Grande valley than in the area east of the Rio Grande valley (table 7). The concentration of dissolved silica also is larger in the Rio Grande valley than in the area east of the Rio Grande valley (table 5).

Ground Water West of the Rio Grande Valley

The specific conductance of ground water west of the Rio Grande valley and east of the ground-water trough ranges from 506 to 890 microsiemens and generally is less than 700 microsiemens (table 5 and pl. 2). Sodium is the dominant cation and sulfate and bicarbonate are the dominant anions (fig. 20). The material-balance model indicates, as illustrated by the relatively large positive sodium after removal of silica, that ion exchange is a dominant process in the evolution of this water (table 7). This may indicate that the sediments in this area contain more clay and silt than do sediments east of the river valley. Chloride concentrations in ground water from this area are smaller than chloride concentrations in ground water west of the ground-water trough, indicating that very little ground water from west of the trough enters the river valley or the flow system east of the trough. The ground-water-quality data support the ground-water-level data that indicate a ground-water trough in this area.

Conclusions

Ground-water recharge due to the infiltration of surface-water inflow derived from the Manzano Mountains occurs along the Hubbell Bench. This ground water flows westward on the Hubbell Bench and into the thicker part of the aquifer west of the Hubbell Spring fault. Water continues moving westward in the aquifer toward the axis of the ground-water trough. The ground-water trough coincides with the Rio Grande valley near and south of Belen and is west of the Rio Grande valley north of Belen (fig. 9). The chemical quality of the ground water on the Hubbell Bench and west of the bench is similar, indicating that the Paleozoic and Mesozoic rocks on the Hubbell Bench do not significantly affect ground-water quality in the area. In general, ground water east of the Rio Grande valley and west of the Hubbell Bench has a specific conductance of less than 400 microsiemens. Bicarbonate is the dominant anion and calcium is the dominant cation, although sodium is dominant in several water samples, probably due to cation exchange.

The specific conductance of ground water in the Rio Grande valley ranges from 281 to 2,170 microsiemens and, in general, is larger than the specific conductance of ground water east of the Rio Grande valley. Bicarbonate and sulfate are the dominant anions and calcium is the dominant cation. In general, the percentage of sodium is larger in ground water west of the Rio Grande valley than in ground water in other parts of the eastern area. This probably is due to cation exchange.

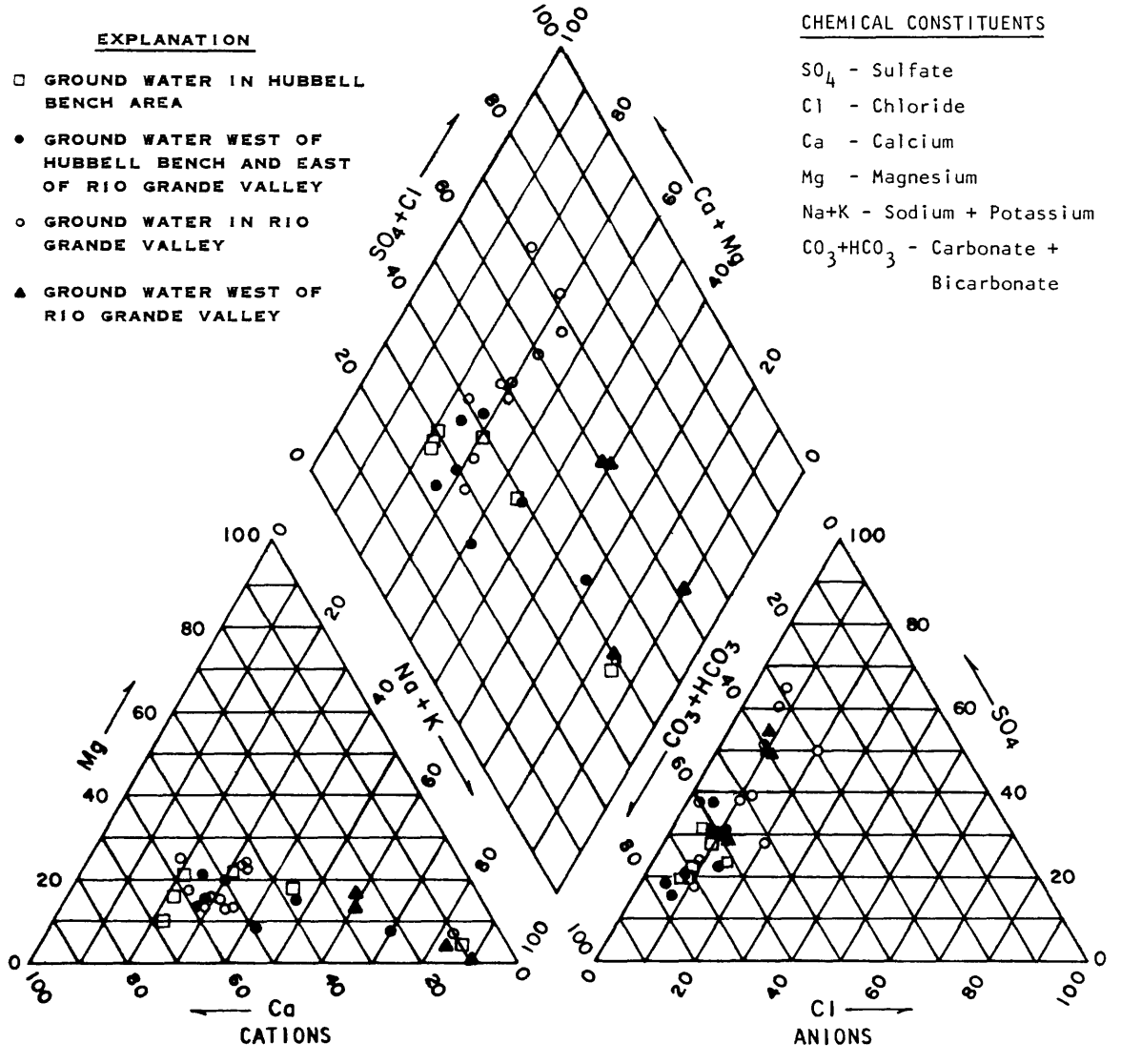

Figure 20.--Piper diagram of selected ground-water analyses in the eastern area.

Table 5. Ground-water-quality data for selected sites in the eastern area

[Well depth, asterisk (*) indicates water level, in feet below land surface and SP indicates spring; ft, feet; °C, degrees Celsius; mg/L, milligrams per liter]

Location	Date sampled	Well depth (ft)	Temperature (°C)	Specific conductance (microsiemens per centimeter at 25 °C)	pH	Calcium (mg/L)	Magnesium (mg/L)	Sodium (mg/L)	Sodium plus potassium (mg/L as sodium)	Potassium (mg/L)	Bicarbonate (mg/L)	Carbonate (mg/L)	Sulfate (mg/L)	Chloride (mg/L)	Fluoride (mg/L)	Silica (mg/L)	Dissolved solids (mg/L)
Ground water on the Hubbell Bench																	
5N.4E.29.142	5-25-80	—	23.0	330	8.5	7	2.0	69	—	2.0	140	0	51	12	0.9	25	—
5N.4E. 9.122	6-18-80	250	19.0	318	8.1	40	9.0	16	—	1.0	150	0	28	8	.4	19	—
5N.4E. 3.114	5-28-80	42	11.0	240	7.7	32	5.0	12	—	1.0	120	0	28	7	.3	17	—
6N.4E.30.144	5-28-80	SP	15.5	340	7.8	52	5.0	19	—	1.0	160	0	34	9	.4	11	—
8N.4E.29.434	2-15-56	SP	15.5	403	7.3	—	—	12	—	—	186	0	29	9	—	—	—
Ground water east of the Rio Grande valley and west of the Hubbell Bench																	
3N.4E. 3.110	6-12-80	322 *	22.4	440	8.1	47	13.0	34	—	3.0	180	0	55	26	0.8	23	—
4N.2E.35.214	11- 4-56	—	21.5	317	7.4	23	6.0	—	34	—	110	0	51	8	.8	32	210
4N.3E.26.144	3-29-50	187	22.0	263	—	20	6.0	—	28	—	98	0	40	7	.6	17	—
4N.3E.18.220	6-12-80	370	24.9	265	8.5	12	3.0	43	—	2.0	97	4	56	5	.7	29	—
4N.2E.15.443	3-27-50	160	20.5	357	—	40	10.0	—	21	—	140	0	40	17	.4	49	—
5N.3E.11.331	6-17-58	—	16.5	391	7.2	—	—	—	—	—	140	0	64	11	—	—	—
5N.3E. 8.222	6-18-80	238	21.9	250	8.0	34	5.0	17	—	2.0	130	0	22	7	.6	40	—
6N.3E. 7.240	6-13-80	295	20.7	315	8.2	37	9.0	23	—	4.0	150	0	37	9	.7	41	—
7N.3E.35.313	7-11-57	345	24.0	257	—	—	—	—	—	—	—	-	—	6	—	—	—
7N.3E.25.220	6-18-80	655	23.0	305	7.9	33	4.0	31	—	2.0	150	0	30	5	.3	26	—
7N.3E.13.434	5-31-57	—	19.0	286	7.6	—	—	—	14	—	150	0	20	4	.8	26	—
8N.3E.32.412	2-14-56	123	18.0	1,020	7.2	—	—	—	—	—	120	0	72	22	—	—	—
8N.2E.24.244	4-30-65	100	—	588	7.8	70	12.0	—	41	—	220	0	92	23	.3	37	398

Table 5. Ground-water-quality data for selected sites in the eastern area - Concluded

Location	Date sampled	Well depth (ft)	Temperature (°C)	Specific conductance (microsiemens per centimeter at 25 °C)	pH	Calcium (mg/L)	Magnesium (mg/L)	Sodium (mg/L)	Sodium plus potassium (mg/L as sodium)	Potassium (mg/L)	Bicarbonate (mg/L)	Carbonate (mg/L)	Sulfate (mg/L)	Chloride (mg/L)	Fluoride (mg/L)	Silica (mg/L)	Dissolved solids (mg/L)
							Ground water in the Rio Grande valley										
4N.2E.32.100	6-12-80	93	22.0	281	8.3	29	9.0	23	—	5.0	150	0	30	13	0.4	56	—
4N.2E. 8.243	4-11-56	38	13.5	631	7.4	—	—	—	43	—	200	0	120	24	—	—	—
4N.2E.18.211	—	—	—	799	7.6	90	16.0	57	—	—	132	0	234	16	.3	44	584
5N.2E.32.143	6-26-58	100 *	—	900	7.5	—	—	—	—	—	270	0	200	45	—	—	—
5N.2E.00.000	9-25-72	—	—	470	7.6	44	13.0	31	—	6.0	158	0	71	36	.6	—	—
6N.2E. 3.344	9-18-51	103	—	879	7.6	100	18.0	—	67	—	280	0	180	39	—	—	—
7N.2E.26.333	7-22-63	—	14.0	861	7.5	110	15.0	—	64	—	300	0	180	33	.5	31	596
7N.2E.26.314	4-16-59	58	15.5	577	8.1	—	—	—	—	—	200	0	—	—	—	—	—
7N.2E.28.234	11-28-56	165	18.5	488	8.0	10	4.0	—	94	—	180	0	68	18	.8	51	344
7N.2E.26.112	3- 9-56	80	15.0	609	7.6	71	13.0	—	33	—	220	0	110	4	.4	35	409
7N.2E.23.212	8- 3-77	165	—	295	8.2	29	9.0	20	—	6.0	130	0	38	11	.4	45	—
7N.2E.13.441	6- 7-71	—	19.0	2,170	7.8	250	41.0	190	—	9.0	486	0	710	61	.1	45	—
7N.2E.28.333	11-15-76	177	—	583	7.8	67	18.0	22	—	5.0	112	0	150	45	.3	32	—
7N.2E.11.210	8-14-51	64	—	1,620	7.6	200	32.0	—	140	—	460	0	440	70	.3	30	1,200
							Ground water west of the Rio Grande valley										
5N.1E.24.344	4-13-56	96	19.0	890	7.5	—	—	—	120	—	200	0	210	44	—	—	—
5N.1E.13.332	11-28-56	519	20.5	720	7.9	37	15.0	—	99	—	180	0	180	24	1.0	31	476
7N.2E.21.332	8- 6-52	607	—	506	—	12	3.0	—	100	—	190	0	76	18	1.0	48	—
7N.2E. 7.114	7-16-75	—	29.5	634	8.7	10	1.0	120	—	6.0	130	0	150	16	1.3	70	—
8N.2E.23.100	1-25-55	85	—	536	—	—	—	—	31	—	210	0	98	18	.8	—	—

Table 6. Saturation index of selected ground-water analyses in the eastern area

Location	Saturation index		
	Calcite	Dolomite	Gypsum
Ground water on the Hubbell Bench			
5N.4E.29.142	0.002	-0.262	-2.573
5N.4E. 9.122	.222	.030	-2.094
5N.4E. 3.114	-.333	-1.350	-2.147
6N.4E.30.144	.139	-.548	-1.915
Ground water east of the Rio Grande valley and west of the Hubbell Bench			
3N.4E. 3.110	0.509	0.731	-1.804
4N.3E.18.220	.111	-.086	-2.289
5N.3E. 8.222	.178	-.213	-2.250
6N.3E. 7.240	.429	.497	-2.025
7N.3E.25.220	.134	-.373	-2.143
Ground water in the Rio Grande valley			
4N.2E.32.100	0.445	0.648	-2.207
7N.2E.13.441	1.055	1.582	-.379

Table 7. Material-balance-model results for selected ground-water analyses in the eastern area

Location	Sodium (Na^+) (millimoles)	Chloride (Cl^-) (millimoles)	Magnesium (Mg^{2+}) (millimoles)	Calcium (Ca^{2+}) (millimoles)	Bicarbonate (HCO_3^-) (millimoles)	Sulfate (SO_4^-) (millimoles)	Silica (Si) (millimoles)	Sodium (Na+) after chloride removal (millimoles)	Calcium (Ca^{2+}) after magnesium removal (millimoles)	Bicarbonate (HCO_3) after magnesium removal (millimoles)	Calcium (Ca^{2+}) after sulfate removal (millimoles)	Calcium (Ca^{2+}) after silica removal (millimoles)	Bicarbonate (HCO_3) after silica removal (millimoles)	Sodium (Na^+) after silica removal (millimoles)	Calcium (Ca^{2+}) after bicarbonate removal (millimoles)	Excess sodium (Na^+) (millimoles)
Ground water on the Hubbell Bench																
5N.4E.29.142	3.00	0.34	0.08	0.17	2.30	0.53	0.42	2.66	0.09	1.97	-0.44	-0.70	0.86	2.08	-1.13	-0.09
5N.4E. 9.122	.70	.23	.37	1.00	2.46	.29	.32	.47	.63	.98	.34	.14	.14	.03	.07	.08
5N.4E. 3.114	.52	.20	.21	.80	1.97	.29	.28	.32	.59	1.14	.30	.12	.39	-.07	-.07	-.11
6N.4E.30.144	.83	.25	.21	1.30	2.62	.35	.18	.57	1.09	1.80	.74	.62	1.31	.32	-.03	.13
Ground water east of the Rio Grande valley and west of the Hubbell Bench																
3N.4E. 3.110	1.48	0.73	0.53	1.17	2.95	0.57	0.38	0.75	0.64	0.81	0.06	-0.17	-0.21	0.21	-0.07	0.03
4N.2E.35.214	1.48	.23	.25	.57	1.80	.53	.53	1.25	.33	.82	-.20	-.54	-.60	.51	-.24	.02
4N.3E.26.144	1.22	.20	.25	.50	1.61	.42	.28	1.02	.25	.62	-.16	-.34	-.13	.63	-.27	.04
4N.3E.18.220	1.87	.14	.12	.30	1.59	.58	.48	1.73	.18	1.10	-.41	-.71	-.19	1.06	-.61	-.09
4N.2E.15.443	.91	.48	.41	1.00	2.30	.42	.82	.43	.59	.65	.17	-.34	-1.52	-.70	.42	.07
5N.3E. 8.222	.74	.20	.21	.85	2.13	.23	.67	.54	.64	1.31	.41	-.00	-.46	-.39	.23	.04
6N.3E. 7.240	1.00	.25	.37	.92	2.46	.39	.68	.75	.55	.98	.17	-.26	-.84	-.21	.16	.06
7N.3E.25.220	1.35	.14	.16	.82	2.46	.31	.43	1.21	.66	1.80	.35	.08	.65	.60	-.25	.05
8N.2E.24.244	1.78	.65	.49	1.75	3.61	.96	.62	1.13	1.25	1.63	.29	-.09	-.01	.28	-.09	.05

Table 7. Material-balance-model results for selected ground-water analyses in the eastern area - Concluded

Location	Sodium (Na^+) (millimoles)	Chloride (Cl^-) (millimoles)	Magnesium (Mg^{2+}) (millimoles)	Calcium (Ca^{2+}) (millimoles)	Bicarbonate (HCO_3^-) (millimoles)	Sulfate (SO_4^-) (millimoles)	Silica (Si) (millimoles)	Sodium (Na+) after chloride removal (millimoles)	Calcium (Ca^{2+}) after magnesium removal (millimoles)	Bicarbonate (HCO_3) after magnesium removal (millimoles)	Calcium (Ca^{2+}) after sulfate removal (millimoles)	Calcium (Ca^{2+}) after silica removal (millimoles)	Bicarbonate (HCO_3) after silica removal (millimoles)	Sodium (Na^+) after silica removal (millimoles)	Calcium (Ca^{2+}) after bicarbonate removal (millimoles)	Excess sodium (Na^+) (millimoles)
Ground water in the Rio Grande valley																
4N.2E.32.100	1.00	0.37	0.37	0.72	2.46	0.31	0.93	0.63	0.35	0.98	0.04	-0.54	-1.50	-0.67	0.21	-0.12
4N.2E.18.211	2.48	.45	.66	2.25	2.16	2.44	.73	2.03	1.59	-.47	-.85	-1.31	-2.42	1.01	-.10	.40
5N.2E.00.000	1.35	1.02	.53	1.10	2.59	.74	.00	.33	.56	.45	-.18	-.18	.45	.33	-.40	-.24
7N.2E.26.333	2.78	.93	.62	2.74	4.92	1.88	.52	1.85	2.13	2.45	.25	-.07	1.08	1.13	-.61	-.04
7N.2E.28.234	4.09	.51	.16	.25	2.95	.71	.85	3.58	.08	2.29	-.62	-1.15	.04	2.40	-1.17	.03
7N.2E.26.112	1.44	.11	.53	1.77	3.61	1.15	.58	1.32	1.24	1.47	.09	-.27	-.08	.51	-.23	.02
7N.2E.23.212	.87	.31	.37	.72	2.13	.40	.75	1.56	.35	.65	-.04	-.51	-1.34	-.49	.16	-.08
7N.2E.13.441	8.26	1.72	1.69	6.24	7.97	7.40	.75	6.54	4.55	1.22	-2.84	-3.31	-.77	5.50	-2.93	-.18
7N.2E.28.333	.96	1.27	.74	1.67	1.84	1.56	.53	-.31	.93	-1.13	-.63	-.96	-2.54	-1.06	.31	-.22
7N.2E.11.210	6.09	1.97	1.32	4.99	7.54	4.58	.50	4.11	3.67	2.28	-.91	-1.22	.95	3.42	-1.70	.01
Ground water west of the Rio Grande valley																
5N.1E.13.332	4.31	0.68	0.62	0.92	2.95	1.88	0.52	3.63	0.31	0.48	-1.57	-1.89	-0.89	2.91	-1.45	0.01
7N.2E.21.332	4.35	.51	.12	.30	3.11	.79	.80	3.84	.18	2.62	-.62	-1.11	.50	2.73	-1.36	.00
7N.2E. 7.114	5.22	.45	.04	.25	2.13	1.56	1.17	4.77	.21	1.97	-1.35	-2.08	-1.13	3.14	-1.52	.06

Southwestern Area

The eastern boundary of the southwestern area is the ground-water trough, which coincides with the Rio Grande near and south of Belen (pl. 2 and fig. 11). This boundary was selected on the basis that it is the easternmost extent of the detectable effects of ground water recharging the aquifer from the west. The southern boundary is the southern margin of the Albuquerque-Belen Basin. The western boundary is formed by the Ladron Mountains, the Lucero uplift, and the southern part of the Rio Puerco fault zone. The northern boundary approximately coincides with T. 9 N. and was selected on the basis that it probably is the northern limit of ground water significantly affected by ground-water inflow from bedrock units older than Cretaceous age along the west margin of the basin (pl. 2).

Ground-water inflow from the Lucero uplift and surface runoff from adjacent areas recharge the aquifer along the western boundary of this area. Water in the aquifer flows eastward or southeastward toward the ground-water trough and the southern end of the Albuquerque-Belen Basin.

The material-balance model was not used to evaluate the evolution of ground water in this area. This is because the assumptions used in the model do not apply to ground water that recharges the aquifer from the Lucero uplift and also because this recharge has such a large effect on ground water in the area.

Comanche Fault Flow System

The Lucero uplift is a west-tilted fault block that marks the boundary between the Colorado Plateau and the Rio Grande rift (Callender and Zilinski, 1976, p. 53). The Lucero uplift has a complex structural history that has been described by Callender and Zilinski (1976). Rocks from Precambrian to Cretaceous age occur along the east flank of the Lucero uplift. Pennsylvanian rocks crop out at the southern end of the uplift, and rocks cropping out along the uplift are progressively younger toward the north (pl. 1). Large travertine deposits occur along the east flank of the uplift. These deposits were formed by chemical precipitation of minerals from water discharging from springs along the Comanche fault.

The Comanche fault has been interpreted as a west-dipping reverse fault (Callender and Zilinski, 1976, p. 55). The fault can be traced along most of the length of the Lucero uplift, and it generally juxtaposes the Madera and Abo Formations west of the fault with the Yeso Formation east of the fault. Along the southern part of the fault, the Madera Formation is juxtaposed with an upthrust block of Precambrian rock (Callender and Zilinski, 1976, p. 55). In this area, the travertine deposits are more extensive than in other areas along the fault. The Pennsylvanian limestone of the Madera and Sandia Formations probably is the source of water discharging from springs along the Comanche fault. These springs probably are the result of ground water being forced to the land surface due to a change in permeability across the fault. The presence of more extensive travertine deposits along the fault where Precambrian rock is in contact with Pennsylvanian limestone seems to indicate further that the Pennsylvanian limestone is the source of the spring water and that the permeability contrast is the mechanism that causes the springs.

Water that discharges from springs along the Comanche fault represents only a part of the water that enters the Albuquerque-Belen Basin along the Lucero uplift. Much of the remaining water enters formations stratigraphically lower than the Yeso Formation on the east side of the Comanche fault and flows eastward until it enters the aquifer (fig. 10). After water enters the aquifer along the west margin of the basin, the water flows eastward toward the ground-water trough (fig. 9).

The specific conductance of water discharging from the springs along the Comanche fault generally is greater than 20,000 microsiemens (table 8). Sodium and chloride are the dominant ions (fig. 21), and the water is considered a brine. Water with large concentrations of sodium and chloride generally is considered to be the end-member water in the chemical evolution of ground water (Freeze and Cherry, 1979, p. 242). This water generally is thought to be relatively old and usually is associated with large sedimentary basins (Freeze and Cherry, 1979, p. 242), possibly indicating that the water does not simply represent local recharge along Mesa Lucero but may also represent sedimentary basin water. It is possible that the ground water discharging along the Comanche fault is ground-water outflow from the southern San Juan Basin (fig. 22).

Mesozoic Rocks Flow System

Mesozoic rocks crop out in the northern part of the Lucero uplift near the Rio San Jose. In this area, the Rio San Jose is a drain for ground water that flows eastward in the Mesozoic rocks flow system. The specific conductance and distribution of dissolved constituents are much different in water from springs and wells in the Mesozoic rocks flow system compared to water discharging from springs along the Comanche fault (Comanche fault flow system) (table 8 and fig. 21). The specific conductance of this water generally is less than 10,000 microsiemens, sulfate is the dominant anion, and sodium is the dominant cation (table 8). Water in the Mesozoic rocks not intercepted by the Rio San Jose moves eastward in through the Mesozoic rocks until the water enters the aquifer. A spring, 8N.2W.7.314, discharges water near the Rio San Jose, but the water is very similar to the water that discharges along the Comanche fault (Comanche fault flow system) (table 8 and fig. 21). As with water from springs along the Comanche fault, water that discharges from this spring probably is derived from deep Pennsylvanian or Permian rocks. This spring probably also leaks upward along a fault.

Mixed Waters

The brine that enters the aquifer along the Lucero uplift is diluted by recharge due to infiltration of surface-water inflow from the west and possibly by direct recharge of precipitation. This is indicated by a general decrease in specific conductance of ground water downgradient and east of the Comanche fault (fig. 23). The concentration of dissolved constituents in the recharge water is small compared to that in the brine. If it is assumed that chloride is conservative in the mixing of the two waters and that the chloride concentration in the recharge water is 1.0 milligram per liter and in the brine is 10,000 milligrams per liter, the mixing ratio of the two waters can be calculated. The mixing ratio of the water is approximately 95 parts recharge water and 5 parts brine (table 9).

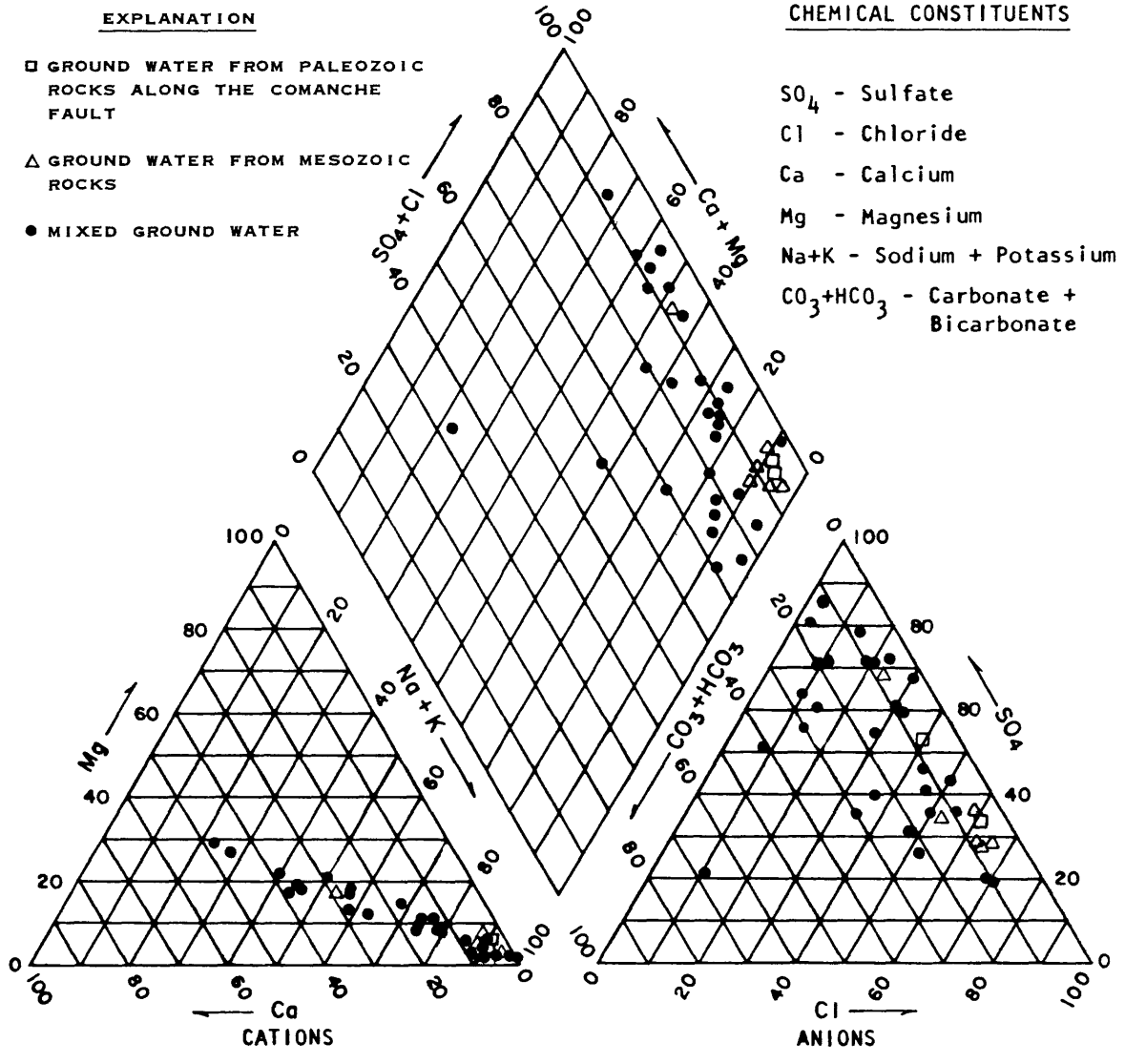

Figure 21.--Piper diagram of selected ground-water analyses in the southwestern area.

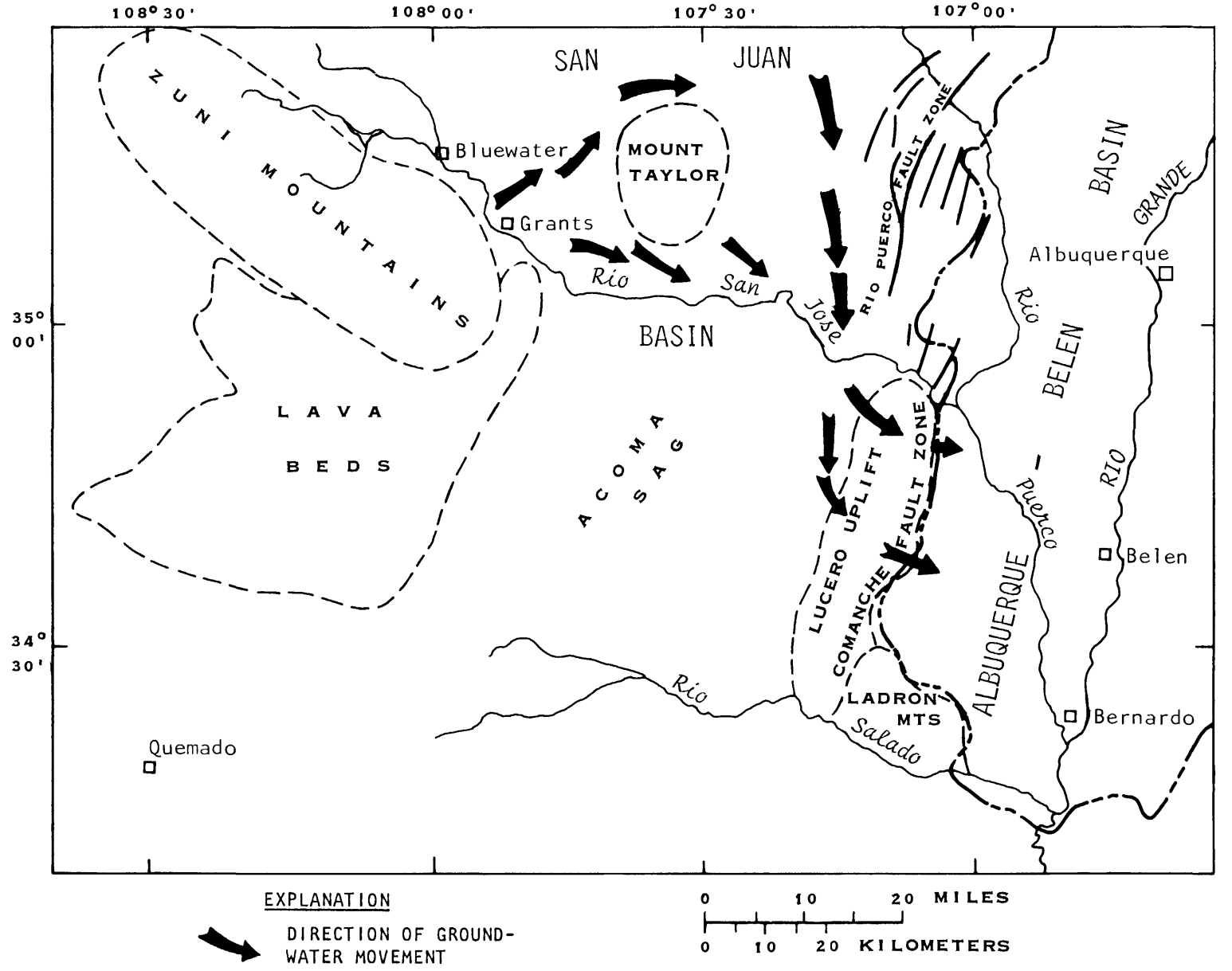

Figure 22.--Possible ground-water flow paths from the San Juan Basin to the Albuquerque-Belen Basin.

EXPLANATION

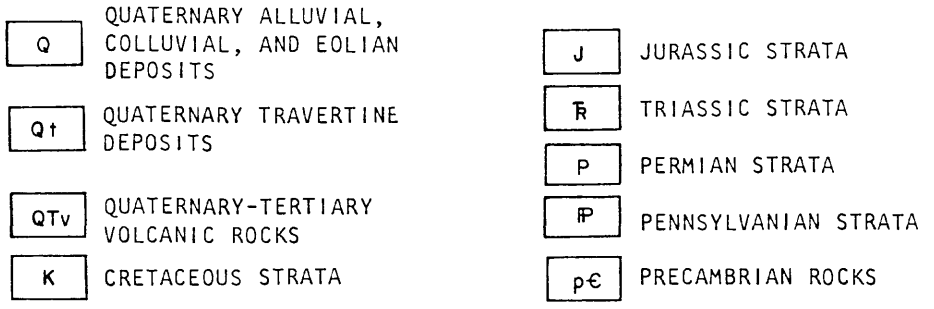

WELL NUMBER	LOCATION	WELL NUMBER	LOCATION
1	4N.1E.09.324	17	7N.1W.23.334
2	4N.1W.12.341	18	7N.1W.31.331
3	4N.1W.15.211	19	7N.2W.06.414
4	4N.1W.28.323	20	7N.2W.10.444
5	4N.2W.02.433	21	7N.2W.18.112
6	4N.3W.25.334	22	7N.2W.19.343
7	5N.1E.28.114	23	7N.2W.29.214
8	5N.1W.14.231	24	7N.3W.13.444
9	5N.1W.32.423	25	8N.1W.24.312
10	5N.2W.21.422	26	8N.2W.12.111
11	5N.3W.34.200	27	8N.2W.20.432
12	6N.1E.33.433	28	8N.2W.24.131
13	6N.1W.29.130	29	8N.2W.30.313
14	6N.2W.13.234	30	8N.3W.11.233
15	6N.2W.16.000	31	8N.3W.12.343
16	6N.3W.35.341	32	8N.3W.12.442

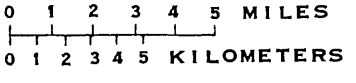

Figure 23.--Specific conductance, sulfate to chloride ratio, and sodium plus potassium to calcium ratio of water from selected wells in the southwestern area.

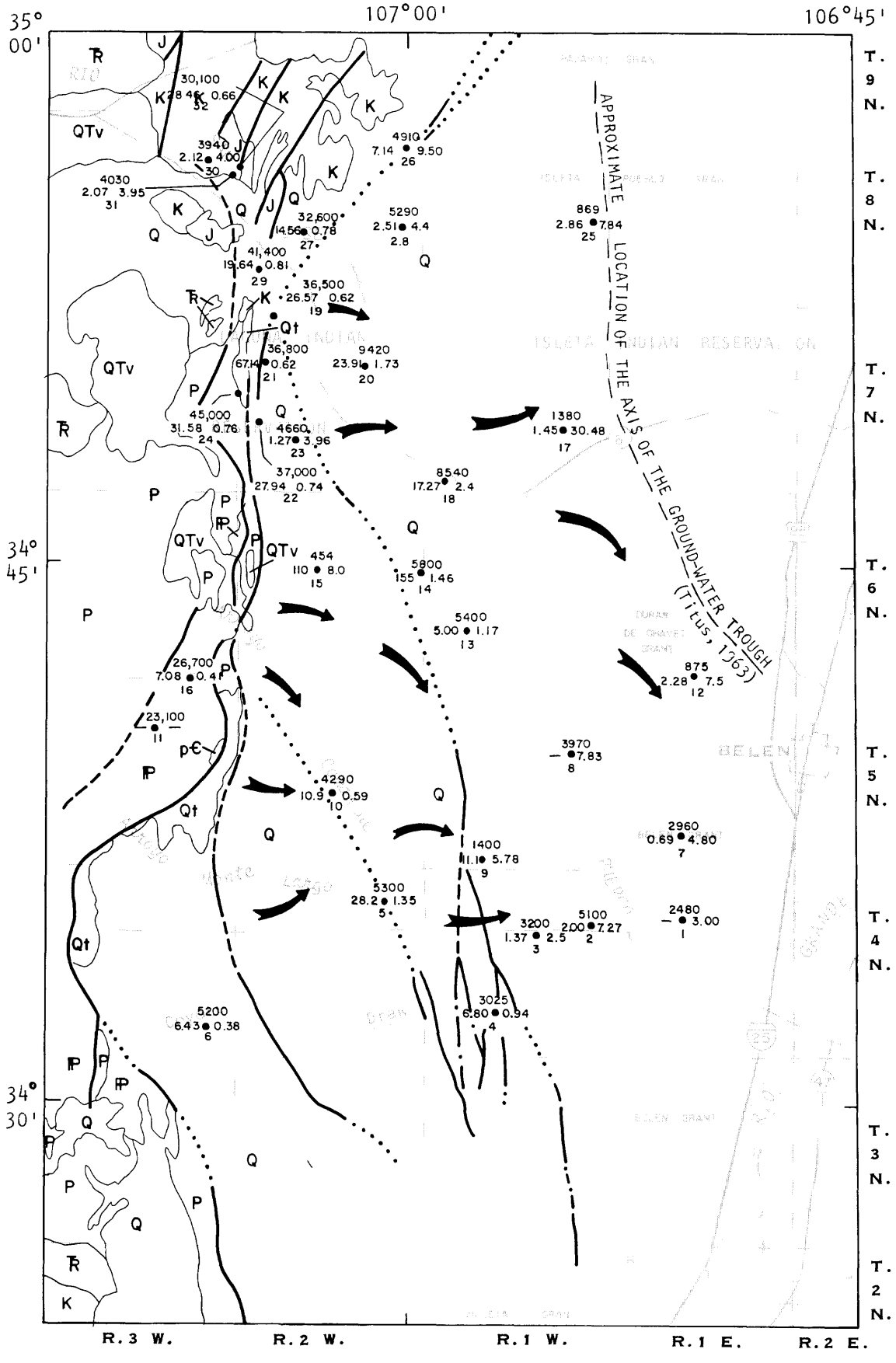
35° 00'
107°00'
106°45'
34° 45'
34° 30'
T. 9 N.
T. 8 N.
T. 7 N.
T. 6 N.
T. 5 N.
T. 4 N.
T. 3 N.
T. 2 N.
R. 3 W.
R. 2 W.
R. 1 W.
R. 1 E.
R. 2 E.
APPROXIMATE LOCATION OF THE AXIS OF THE GROUND-WATER TROUGH (Titus, 1963)
QTv
Qt
Q
P
K
J
Tr
pC
30,100 28.46 0.66 32
3940 2.12 4.00 30
4030 2.07 3.95 31
4910 7.14 9.50 26
5290 2.51 4.4 2.8
32,600 14.56 0.78 27
41,400 19.64 0.81 29
36,500 26.57 0.62 19
36,800 67.14 0.62 21
9420 23.91 1.73 20
45,000 31.58 0.76 24
4660 1.27 3.96 23
37,000 27.94 0.74 22
8540 17.27 2.4 18
869 2.86 7.84 25
1380 1.45 30.48 17
454 110 8.0 15
5800 155 1.46 14
5400 5.00 1.17 13
875 2.28 7.5 12
26,700 7.08 0.41 16
23,100 11
4290 10.9 0.59 10
3970 7.83 8
1400 1.1 5.78 9
2960 0.69 4.80 7
5300 28.2 1.35 5
3200 1.37 2.5 3
5100 2.00 7.27 2
2480 3.00 1
5200 6.43 0.38 6
3025 6.80 0.94 4

Table 8. Ground-water-quality data for selected sites in the southwestern area

[Well depth, SP indicates spring; ft, feet; °C, degrees Celsius; mg/L, milligrams per liter]

Location	Date sampled	Well depth (ft)	Temperature (°C)	Specific conductance (microsiemens per centimeter at 25 °C)	pH	Calcium (mg/L)	Magnesium (mg/L)	Sodium (mg/L)	Sodium plus potassium (mg/L as sodium)	Potassium (mg/L)	Bicarbonate (mg/L)	Carbonate (mg/L)	Sulfate (mg/L)	Chloride (mg/L)	Fluoride (mg/L)	Silica (mg/L)	Dissolved solids (mg/L)
							Comanche fault flow system										
5N.3W.34.200	3- 3-54	80	15.5	23,100	—	400	300.0	—	—	—	1,230	0	—	6,800	—	—	—
6N.3W.35.341	5- 1-57	SP	—	26,700	6.6	823	460.0	—	5,830	—	2,550	0	3,250	7,900	16.0	14	—
7N.2W.19.343	5-16-75	—	21.5	37,000	8.3	340	230.0	9,500	—	280	1,490	0	7,400	10,000	2.2	23	—
7N.3W.13.444	4-22-75	—	—	45,000	8.7	380	230.0	12,000	—	310	1,960	54	9,100	12,000	2.2	26	—
7N.2W.18.112	4-22-75	SP	13.5	36,800	8.3	140	160.0	9,400	—	320	1,920	0	6,200	10,000	2.4	32	—
7N.2W. 6.414	4-22-75	SP	13.5	36,500	6.9	350	350.0	9,300	—	260	2,460	0	6,200	10,000	3.8	22	—
8N.2W.30.313	4-21-75	SP	—	41,400	7.3	560	350.0	11,000	—	320	1,530	0	8,900	11,000	3.8	19	—
8N.2W.20.432	4-21-75	—	24.0	32,600	7.1	570	150.0	8,300	—	280	2,900	0	6,100	7,800	3.5	22	—
8N.3W.12.442	4-21-75	—	—	30,100	8.3	260	130.0	7,400	—	440	1,780	0	5,100	7,700	2.4	17	—
							Mesozoic rocks flow system										
8N.3W.12.343	4-21-75	—	16.5	4,030	7.9	270	100.0	560	—	12.0	232	0	1,500	380	0.8	30	—
8N.3W.11.233	4-21-75	—	—	3,940	7.8	250	100.0	530	—	12.0	219	0	1,400	350	.8	31	—
9N.2W.10.300	3- 1-65	445	—	5,870	8.4	24	13.0	—	1,480	—	610	12	2,600	78	2.9	7	0
							Mixed waters										
4N.3W.25.334	1- 5-50	SP	16.0	5,200	—	138	67.0	—	887	—	354	0	471	1,250	0.8	24	—
4N.1W.28.323	6- 3-80	260	20.5	3,025	7.5	75	33.0	510	—	13.0	250	0	500	530	1.6	15	—
4N.1W.15.211	6- 4-80	268	21.0	3,200	7.3	270	87.0	370	—	12.0	180	0	1,100	440	.5	15	—
4N.1W.12.341	6- 4-80	—	15.2	5,100	7.3	360	160.0	720	—	11.0	240	0	2,400	330	.6	16	—
4N.1E. 9.324	4-24-56	400	23.0	2,480	7.2	—	—	—	190	—	98	0	870	290	—	—	—
4N.2W. 2.433	6- 4-80	431	18.5	5,300	7.7	39	17.0	1,100	—	32.0	950	0	920	680	4.1	53	—
5N.1W.32.423	5-27-80	412	22.0	1,400	7.9	27	11.0	300	—	9.0	230	0	460	83	1.9	21	—
5N.1E.28.114	4-24-56	393	22.0	2,960	7.2	320	120.0	—	220	—	170	0	1,200	250	.2	24	2,420
5N.2W.21.422	6- 5-80	620	21.5	4,290	7.5	78	32.0	850	—	26.0	590	0	560	850	2.2	18	—
5N.1W.14.231	5-24-56	99	17.0	3,970	7.2	—	—	—	—	—	420	0	1,800	230	—	—	—
6N.1E.33.433	6- 6-80	556	20.7	875	8.0	57	17.0	130	—	6.0	240	0	240	32	.9	24	—

Table 8. Ground-water-quality data for selected sites in the southwestern area – Concluded

Location	Date sampled	Well depth (ft)	Temperature (°C)	Specific conductance (microsiemens per centimeter at 25 °C)	pH	Calcium (mg/L)	Magnesium (mg/L)	Sodium (mg/L)	Sodium plus potassium (mg/L as sodium)	Potassium (mg/L)	Bicarbonate (mg/L)	Carbonate (mg/L)	Sulfate (mg/L)	Chloride (mg/L)	Fluoride (mg/L)	Silica (mg/L)	Dissolved solids (mg/L)
							Mixed waters — Concluded										
6N.1W.29.130	6- 6-80	567	18.8	5,400	8.0	220	71.0	1,100	—	15.0	240	0	1,400	1,200	0.6	17	—
6N.2W.13.234	5-29-57	133	18.0	5,800	8.3	9	10.0	—	1,400	—	870	8	1,200	820	5.0	22	3,880
6N.2W.16.000	8-19-53	330	—	454	—	—	—	—	110	—	210	24	32	4	.2	14	—
7N.2W.29.214	5-16-75	—	19.0	4,660	7.7	410	110.0	520	—	34.0	117	0	1,900	480	1.3	13	—
7N.1W.23.334	6- 6-80	—	16.2	1,380	8.0	110	35.0	160	—	9.0	96	0	640	21	1.0	26	—
7N.2W.10.444	6- 5-75	—	—	9,420	8.3	92	30.0	2,200	—	33.0	464	0	2,600	1,500	1.3	15	—
7N.1W.31.331	4-26-56	97	18.0	8,540	7.7	110	55.0	—	1,900	—	910	0	2,400	1,000	.4	27	6,170
8N.2W.24.131	—	—	18.0	5,290	7.3	330	140.0	—	830	—	270	0	2,200	500	.8	13	4,210
8N.1W.24.312	—	—	21.5	869	7.8	49	15.0	—	140	—	86	0	290	37	.5	29	—
8N.2W.12.111	4-29-57	—	16.5	4,910	7.4	140	43.0	—	1,000	—	680	0	1,900	200	2.0	16	3,690
							Rio Salado area										
1N.2W. 1.330	8-23-49	44	—	4,830	—	150	68.0	—	860	—	300	0	840	1,000	1.0	18	—
1N.1E. 5.100	2-15-50	150	—	3,910	—	140	75.0	—	640	—	260	0	900	640	.6	26	—
2N.2W.36.440	8-23-49	320	—	29,400	—	490	140.0	—	8,500	—	280	0	13,000	4,400	—	18	—
2N.1E. 9.220	8-23-49	285	—	820	—	14	3.0	—	160	—	110	6	240	28	1.1	34	—
3N.1E.34.320	8-24-49	155	—	850	—	26	10.0	—	140	—	120	14	220	39	—	—	—
3N.1W.25.444	5- -44	85	—	3,520	—	110	50.0	—	620	—	280	0	710	610	—	—	—
3N.1W.21.331	5-29-80	405	19.0	1,550	7.9	91	41.0	220	—	11.0	230	0	280	320	1.0	23	—
3N.2W.22.343	1- 6-50	40	—	710	—	72	28.0	—	40	—	300	0	76	30	1.4	33	—

Table 9. Sulfate to chloride ratio, sodium plus potassium to calcium ratio, and mixing ratio for selected ground-water analyses

[Specific conductance in microsiemens per centimeter at 25 °Celsius]

Location	Specific conductance	Sulfate to chloride	Sodium plus potassium to calcium	Mixing ratio
Mixed waters				
4N.1W.28.323	3,025	0.94	6.97	5:95
4N.1W.15.211	3,200	2.5	1.4	4:96
4N.1W.12.341	5,100	7.27	2.0	3:97
4N.1E.9.324	2,480	3.0	-	3:97
4N.2W.2.433	5,300	1.35	29	7:93
4N.3W.25.334	5,200	2.7	6.4	12:88
5N.1W.32.423	1,400	5.5	11.4	1:99
5N.1E.28.114	2,960	4.8	.69	3:97
5N.1W.14.231	3,970	7.83	-	2:98
5N.2W.21.422	4,290	.65	10.8	8:92
6N.1W.29.130	5,400	1.17	5.1	12:88
6N.2W.13.234	5,800	1.46	155	8:92
6N.2W.16.000	454	8.0	-	0.4:99.6
7N.1W.23.334	1,380	30.48	1.45	0.2:99.8
7N.1W.31.331	8,540	2.40	17.27	10:90
7N.2W.10.444	9,420	1.73	23.91	15:85
7N.2W.29.214	4,660	3.96	1.27	5:95
8N.1W.24.312	869	7.84	2.86	0.4:99.6
8N.2W.12.111	4,910	9.50	7.14	2:98
8N.2W.24.131	5,290	4.40	2.51	5:95
Brine				
6N.3W.35.341	26,700	0.41	7.1	--
7N.2W.19.343	37,000	.74	28.8	--
7N.3W.13.444	45,000	.76	32.4	--
7N.2W.18.112	36,800	.62	69.4	--
7N.2W.6.414	36,500	.62	27.3	--
8N.2W.30.313	41,400	.81	20.2	--
8N.2W.20.432	32,600	.78	15.1	--
8N.3W.12.442	30,100	.66	30.2	--

If the assumption is made that the major ions remain in solution (no chemical reactions occur) during the mixing of the local recharge water and the brine, the ratio of sulfate to chloride in the mixed waters (regional water) is approximately the same as the ratio in the brine. This is true because of the comparatively small concentrations of ions in the recharge water. The data in table 9 indicate that there is a change in the ratio of sulfate to chloride in the mixed water compared to the brine. The sulfate to chloride ratio for the mixed waters ranges from 0.65 to 30.48 (table 9 and fig. 23). The sulfate to chloride ratio for the brine is approximately 0.7. This may indicate that chemical reactions are taking place as the waters mix and move through the aquifer. Because of its chemical properties, the chloride ion can be assumed to be conservative as compared to other ions in water, suggesting that sulfate ions are introduced to the water as the water moves through the aquifer. Correspondingly, the ratio of the concentrations of sodium plus potassium ions to calcium ions also changes as the waters mix. The ratio in the brine is approximately 30, whereas the ratio in the mixed waters ranges from 0.7 to 155 (table 9 and fig. 23). In general, the ratio is less than 7.0. This means that there is an increase in calcium as compared to sodium plus potassium as the water mixes and moves through the aquifer. The increase in sulfate and calcium may be explained by the dissolution of gypsum. Gypsum probably is found in the sediments of the area because of the presence of playa-type deposits (Kelley, 1977, p. 16-17). Near San Acacia (fig. 2), rocks formed in playas of approximately the same age contain beds of gypsum as much as 5 feet thick.

The specific conductance of mixed waters varies considerably throughout the area (fig. 23). The sulfate to chloride ratios and the sodium plus potassium to calcium ratios also are variable (table 9 and fig. 23). If mixing were uniform throughout the area and the chemical reactions were the same, the changes in specific conductance and ion ratios would be expected to be more uniform, and areal trends would be expected. Because the changes in specific conductance and ion ratios between water in wells are so varied, it is difficult to make generalizations about the distribution of recharge and the type of chemical reactions occurring. A difference in the ion ratios of the brine compared to the mixed water that can be explained by dissolution of gypsum is indicated in table 9. In general, most recharge probably occurs along arroyos; thus, wells near arroyos may yield water mixed with runoff that has infiltrated through the arroyo channels (smaller specific conductance). The chemical composition of this recharge water also probably is variable, which may explain the variability of the ion ratios in the area.

Infiltration of water from the Rio Puerco also recharges the aquifer. Water infiltrating through the bed of the Rio Puerco is expected to have a significantly larger specific conductance than recharge water resulting from runoff from precipitation that infiltrates through the beds of ephemeral channels. The specific conductance is approximately 2,000 microsiemens, and sodium is the dominant cation and sulfate the dominant anion in water from the Rio Puerco near Bernardo (table 2). Recharge water from the Rio Puerco mixing with ground water is expected to decrease the specific conductance of the regional ground water (mixed ground water).

The regional ground water in the southwest area becomes less saline as it moves eastward toward the ground-water trough. Water from wells 6N.1E.33.433, 7N.1W.23.334, and 8N.1W.24.312, which are near the axis of the trough, has a specific-conductance range between 869 and 1,380 microsiemens (fig. 23). In general, sulfate is the dominant anion and sodium plus potassium is the dominant cation (table 8). The composition of this water probably is similar to any regional ground water along the axis or near the margins of the trough. The chemistry of this water is similar to the chemistry of water in the Rio Grande valley south of the trough (2N.1E.9.220 and 3N.1E.34.320) (pl. 2 and table 8).

Rio Salado Area

Well 2N.2W.36.440 is completed in the Popotosa Formation and was reported to flow (Spiegel, 1955, p. 85). Water from this well has a sulfate concentration of 13,000 milligrams per liter and a much larger specific conductance than other water in the area (table 8). This water may represent water in confined aquifers underlying the Popotosa Formation, water moving up along the faults, or water that has been in the ground-water system for a long time. Water from well 1N.2W.1.330 probably represents ground-water underflow of the Rio Salado. This water is similar in quality to water discharging from springs along the Rio Salado upstream from this well (Spiegel, 1955, p. 94).

Well 3N.2W.22.343 is on an alluvial fan along the Ladron Mountains. In this area of the Ladron Mountains, Precambrian rocks are exposed (pl. 1). Water from well 3N.2W.22.343 represents precipitation that has infiltrated and recharged the ground-water system. The water has a very small specific conductance compared to other water in the area (pl. 2), indicating that the ground water has been in contact with relatively insoluble minerals in the alluvial fans.

Wells 1N.1E.5.100, 2N.1E.9.220, and 3N.1E.34.320 are located in or near the Rio Grande valley (pl. 2). The water from wells 2N.1E.9.220 and 3N.1E.34.320 contains smaller concentrations of dissolved constituents than does water from well 1N.1E.5.100 (table 8). The water from 1N.1E.5.100 contains 640 milligrams per liter of chloride, which is approximately 20 times more chloride than in water from the other wells in or near the river valley. Large chloride concentrations also occur in ground water in the northern Socorro Basin (the basin downgradient from the Albuquerque-Belen Basin). Simonett (1981), in a study of the effects of irrigation near San Acacia, determined that applied surface water that infiltrates after irrigation is forced out of the aquifer under the fields and into drains by water with large chloride concentrations. Simonett's (1981) conclusions imply that there are upward vertical gradients (upward movement of ground water) in the northern Socorro Basin. This upward movement of ground water probably also occurs in the southern Albuquerque-Belen Basin, probably caused by a decrease in cross-sectional area for ground-water flow between basins. The thickness and width of the aquifer are less in this area than in adjacent parts of the Albuquerque-Belen and Socorro Basins (Birch, 1980). Ground water from wells 1N.1E.5.100, 2N.1E.9.220, and 3N.1E.34.320 indicates that the upwelling does not significantly affect shallow ground water (ground water less than approximately 300 feet deep) as far north as well 2N.1E.9.220, but that water from well 1N.1E.5.100 is significantly affected by upwelling.

Conclusions

Sodium chloride brine enters the southwestern area along the western margin. The brine flows eastward toward the ground-water trough and mixes with the water in the aquifer and recharge water. The specific conductance of this mixed ground water is larger than that in most ground water in the Albuquerque-Belen Basin. The mixed ground water also dissolves gypsum as it moves through the aquifer. This trend is shown in Piper diagrams by a general increase in the percentages of calcium and sulfate of the mixed ground water in comparison to the percentages of calcium and sulfate in the brine. Ground water also mixes with water infiltrating through the bed of the Rio Puerco. Recharge from the Rio Puerco probably decreases the specific conductance of ground water in the aquifer. Mountain-front runoff derived from Precambrian outcrops in the Ladron Mountains has a much smaller specific conductance than most ground water in the aquifer. In areas where this recharge mixes with ground water, the specific conductance of the mixed water is expected to be smaller than that in most ground water in the southwestern area.

Ground water with large concentrations of chloride in the southern part of the southwestern area probably is due to upward movement of deep basin water. This probably is the result of a constriction to ground-water flow between the Albuquerque-Belen and Socorro Basins (fig. 1).

Northern Area

The northern area of the Albuquerque-Belen Basin is bounded on the east by the Manzanita and Sandia Mountains (pl. 2). These mountains are fault-block mountains composed of a Precambrian core and capped by Paleozoic limestone that dips to the east. A bench along the west side of these mountains is composed of Paleozoic, Mesozoic, and Tertiary rocks and is covered with a thin layer of the aquifer. Springs commonly are located near the fault that separates the bench and the thick section of the aquifer. The western boundary of the northern area is comprised of the Cretaceous rocks that bound the Albuquerque-Belen Basin. These rocks consist of deep-water marine shale, beach sandstone, and continental sandstone and shale. The area is bounded on the north by the Jemez volcanic complex, which consists of interbedded volcanic rocks and volcaniclastic sediments, Paleozoic rocks, Mesozoic rocks, and Tertiary basin-fill sediments. The western half of the southern boundary to this area is near the northern limit of ground water in the aquifer significantly affected by ground-water inflow from bedrock units older than Cretaceous age along the west margin of the basin. The eastern half of the southern boundary of this area is just north of Los Lunas (pl. 2). This boundary is based on a slight difference in specific conductance north and south of the boundary.

Recharge to the aquifer in this area occurs along the east, west, and northern boundaries. On the east, recharge occurs as infiltration of runoff from precipitation on Precambrian and Paleozoic rocks of the Manzanita and Sandia Mountains. On the west, recharge occurs as ground-water inflow from adjacent bedrock units and from infiltration of runoff from precipitation. On the north, the aquifer is recharged by infiltration of runoff from the Jemez volcanic complex, ground-water inflow from the Jemez volcanic complex, and ground-water inflow from the adjacent Santo Domingo Basin (figs. 1 and 2). Ground water in the aquifer moves from the east and west boundaries of the area toward the ground-water trough. In the northern part of the area, ground water moves south or southeast (fig. 9).

Water Derived from Paleozoic Rocks

Two springs (8N.4E.9.314 and 9N.4E.24.114) and a well (9N.4E.35.200) west of the Manzanita Mountains derive water from Paleozoic limestone, shale, and sandstone. Water from spring 8N.4E.9.314 contains 217 milligrams per liter of sulfate (table 10). This spring issues from the Yeso Formation, which contains gypsum beds. Dissolution of gypsum probably is the reason for the relatively large sulfate concentration in this water. Waters from spring 9N.4E.24.114 and well 9N.4E.35.200 have chloride concentrations of 355 and 120 milligrams per liter, respectively. These concentrations are larger than those in water from other wells or springs in this area. The large chloride concentrations may be due to dissolution of salt crystals in the marine limestone or may represent water that has a long residence time in the Paleozoic rocks. The distribution of anions in water from spring 9N.4E.24.114 and well 9N.4E.35.200 is very similar to the distribution of anions in water from well 9N.4E.20.221 downgradient from spring 9N.4E.24.114. The water from

well 9N.4E.20.221 may represent a mixture of ground water similar to water from spring 9N.4E.24.114 and recharge water. This would explain the smaller specific conductance of water from well 9N.4E.20.221 (704 microsiemens) compared to the specific conductance of water from spring 9N.4E.24.114 (2,540 microsiemens) and the similarity in the distribution of anions.

Recharge from the East

Water from wells 9N.4E.4.213, 10N.4E.34.214, 10N.4E.24.344, and spring 10N.4E.13.242, located near Tijeras Arroyo, is of similar character; calcium is the dominant cation, and the specific conductance ranges from 569 to 963 microsiemens (table 10). This water represents recharge or inflow from the Sandia Mountains.

North and west of the previously discussed area, water from wells 10N.3E.36.132, 10N.4E.22.342, 10N.4E.22.344, 11N.4E.1.314, 12N.4E.35.234, 9N.3E.11.241, 10N.3E.35.111, 10N.4E.20.111, and 10N.3E.11.200 has a specific conductance generally less than 500 microsiemens (table 10), and calcium and bicarbonate are the dominant ions (fig. 24). This water probably is representative of ground water recharged to the aquifer from the Sandia Mountains.

Water from wells 10N.3E.36.132, 9N.3E.11.241, and 10N.4E.20.111 is supersaturated or at saturation with respect to calcite, implying that the dissolution of calcite may be a dominant process affecting the chemistry of this water. Examination of the material-balance-model results shows that the concentration of sulfate is relatively small, indicating that gypsum dissolution is not a major reaction in the evolution of ground-water quality in recharge water from the east (table 11). The model results also show a negative sodium concentration after the removal of silica, indicating that the assumed plagioclase-alteration reaction probably is not correct (table 11).

Water Derived from Cretaceous Rocks

Several wells on the west side of the area, 10N.2W.25.114, 10N.2W.25.432, 10N.2W.11.432, 10N.1W.21.132, 12N.1W.14.111, and 12N.1W.17.100, derive water from Cretaceous rocks or water affected by water from Cretaceous rocks. Sulfate is the dominant anion and sodium is the dominant cation (fig. 24). The large sulfate concentration probably is due to the dissolution of gypsum in the Cretaceous rocks. Dissolution of gypsum usually results in large concentrations of calcium; however, this water does not have large calcium concentrations. The large sodium concentrations and small calcium concentrations probably are due to ion exchange (calcium for sodium) on the clay in the Cretaceous rocks. The relatively large positive sodium concentrations after silica is removed and the relatively large sulfate concentrations in the results of the material-balance model indicate that ion exchange and the dissolution of gypsum are the dominant chemical processes in the evolution of ground water derived from Cretaceous rocks (table 11). This sodium sulfate water probably is representative of inflow from the Cretaceous rocks along the west side of the basin.

Table 10. Ground-water-quality data for selected sites in the northern area

[Well depth, asterisk (*) indicates water level, in feet below land surface, and SP indicates spring; E, estimated; ft, feet; °C, degrees Celsius; mg/L, milligrams per liter]

Location	Date sampled	Well depth (ft)	Temperature (°C)	Specific conductance (microsiemens per centimeter at 25 °C)	pH	Calcium (mg/L)	Magnesium (mg/L)	Sodium (mg/L)	Sodium plus potassium (mg/L as sodium)	Potassium (mg/L)	Bicarbonate (mg/L)	Carbonate (mg/L)	Sulfate (mg/L)	Chloride (mg/L)	Fluoride (mg/L)	Silica (mg/L)	Dissolved solids (mg/L)
Water derived from Paleozoic rocks																	
8N.4E. 9.314	2-27-56	SP	13.5	836	7.4	—	—	—	—	—	217	0	217	30	—	—	—
9N.4E.35.200	8-21-44	81	16.5	1,480	7.5	180	36.0	—	98	—	700	0	59	120	—	—	892
9N.4E.24.114	7-25-45	SP	17.0	2,540	—	224	51.0	—	290	—	956	0	100	355	0.8	16	—
9N.4E.20.221	7- 9-57	—	23.0	704	7.6	66	19.0	—	58	—	280	0	59	48	1.3	28	427
10N.4E. 3.223	5- 7-56	291	24.5	466	7.7	65	10.0	—	22	—	200	0	54	14	1.4	23	298
Recharge from the east																	
10N.3E.36.132	5-19-56	997	20.0	318	7.8	32	7.0	—	25	—	130	0	36	9	0.4	38	231
9N.4E. 4.213	3-30-72	—	22.5	569	7.5	65	12.0	35	—	3.0	190	0	82	20	.7	28	368
10N.4E.34.214	9-27-57	1,200	14.3	636	7.3	79	22.0	—	26	—	240	0	100	16	.6	20	—
10N.4E.24.344	11-13-63	110	—	734	7.8	74	29.0	—	41	—	220	0	170	18	—	22	—
10N.4E.22.342	4- 6-65	1,341	23.3	472	7.7	59	9.0	28	—	—	192	0	63	11	.6	25	308
10N.4E.22.344	10- 4-73	—	24.5	339	8.0	37	3.0	28	—	2.0	151	0	33	7	.7	24	266
10N.4E.13.242	5- 7-56	SP	13.5	963	7.7	149	31.0	—	29	—	497	0	121	18	1.6	34	628
11N.4E. 1.314	5- 8-56	—	17.0	297	7.2	42	7.0	—	12	—	163	0	16	6	1.2	20	186
11N.4E.16.341	5- 1-57	750	20.5	331	7.5	43	7.0	—	17	—	170	0	21	6	.6	26	197
12N.4E.35.234	9-21-50	175	—	616	—	76	7.0	—	36	—	290	0	71	9	4.0	21	—
9N.3E.11.241	4-26-57	341	19.5	639	7.8	83	11.0	—	28	—	140	0	46	9	.6	41	490
10N.3E.35.111	7-11-57	1,000	—	292	7.9	33	7.0	—	19	—	130	0	30	9	.4	38	200
10N.4E.20.111	8- 8-58	1,280	21.5	315	7.9	40	1.0	—	26	—	130	0	19	22	.5	28	206
10N.4E. 8.434	1-21-74	571 *	24.0	284	7.9	32	1.0	24	—	2.0	123	0	19	13	.8	32	182
10N.3E.11.200	5-15-52	246 *	—	313	8.0	40	5.0	—	20	—	140	0	34	8	.3	41	—
10N.4E. 4.221	4-13-65	1,329	23.9	285	7.9	37	2.0	23	—	—	148	0	18	5	.8	26	190
11N.3E.35.244	11- 5-60	—	17.0	275	8.1	34	4.0	—	21	—	130	0	28	10	.4	33	181
11N.3E.34.141	5- 1-57	150	16.5	291	7.7	34	9.0	—	13	—	130	0	31	10	.4	35	190
12N.4E.17.424	5- 7-56	E350	20.0	329	7.9	40	6.0	—	24	—	140	0	39	12	.6	47	241

Table 10. Ground-water-quality data for selected sites in the northern area - Continued

Location	Date sampled	Well depth (ft)	Temperature (°C)	Specific conductance (microsiemens per centimeter at 25 °C)	pH	Calcium (mg/L)	Magnesium (mg/L)	Sodium (mg/L)	Sodium plus potassium (mg/L as sodium)	Potassium (mg/L)	Bicarbonate (mg/L)	Carbonate (mg/L)	Sulfate (mg/L)	Chloride (mg/L)	Fluoride (mg/L)	Silica (mg/L)	Dissolved solids (mg/L)
							Water derived from Cretaceous rocks										
10N.2W.25.432	6- 6-67	193	20.5	919	8.3	58	26.0	—	110	—	180	4	280	21	0.9	23	—
10N.1W.21.132	6- 6-67	205	21.5	951	8.4	47	6.0	—	160	—	160	6	300	20	.3	19	—
10N.2W.11.432	6- 6-67	128 *	18.5	3,080	—	—	—	—	—	—	—	0	1,300	14	—	—	—
10N.2W.25.114	10-26-67	—	—	1,930	8.2	100	20.0	310	—	—	220	0	780	30	—	18	1,370
11N.1W.28.224	4-23-57	96	13.0	371	7.5	34	8.0	—	33	—	150	0	46	10	1.0	59	282
12N.1W.17.100	4-28-61	225	—	10,000	8.6	56	14.0	—	2,600	—	510	26	3,400	1,300	1.3	9	—
12N.1W.14.111	6-20-80	120	20.0	1,180	8.3	19	6.0	240	—	3.0	410	0	210	5	1.9	27	—
							Local recharge water in the Jemez area										
14N.3E. 3.434	5- 8-59	637	—	357	7.7	—	—	—	—	—	130	0	52	12	—	—	—
14N.2E. 5.320	4-18-57	130	14.5	399	7.8	48	11.0	—	13	—	130	0	29	3	0.4	18	247
15N.2E.22.423	1-20-60	333	—	458	7.9	45	5.0	—	45	—	160	0	47	34	.6	30	290
15N.2E.12.431	4- 4-74	—	17.0	490	7.9	49	2.0	56	—	6.0	228	0	57	4	.4	36	—
							Water associated with the Jemez area										
12N.4E. 6.213	5- 1-57	500	18.0	501	7.8	37	11.0	—	56	—	170	0	53	46	0.8	—	339
12N.4E. 5.214	9-25-74	—	27.0	642	—	41	7.0	79	—	8.0	200	0	40	72	1.0	73	—
13N.3E.36.123	2-21-75	—	—	860	7.7	98	15.0	55	—	6.0	223	0	170	47	.4	29	—
13N.4E.29.421	7-26-52	128	—	524	7.6	30	6.0	—	81	—	230	0	46	28	1.4	91	—
13N.3E.25.244	5-18-56	119	—	1,830	7.6	200	30.0	—	140	—	110	0	310	360	.6	41	1,300
13N.4E.19.234	6-27-63	360	—	1,350	8.0	100	29.0	—	130	—	170	0	160	250	.6	46	—
13N.3E. 3.223	4-18-57	183	16.0	736	7.4	81	19.0	—	44	—	130	0	170	32	.8	36	503
14N.4E.31.444	4-25-50	100	—	1,660	7.5	110	17.0	—	240	—	240	0	360	200	.9	25	—
14N.3E.22.311	8-12-54	63	—	624	—	0	—	—	—	—	220	0	—	42	—	58	0
14N.2E.23.321	4-18-57	360 *	—	783	7.4	—	—	—	—	—	130	0	98	110	—	—	—
14N.3E.18.340	4-18-57	130	16.5	2,570	7.3	250	49.0	—	220	—	190	—	450	480	—	32	1,650
15N.1E.26.222	3-24-59	117	—	6,510	7.7	250	14.0	—	1,490	—	420	0	3,050	280	1.2	11	5,320
15N.2E. 6.222	4- 4-54	177	—	5,920	—	180	31.0	—	1,190	—	180	0	290	1,140	5.0	91	3,680
15N.2E.36.314	12-19-51	18	—	1,910	7.7	92	17.0	—	310	—	300	0	350	260	1.7	3	—

Table 10. Ground-water-quality data for selected sites in the northern area - Continued

Location	Date sampled	Well depth (ft)	Temperature (°C)	Specific conductance (microsiemens per centimeter at 25 °C)	pH	Calcium (mg/L)	Magnesium (mg/L)	Sodium (mg/L)	Sodium plus potassium (mg/L as sodium)	Potassium (mg/L)	Bicarbonate (mg/L)	Carbonate (mg/L)	Sulfate (mg/L)	Chloride (mg/L)	Fluoride (mg/L)	Silica (mg/L)	Dissolved solids (mg/L)
Water with anomalous chloride concentrations northeast of Albuquerque																	
10N.4E. 5.122	1- 9-59	1,224	23.5	600	7.9	64	4.0	—	50	—	150	0	27	96	0.3	32	370
11N.4E.31.412	1-28-59	1,200	22.0	585	8.1	64	6.0	—	41	—	140	0	34	84	.2	33	357
11N.4E.28.111	6-20-79	725 *	26.0	422	7.7	44	2.0	43	—	4.0	110	0	31	61	.7	30	—
11N.4E.20.232	3-24-80	1,785	29.0	580	7.7	37	6.0	74	—	6.0	160	0	37	86	1.1	41	—
12N.4E.30.124	5- 7-56	—	17.0	631	7.8	70	19.0	—	36	—	210	0	84	44	.4	35	416
12N.4E.32.242	5- 7-56	579 *	18.5	735	7.7	73	15.0	—	56	—	180	0	63	100	.2	48	488
Water from the area west of Albuquerque where ion exchange is dominant																	
8N.1E. 1.342	5-28-57	430	20.0	475	8.1	27	7.0	—	66	—	140	0	96	12	1.2	44	338
10N.2E.36.413	5-18-65	60	—	545	8.2	39	11.0	—	65	—	190	0	100	14	.5	47	364
10N.2E.33.240	8-25-73	1,200	30.0	524	8.9	6	—	110	—	2.0	165	5	84	13	1.1	40	340
10N.2E.25.213	5-21-57	360	19.0	556	7.7	33	6.0	—	81	—	180	0	110	17	.6	60	390
10N.2E.21.343	4- 6-65	1,180	31.0	495	9.1	1	1.0	—	110	—	150	19	69	9	1.0	42	332
10N.1E.30.222	8- 4-60	—	—	1,420	7.8	110	27.0	180	—	7.0	100	0	630	20	.6	15	1,090
10N.3E.20.344	5-22-57	418	—	405	7.9	30	9.0	—	41	—	140	0	48	22	.4	81	314
10N.2E.24.233	5-21-57	336	16.5	454	7.7	33	6.0	—	56	—	160	0	78	15	.6	62	327
10N.1E.18.331	11-17-54	275	18.0	364	—	—	—	—	40	—	150	0	34	16	.8	21	—
10N.2E.12.412	5-21-57	1,000	21.0	499	7.7	36	8.0	—	62	—	180	0	87	12	.4	64	361
10N.2E. 9.133	9-25-78	1,675	28.0	450	8.7	4	—	110	—	2.0	200	0	57	6	1.3	30	—
10N.2E. 2.313	9-14-78	1,452	26.0	560	7.9	10	2.0	97	—	4.0	150	0	99	18	1.1	50	—
11N.1E.26.424	5- 9-56	935	—	572	10.1	19	2.0	—	110	—	40	73	100	22	.8	7	353
11N.1W.11.424	4-23-57	282	18.5	397	7.6	23	6.0	—	57	—	160	0	49	10	.6	25	246
11N.2E. 2.343	4-15-65	1,000	—	363	7.8	34	8.0	—	32	—	160	0	36	10	.5	61	276
11N.2E. 3.213	5- 2-80	1,363	23.0	485	7.7	13	3.0	87	—	6.0	160	0	90	10	1.0	66	—
12N.1E.22.222	4- 6-56	1,540	21.5	373	7.7	—	—	—	—	—	150	0	43	4	—	—	—
12N.3E.30.121	12-12-74	420 *	16.0	348	7.5	31	6.0	30	—	6.0	142	0	37	7	.4	60	251
12N.2E.14.433	12-12-74	637 *	19.5	367	—	18	4.0	53	—	5.0	127	0	43	7	.4	50	263

Table 10. Ground-water-quality data for selected sites in the northern area - Concluded

Location	Date sampled	Well depth (ft)	Temperature (°C)	Specific conductance (microsiemens per centimeter at 25 °C)	pH	Calcium (mg/L)	Magnesium (mg/L)	Sodium (mg/L)	Sodium plus potassium (mg/L as sodium)	Potassium (mg/L)	Bicarbonate (mg/L)	Carbonate (mg/L)	Sulfate (mg/L)	Chloride (mg/L)	Fluoride (mg/L)	Silica (mg/L)	Dissolved solids (mg/L)
Water from the Rio Grande valley																	
8N.3E.14.231	3-22-56	—	22.0	360	7.6	—	—	—	—	—	140	0	35	10	—	—	—
8N.2E. 1.312	10- 2-56	74	14.0	499	7.6	0	—	—	—	—	160	0	95	14	—	—	—
9N.2E.35.400	8- 3-63	235	15.5	936	7.8	110	11.0	—	88	—	320	0	200	38	0.4	37	642
9N.2E.35.113	10- 2-56	115	16.0	660	7.5	—	—	—	—	—	200	0	130	28	—	—	—
9N.3E. 8.300	8-16-46	39	—	327	—	40	6.0	—	22	—	160	0	29	10	.6	—	—
9N.2E.12.322	10- 2-56	240	—	823	7.9	—	—	—	—	—	260	0	190	24	—	—	—
9N.2E. 3.342	10- 5-56	140	20.0	475	7.7	—	—	—	—	—	150	0	77	22	—	—	—
10N.3E.19.111	4-26-57	100	14.0	556	7.7	63	13.0	—	38	—	190	0	110	16	.4	33	370
11N.3E.22.314	9- -69	150	—	958	8.4	100	11.0	—	110	—	330	8	220	22	.2	28	—
11N.3E.20.143	1-17-60	64	15.0	1,070	7.6	170	23.0	51	—	6.0	370	0	280	28	.5	33	—
11N.3E.21.132	4-23-65	201	—	365	7.6	40	9.0	—	22	—	132	0	47	18	.3	30	243
11N.3E.15.121	4-23-65	168	—	281	8.0	35	5.0	17	—	—	122	0	30	8	.4	26	187
12N.3E.35.243	5- 8-56	15	10.5	521	7.8	63	10.0	—	38	—	190	0	94	18	.4	24	348
12N.3E.33.400	4-23-62	47	—	1,020	7.6	160	10.0	—	69	—	430	0	190	21	.4	30	709
12N.3E.27.222	5- 1-57	70	15.0	906	7.5	120	22.0	—	58	—	380	0	150	17	.4	34	612
12N.3E.24.423	2-27-61	96	15.0	929	7.7	130	19.0	—	58	—	370	0	160	20	.4	36	648
Water from the Rio Grande valley with large silica concentrations																	
9N.3E.18.413	9-18-61	—	—	735	7.5	97	12.0	26	—	6.0	140	0	49	51	0.5	55	—
9N.2E.11.241	6-23-61	33	16.5	1,280	7.7	172	23.0	—	90	—	288	0	370	68	—	39	—
9N.3E. 5.234	5- 2-57	92	20.5	296	7.8	32	9.0	—	14	—	130	0	31	6	.6	57	221
10N.3E.32.421	6-25-80	—	26.0	400	7.6	28	7.0	40	—	9.0	120	0	47	33	—	78	—
10N.3E.21.433	4-26-57	323	—	467	8.0	53	14.0	—	21	—	110	0	94	30	.4	45	324
10N.3E.17.343	5- 1-57	520	18.0	889	7.5	110	29.0	—	40	—	230	0	210	52	.4	61	633
10N.2E.14.211	4-26-57	162	16.0	583	8.0	58	14.0	—	45	—	170	0	120	20	.4	51	406
10N.3E. 8.443	5-21-57	351	20.0	585	7.7	63	13.0	—	41	—	180	0	110	24	.4	64	427
10N.2E. 2.212	4-26-57	250	—	614	7.7	61	19.0	—	38	—	170	0	130	26	.6	75	436
11N.3E.31.231	5-21-57	824	18.8	308	7.9	30	7.0	—	23	—	130	0	31	9	.4	67	250
11N.2E.22.441	4-25-57	240	20.0	2,300	7.4	220	58.0	—	270	—	220	0	1,100	31	.6	15	1,850
12N.3E.31.134	4-27-65	350	—	501	7.8	57	10.0	—	29	—	130	0	58	51	.5	52	343
13N.4E. 1.243	5-11-53	235	—	1,520	—	167	38.0	—	140	—	490	0	380	53	.5	74	1,100
13N.4E.11.113	7-26-52	32	—	1,320	7.3	100	25.0	—	180	—	630	0	170	39	.6	68	902

Table 11. Material-balance-model results for selected ground-water analyses in the northern area

Location	Sodium (Na^+) (milli-moles)	Chlo-ride (Cl^-) (milli-moles)	Magne-sium (Mg^{2+}) (milli-moles)	Calcium (Ca^{2+}) (milli-moles)	Bicar-bonate (HCO_3^-) (milli-moles)	Sul-fate (SO_4^-) (milli-moles)	Silica (Si) (milli-moles)	Sodium (Na+) after chlo-ride removal (milli-moles)	Calcium (Ca^{2+}) after magne-sium removal (milli-moles)	Bicar-bonate (HCO_3) after magne-sium removal (milli-moles)	Calcium (Ca^{2+}) after sul-fate removal (milli-moles)	Calcium (Ca^{2+}) after silica removal (milli-moles)	Bicar-bonate (HCO_3) after silica removal (milli-moles)	Sodium (Na^+) after silica removal (milli-moles)	Calcium (Ca^{2+}) after bicar-bonate removal (milli-(moles)	Excess sodium (Na^+) (milli-moles)
Water derived from Paleozoic rocks																
9N.4E.24.114	12.53	10.01	2.10	5.59	15.67	1.04	0.27	2.51	3.49	7.28	2.45	2.28	6.57	2.14	-1.00	0.07
9N.4E.20.221	2.52	1.35	.78	1.65	4.59	.61	.47	1.17	.87	1.46	.25	-.04	.22	.52	-.15	.11
10N.4E. 3.223	.96	.39	.41	1.62	3.28	.56	.38	.56	1.21	1.63	.65	.41	.62	.03	.10	.12
Recharge from the east																
9N.4E. 4.213	1.52	0.56	0.49	1.62	3.11	0.85	0.47	0.96	1.13	1.14	0.27	-0.02	-0.10	0.31	0.03	0.19
9N.3E.11.241	1.22	.25	.45	2.07	2.30	.48	.68	.96	1.62	.49	1.14	.71	-1.33	.01	1.38	1.38
10N.4E.34.214	1.13	.45	.90	1.97	3.93	1.04	.33	.68	1.07	.31	.02	-.18	-.57	.22	.10	.21
10N.4.5E.24.3	1.78	.51	1.19	1.85	3.61	1.77	.37	1.28	.65	-1.17	-1.12	-1.35	-2.14	.76	-.28	.11
10N.4E.22.342	1.22	.31	.37	1.47	3.15	.66	.42	.91	1.10	1.67	.45	.19	.56	.33	-.09	.07
10N.4E.22.344	1.22	.20	.12	.92	2.48	.34	.40	1.02	.80	1.98	.46	.21	.92	.46	-.25	-.02
10N.4E.13.242	1.26	.51	1.28	3.72	8.15	1.26	.57	.75	2.44	3.05	1.18	.83	1.54	-.04	.06	.04
10N.3E.36.132	1.09	.25	.29	.80	2.13	.38	.63	.83	.51	.98	.14	-.26	-.70	-.05	.09	.07
10N.3E.35.111	.83	.25	.29	.82	2.13	.31	.63	.57	.54	.98	.22	-.17	-.70	-.31	.18	.02
10N.4E.20.111	1.13	.62	.04	1.00	2.13	.20	.47	.51	.96	1.97	.76	.47	.73	-.14	.10	.03
10N.4E. 8.434	1.04	.37	.04	.80	2.02	.20	.53	.68	.76	1.85	.56	.23	.44	-.07	.01	-.02
10N.3E.11.200	.87	.23	.21	1.00	2.30	.35	.68	.64	.79	1.47	.44	.01	-.34	-.31	.18	.03
10N.4E. 4.221	1.00	.14	.08	.92	2.43	.19	.43	.86	.84	2.10	.65	.38	.95	.26	-.09	.04
11N.4E. 1.314	.52	.17	.29	1.05	2.67	.17	.33	.35	.76	1.52	.59	.39	.64	-.11	.07	.01
11N.3E.35.244	.91	.28	.16	.85	2.13	.29	.55	.63	.68	1.47	.39	.05	.01	-.14	.04	-.02
11N.3E.34.141	.57	.28	.37	.85	2.13	.32	.58	.28	.48	.65	.16	-.21	-.90	-.53	.24	-.02
11N.4E.16.341	.74	.17	.29	1.07	2.79	.22	.43	.57	.78	1.64	.57	.30	.48	-.03	.05	.04
12N.4E.35.234	1.57	.25	.70	1.90	4.75	.74	.35	1.31	1.20	1.96	.46	.24	1.03	.82	-.27	.14
12N.4E.32.242	2.44	2.82	.62	1.82	2.95	.66	.80	-.39	1.20	.48	.55	.05	-1.64	-1.50	.87	.12
12N.4E.17.424	1.04	.34	.25	1.00	2.30	.41	.78	.71	.75	1.31	.34	-.14	-.77	-.39	.24	.05
Water derived from Cretaceous rocks																
10N.2W.25.432	4.78	0.59	1.07	1.45	2.95	2.92	0.38	4.19	0.38	-1.33	-2.54	-2.78	-2.35	3.66	-1.61	0.22
10N.1W.21.132	6.96	.56	.25	1.17	2.62	3.13	.32	6.40	.93	1.64	-2.20	-2.40	.79	5.95	-2.79	.18
11N.1W.28.224	1.44	.28	.33	.85	2.46	.48	.98	1.15	.52	1.14	.04	-.57	-1.47	-.22	.16	.05
12N.1W.17.100	113.09	36.67	.58	1.40	8.36	35.42	.15	76.42	.82	6.06	-34.60	-34.69	5.65	76.21	-37.52	.59
12N.1W.14.111	10.44	.14	.25	.47	6.72	2.19	.45	10.30	.23	5.73	-1.96	-2.24	4.54	9.67	-4.51	.33

Table 11. Material-balance-model results for selected ground-water analyses in the northern area - Continued

Location	Sodium (Na^+) (milli-moles)	Chlo-ride (Cl^-) (milli-moles)	Magne-sium (Mg^{2+}) (milli-moles)	Calcium (Ca^{2+}) (milli-moles)	Bicar-bonate (HCO_3^-) (milli-moles)	Sul-fate (SO_4^-) (milli-moles)	Silica (Si) (milli-moles)	Sodium (Na+) after chlo-ride removal (milli-moles)	Calcium (Ca^{2+}) after magne-sium removal (milli-moles)	Bicar-bonate (HCO_3) after magne-sium removal (milli-moles)	Calcium (Ca^{2+}) after sul-fate removal (milli-moles)	Calcium (Ca^{2+}) after silica removal (milli-moles)	Bicar-bonate (HCO_3) after silica removal (milli-moles)	Sodium (Na^+) after silica removal (milli-moles)	Calcium (Ca^{2+}) after bicar-bonate removal (milli-(moles)	Excess sodium (Na^+) (milli-moles)
Local recharge in the Jemez area																
14N.2E. 5.320	0.57	0.08	0.45	1.20	2.13	0.30	0.30	0.48	0.75	0.32	0.44	0.26	-0.48	0.06	0.49	0.53
15N.2E.22.423	1.96	.96	.21	1.12	2.62	.49	.50	1.00	.92	1.80	.43	.12	.47	.30	-.12	.03
15N.2E.12.431	2.44	.11	.08	1.22	3.74	.59	.60	2.32	1.14	3.41	.55	.17	1.82	1.49	-.73	.01
Water associated with the Jemez area																
12N.4E. 5.214	3.44	2.03	0.29	1.02	3.28	0.42	1.22	1.41	0.74	2.13	0.32	-0.44	-1.10	-0.29	0.11	-0.03
13N.3E.36.123	2.39	1.33	.62	2.45	3.66	1.77	.48	1.07	1.83	1.19	.06	-.24	-.10	.39	-.20	.00
13N.4E.29.421	3.52	.79	.25	.75	3.77	.48	1.52	2.73	.50	2.78	.02	-.92	-1.24	.62	-.30	.01
13N.3E.25.244	6.09	10.16	1.23	4.99	1.80	3.23	.68	-4.07	3.76	-3.13	.53	.10	-4.95	-5.02	2.57	.07
13N.4E.19.234	5.65	7.05	1.19	2.50	2.79	1.67	.77	-1.40	1.30	-1.98	-.36	-.84	-4.02	-2.47	1.17	-.06
13N.3E. 3.223	1.91	.90	.78	2.02	2.13	1.77	.60	1.01	1.24	-1.00	-.53	-.91	-2.59	.18	.39	.48
14N.4E.31.444	10.44	5.64	.70	2.74	3.93	3.75	.42	4.80	2.05	1.14	-1.70	-1.96	.03	4.22	-1.98	.13
14N.3E.18.340	9.57	13.54	2.02	6.24	3.11	4.69	.53	-3.97	4.22	-4.95	-.47	-.80	-6.36	-4.71	2.38	.03
Water with anomalous chloride concentrations northeast of Albuquerque																
10N.4E. 5.122	2.17	2.71	0.16	1.60	2.46	0.28	0.53	-0.53	1.43	1.80	1.15	0.82	0.38	-1.28	0.63	-0.01
11N.4E.31.412	1.78	2.37	.25	1.60	2.30	.35	.55	-.59	1.35	1.31	1.00	.65	-.15	-1.35	.73	.05
11N.4E.28.111	1.87	1.72	.08	1.10	1.80	.32	.50	.15	1.02	1.47	.69	.38	.15	-.55	.31	.03
11N.4E.20.232	3.22	2.43	.25	.92	2.62	.39	.68	.79	.68	1.64	.29	-.13	-.18	-.16	-.05	-.12
12N.4E.30.124	1.57	1.24	.78	1.75	3.44	.88	.58	.32	.96	.32	.09	-.27	-1.23	-.49	.34	.10
Water from the area west of Albuquerque where ion exchange is dominant																
8N.1E. 1.342	2.87	0.34	0.29	0.67	2.30	1.00	0.73	2.53	0.39	1.14	-0.61	-1.07	-0.80	1.51	-0.67	0.09
10N.2E.36.413	2.83	.39	.45	.97	3.11	1.04	.78	2.43	.52	1.30	-.52	-1.01	-.78	1.34	-.62	.05
10N.2E.25.213	3.52	.48	.25	.82	2.95	1.15	1.00	3.04	.58	1.96	-.57	-1.19	-.69	1.65	-.85	-.02
10N.2W.25.114	13.48	.85	.82	2.50	3.61	8.13	.30	12.64	1.67	.32	-6.45	-6.64	-.48	12.22	-6.40	-.29
10N.2E.21.343	4.78	.25	.04	.02	2.46	.72	.70	4.53	-.02	2.29	-.73	-1.17	.44	3.56	-1.39	.39
10N.1E.30.222	7.83	.56	1.11	2.74	1.64	6.56	.25	7.27	1.63	-2.80	-4.93	-5.08	-3.47	6.92	-3.35	.11
10N.3E.20.344	1.78	.62	.37	.75	2.30	.50	1.35	1.16	.38	.81	-.12	-.96	-2.77	-.72	.42	.06
10N.2E.24.233	2.44	.42	.25	.82	2.62	.81	1.03	2.01	.58	1.64	-.24	-.88	-1.11	.57	-.33	-.04
10N.2E.12.412	2.70	.34	.33	.90	2.95	.91	1.07	2.36	.57	1.63	-.34	-1.00	-1.20	.87	-.40	.03
10N.2E. 2.313	4.22	.51	.08	.25	2.46	1.03	.83	3.71	.17	2.13	- .86	-1.38	- .08	2.55	-1.34	- .07

Table 11. Material-balance-model results for selected ground-water analyses in the northern area - Concluded

Location	Sodium (Na^+) (milli-moles)	Chloride (Cl^-) (milli-moles)	Magnesium (Mg^{2+}) (milli-moles)	Calcium (Ca^{2+}) (milli-moles)	Bicarbonate (HCO_3^-) (milli-moles)	Sulfate (SO_4^-) (milli-moles)	Silica (Si) (milli-moles)	Sodium (Na+) after chloride removal (milli-moles)	Calcium (Ca^{2+}) after magnesium removal (milli-moles)	Bicarbonate (HCO_3) after magnesium removal (milli-moles)	Calcium (Ca^{2+}) after sulfate removal (milli-moles)	Calcium (Ca^{2+}) after silica removal (milli-moles)	Bicarbonate (HCO_3) after silica removal (milli-moles)	Sodium (Na^+) after silica removal (milli-moles)	Calcium (Ca^{2+}) after bicarbonate removal (milli-(moles)	Excess sodium (Na^+) (milli-moles)
Water from the area west of Albuquerque where ion exchange is dominant - Concluded																
11N.1E.26.424	4.78	0.62	0.08	0.47	0.66	1.04	0.12	4.16	0.39	0.33	-0.65	-0.73	-0.00	3.99	-0.73	1.27
11N.2E.22.441	11.74	.87	2.39	5.49	3.61	11.46	.25	10.87	3.10	-5.94	-8.36	-8.51	-6.60	10.52	-5.21	.05
11N.1W.11.424	2.48	.28	.25	.57	2.62	.51	.42	2.20	.33	1.64	-.18	-.44	.53	1.62	-.71	.10
11N.2E. 2.343	1.39	.28	.33	.85	2.62	.38	1.02	1.11	.52	1.31	.14	-.49	-1.39	-.31	.21	.05
11N.2E. 3.213	3.78	.28	.12	.32	2.62	.94	1.10	3.50	.20	2.13	-.74	-1.42	-.79	1.97	-1.03	-.04
12N.3E.30.121	1.30	.20	.25	.77	2.33	.39	1.00	1.11	.53	1.34	.14	-.48	-1.32	-.29	.18	.03
12N.2E.14.433	2.31	.20	.16	.45	2.08	.45	.83	2.11	.28	1.42	-.16	-.68	-.79	.95	-.29	.19
Water from the Rio Grande valley																
9N.2E.35.400	3.83	1.07	0.45	2.74	5.25	2.08	0.62	2.76	2.29	3.44	0.21	-0.18	1.80	1.90	-1.07	-0.13
10N.3E.19.111	1.65	.45	.53	1.57	3.11	1.15	.55	1.20	1.04	.98	-.11	-.45	-.48	.44	-.21	.01
11N.3E.22.314	4.78	.62	.45	2.50	5.41	2.29	.47	4.16	2.04	3.60	-.25	-.54	2.36	3.51	-1.72	.04
11N.3E.20.143	2.22	.79	.95	4.24	6.07	2.92	.55	1.43	3.30	2.28	.38	.04	.82	.66	-.37	-.04
11N.3E.21.132	.96	.51	.37	1.00	2.16	.49	.50	.45	.63	.68	.14	-.17	-.64	-.25	.15	.03
11N.3E.15.121	.74	.23	.21	.87	2.00	.31	.43	.51	.67	1.18	.36	.09	.03	-.09	.07	.03
12N.3E.35.243	1.65	.51	.41	1.57	3.11	.98	.40	1.15	1.16	1.47	.18	-.07	.41	.59	-.27	.02
12N.3E.33.400	3.00	.59	.41	3.99	7.05	1.98	.50	2.41	3.58	5.40	1.60	1.29	4.08	1.71	-.75	.11
12N.3E.27.222	2.52	.48	.90	2.99	6.23	1.56	.57	2.04	2.09	2.61	.53	.17	1.10	1.25	-.38	.25
12N.3E.24.423	2.52	.56	.78	3.24	6.07	1.67	.60	1.96	2.46	2.94	.80	.42	1.35	1.12	-.25	.31
Water from the Rio Grande valley with large silica concentrations																
9N.3E.18.413	1.13	1.44	0.49	2.42	2.30	0.51	0.92	-0.31	1.93	0.32	1.42	0.85	-2.11	-1.59	1.90	1.11
9N.2E.11.241	3.91	1.92	.95	4.29	4.72	3.85	.65	2.00	3.35	.94	-.51	-.91	-.79	1.09	-.52	.03
9N.3E. 5.234	.61	.17	.37	.80	2.13	.32	.95	.44	.43	.65	.11	-.49	-1.87	-.88	.45	.01
10N.3E.32.421	1.74	.93	.29	.70	1.97	.49	1.30	.81	.41	.82	-.08	-.89	-2.64	-1.00	.43	-.07
10N.3E.21.433	.91	.85	.58	1.32	1.80	.98	.75	.07	.75	-.50	-.23	-.70	-2.49	-.98	.55	.06
10N.3E.17.343	1.74	1.47	1.19	2.74	3.77	2.19	1.02	.27	1.55	-1.00	-.64	-1.27	-3.70	-1.14	.58	.01
10N.2E.14.211	1.96	.56	.58	1.45	2.79	1.25	.85	1.39	.87	.48	-.38	-.91	-1.77	.21	-.02	.08
10N.3E. 8.443	1.78	.68	.53	1.57	2.95	1.15	1.07	1.11	1.04	.81	-.11	-.77	-2.02	-.38	.24	.05
10N.2E. 2.212	1.65	.73	.78	1.52	2.79	1.35	1.25	.92	.74	-.34	-.61	-1.39	-3.66	-.82	.44	.03
11N.3E.31.231	1.00	.25	.29	.75	2.13	.32	1.12	.75	.46	.98	.14	-.56	-1.99	-.81	.44	.03
12N.3E.31.134	1.26	1.44	.41	1.42	2.13	.60	.87	-.18	1.01	.49	.41	-.13	-1.82	.00	.77	.08

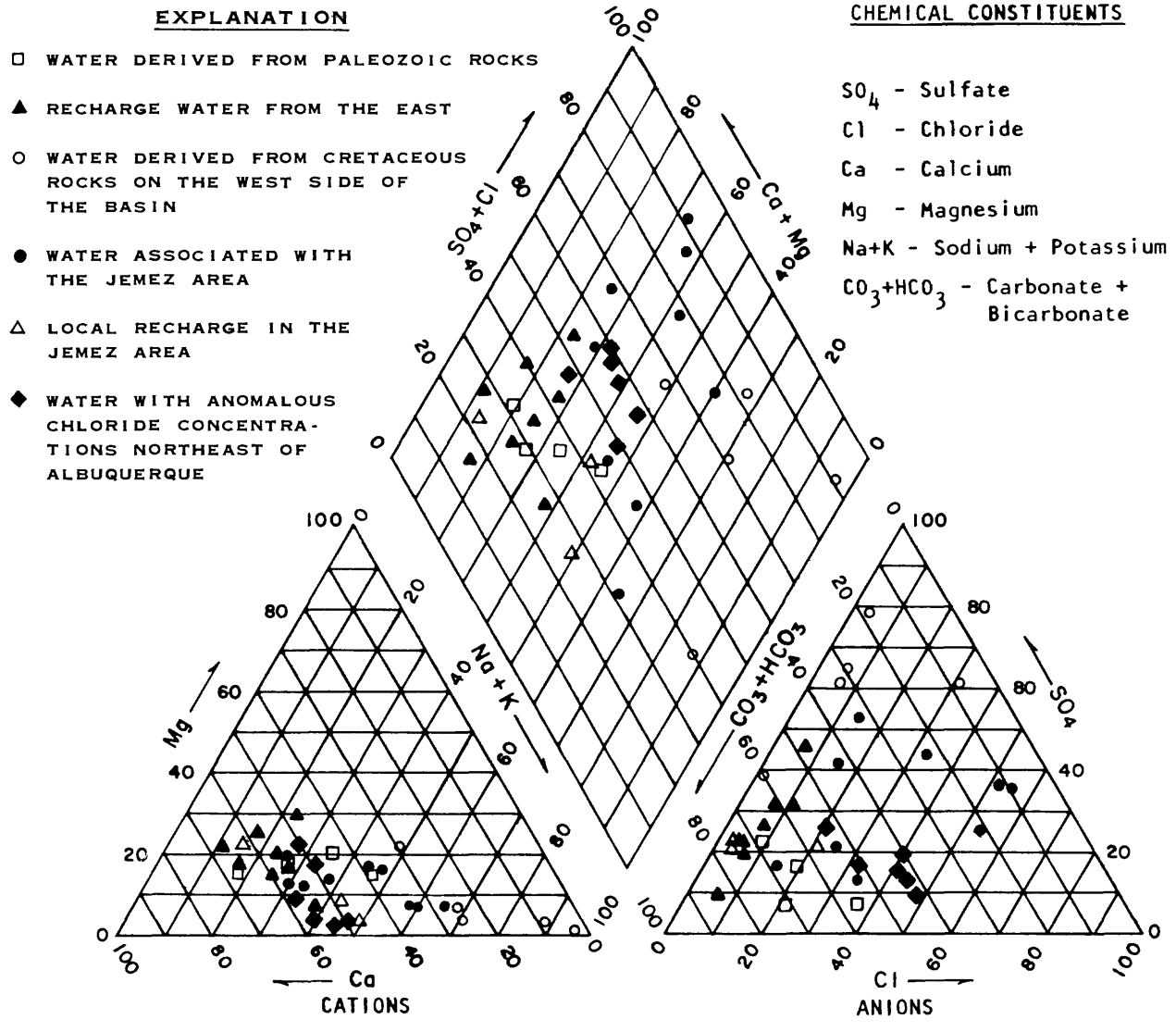

Figure 24.--Piper diagram of selected water analyses in the northern area.

Water from well 11N.1W.28.224 has a specific conductance of 371 microsiemens, which is much smaller than the specific conductance of other water in this area along the west side of the basin. This water may represent recharge from the Rio Puerco as opposed to inflow from the Cretaceous rocks to the west.

Inflow from the San Juan Basin

In the San Ysidro area (pl. 2), there probably are two different sources of ground-water inflow to the aquifer: (1) inflow from the San Juan Basin and (2) inflow from the Jemez volcanic complex.

Several springs and wells west of San Ysidro derive water from the Paleozoic and Mesozoic rocks of the San Juan Basin. The specific conductance of water from these springs and wells generally is greater than 5,000 microsiemens. Sodium generally is the dominant cation and sulfate and chloride are the dominant anions. The presence of springs and flowing wells west of San Ysidro indicates that water in the Paleozoic and Mesozoic rocks is under confined conditions. In areas where permeable Paleozoic and Mesozoic rocks are in fault contact with the aquifer, this mineralized ground water is expected to flow into the aquifer. Water from well 15N.1E.26.222 probably represents inflow water of this type (table 10). The quantity and extent of ground-water inflow from the San Juan Basin in this area are not known.

Local Recharge Water in the Jemez Area

Inflow from the Jemez volcanic complex consists of local recharge water and water from the geothermal reservoir. Major differences exist in the chemical composition of these two waters.

Water from wells 14N.3E.3.434, 14N.2E.5.320, 15N.2E.22.423, and 15N.2E.12.431 (table 10) in the Jemez area represents local recharge water and has a specific conductance of less than 500 microsiemens. Bicarbonate is the dominant anion and sodium and calcium are the dominant cations (fig. 24). The chloride concentration in this water generally is less than 30 milligrams per liter, and the silica concentration is about 30 milligrams per liter. The moderately large silica concentrations in water not derived from the geothermal reservoir may be due to weathering of plagioclase to calcium montmorillonite, as assumed by the material-balance model, or may be due to the dissolution of volcanic glass in the sediments associated with the Jemez volcanic complex.

Water Associated with the Jemez Area

Trainer (1974, p. 344) indicated that the fault zones near Cañon de San Diego (San Diego Canyon) and San Ysidro (pl. 2) may be drains or conduits for flow from the Jemez geothermal reservoir to the aquifer. Other fault zones probably exist along the southern side of the Jemez volcanic complex that also are conduits for flow from the geothermal reservoir to the aquifer. Water from the geothermal reservoir probably mixes with local recharge as the geothermal water moves southward out of the Jemez volcanic complex toward and into the aquifer. Water from the geothermal reservoir also discharges into the Jemez River in the Jemez Springs area. Infiltration of water from the Jemez River in the Albuquerque-Belen Basin is a process whereby water with large silica and chloride concentrations from the geothermal reservoir could recharge the aquifer.

Water discharging from springs associated with faults near Jemez Springs has chloride concentrations as large as 1,500 milligrams per liter and silica concentrations as large as 100 milligrams per liter, indicating that the water was partially derived from the Jemez geothermal reservoir (Trainer, 1974, p. 342-344). Water derived from well 15N.2E.6.222 (table 10) has a chloride concentration of 1,140 milligrams per liter and a silica concentration of 91 milligrams per liter. The large silica and chloride concentrations indicate that the water represents a mixture of water from the geothermal reservoir moving into the aquifer and local recharge water. Similarly, water from several wells south of the Jemez volcanic complex near Bernalillo (wells 12N.4E.6.213, 12N.4E.5.214, 13N.3E.36.123, 13N.4E.29.421, 13N.3E.25.244, and 13N.4E.19.234) has anomalously large silica or chloride concentrations (fig. 25). These wells are on the same general trend as a set of faults associated with the volcanic rocks on Santa Ana Mesa (fig. 25). These faults may be conduits for geothermal fluids from the Jemez geothermal reservoir. These wells are south of the Jemez River (fig. 25), thus the geothermal component of water derived from these wells may simply be the result of infiltration of water from the Jemez River that has moved southward in the aquifer.

The material-balance-model results indicate that there is a negative sodium concentration after removal of chloride in water from wells 13N.3E.25.244, 13N.4E.19.234, and 14N.3E.18.340 (table 11). This negative sodium indicates either that the assumption of the model that chloride and sodium are input to the water in a 1:1 ratio is not correct or that sodium is removed from the water. Very few processes remove sodium from water, which suggests that chloride is input to the system in a ratio with sodium different than 1:1.

Water with Anomalous Chloride Concentrations Northeast of Albuquerque

Several wells northeast of Albuquerque have relatively large chloride concentrations, as much as 100 milligrams per liter (table 10). Examination of the Piper diagram (fig. 24) indicates that the percentage of chloride in water from several of these wells is greater than 40. This large percentage of chloride is similar to those in water from wells associated with the Jemez area (fig. 24). The wells that derive water with anomalous chloride concentrations northeast of Albuquerque are along the same trend as the faults on Santa Ana Mesa, the rift-zone boundary faults along the west side of the Sandia Mountains, and wells with large silica and chloride concentrations near Bernalillo (fig. 25). The material-balance-model results indicate a negative sodium concentration after removal of chloride in two samples and a negative sodium concentration after removal of silica in all samples. This indicates that either chloride is not input to the water at a 1:1 ratio with sodium or that the alteration of plagioclase reaction assumed for the model is not correct.

Wells upgradient from the wells yielding water with anomalous chloride concentrations yield water with small chloride concentrations (fig. 25). This indicates that there is mixing of the upgradient water with small chloride concentrations and the water with large chloride concentrations to form the water with anomalous chloride concentrations.

If the concentrations of individual dissolved constituents in the upgradient water are subtracted from the water with anomalous chloride concentrations, the results give an indication of the relative composition of the water with large chloride concentrations (chloride input water) (table 12). Chloride and sodium are the only constituents that predominate in the chloride input water (table 12). Wells that yield the water with anomalous chloride concentrations generally are more than 1,000 feet deep, and the silica concentration in water from several of these wells is greater than 40 milligrams per liter (table 10). The anomalously large chloride and silica concentrations in water from these wells and the small chloride concentrations in water upgradient from these wells may indicate that geothermal water is moving up along faults in this area.

Table 12. Calculation of the composition of upward-moving ground water in the area northeast of Albuquerque

[Concentrations in millimoles]

Location	Sodium	Chloride	Sulfate	Magnesium	Calcium	Bicarbonate	Remarks
10N.4E.5.122	2.18	2.70	0.28	0.17	1.60	1.23	Water with anomalous chloride concentrations
10N.4E.4.221	1.00	.14	.19	.08	.92	1.21	Upgradient water
Excess	1.18	2.56	0.09	0.09	0.68	0.02	Chloride input water
11N.4E.20.232	3.22	2.43	0.39	0.25	0.92	1.31	Water with anomalous chloride concentrations
11N.4E.16.341	.74	.17	.22	.29	1.07	1.40	Upgradient water
Excess	2.48	2.26	0.17	-0.04	-0.15	-0.09	Chloride input water

EXPLANATION

FAULT--Dashed where approximately located, dotted where concealed

5100 POTENTIOMETRIC CONTOUR--Shows altitude at which water level would have stood in tightly cased wells, 1960. Dashed where approximately located. Contour intervals 10 and 50 feet. Datum is sea level. Contours from Bjorklund and Maxwell, 1961

15
28
91 WELL--Top number is well number (see list below). Middle number is chloride concentration, in milligrams per liter. Bottom number is silica concentration as Si, in milligrams per liter. — indicates no value

WELL NUMBER	LOCATION
1	10N.4E.04.221
2	10N.4E.05.122
3	11N.4E.16.341
4	11N.4E.20.232
5	11N.4E.28.111
6	11N.4E.31.412
7	12N.4E.05.214
8	12N.4E.06.213
9	12N.4E.17.424
10	12N.4E.30.124
11	12N.4E.32.242
12	13N.3E.25.244
13	13N.3E.36.123
14	13N.4E.19.234
15	13N.4E.29.421

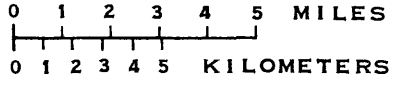

Figure 25.--Concentrations of chloride and silica in water from selected wells in the Bernalillo and Albuquerque areas.

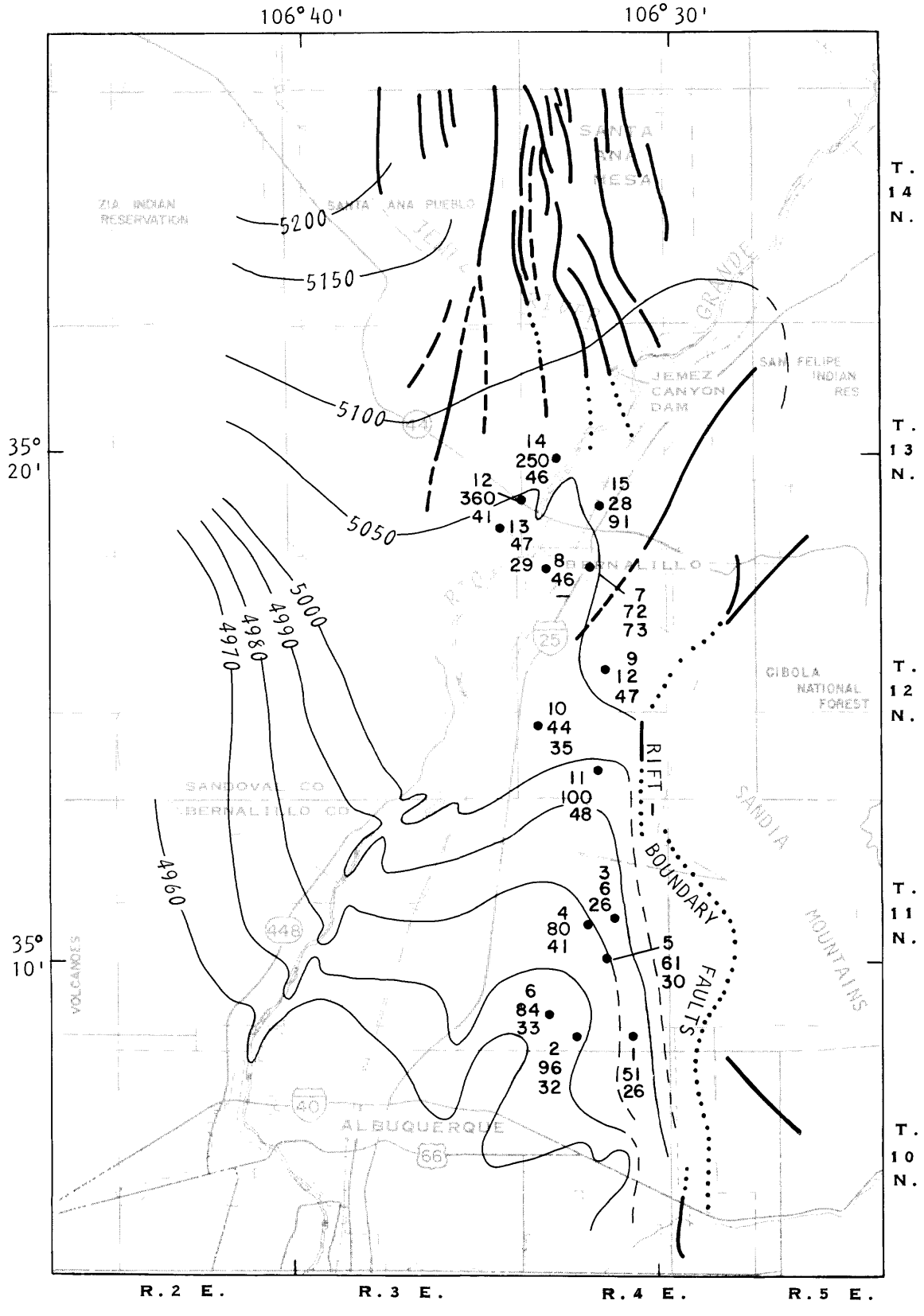
106° 40'
106° 30'
35° 20'
35° 10'
T. 14 N.
T. 13 N.
T. 12 N.
T. 11 N.
T. 10 N.
R. 2 E.
R. 3 E.
R. 4 E.
R. 5 E.
ZIA INDIAN RESERVATION
SANTA ANA PUEBLO
SANTA ANA MESA
JEMEZ CANYON DAM
SAN FELIPE INDIAN RES
CIBOLA NATIONAL FOREST
SANDOVAL CO.
BERNALILLO CO.
SANDIA MOUNTAINS
VOLCANOES
ALBUQUERQUE
RIFT BOUNDARY FAULTS
5200
5150
5100
5050
5000
4990
4980
4970
4960
14 250 46
12 360 41
13 47
15 28 91
8 29 46
7 72 73
9 12 47
10 44 35
11 100 48
3 6 26
4 80 41
5 61 30
6 84 33
2 96 32
1 151 26

Water from the Area West of Albuquerque Where Ion Exchange is Dominant

Water from wells in a large area west and north of Albuquerque has sodium as the dominant cation and very small concentrations of calcium (fig. 26 and table 10). The material-balance-model results indicate that in most water samples there is a relatively large positive sodium concentration after removal of silica (table 11). This indicates that cation exchange is a dominant process in the chemical evolution of ground water in this area.

Sediments west of Albuquerque consist of coarse-grained alluvial sediments that are underlain by fine-grained, closed-basin sediments. These closed-basin sediments (middle red member equivalent) contain substantial silt and clay. The extent of these fine-grained sediments as defined from geophysical logs is shown in figure 27. This area of fine-grained sediments seems to correspond with the area where ion exchange in ground water is the dominant process, although the area where ground water is affected by ion exchange is east of the line of zero thickness of the fine-grained sediments (fig. 27). The northern extent of the area of fine-grained sediments could not be determined because of the lack of geophysical and driller's logs. Ground water that contains relatively large concentrations of sodium with respect to calcium extends north of the area defined from geophysical logs as being underlain by fine-grained sediments, indicating that fine-grained sediments probably extend north of well 12N.2E.14.433, as interpreted from the chemistry of water from this well.

In this case, the water-quality data were useful in interpreting the geology of the area. The examination of water-quality data may be a very useful technique in defining areas underlain by sediments with large proportions of clay having large ion-exchange capacities.

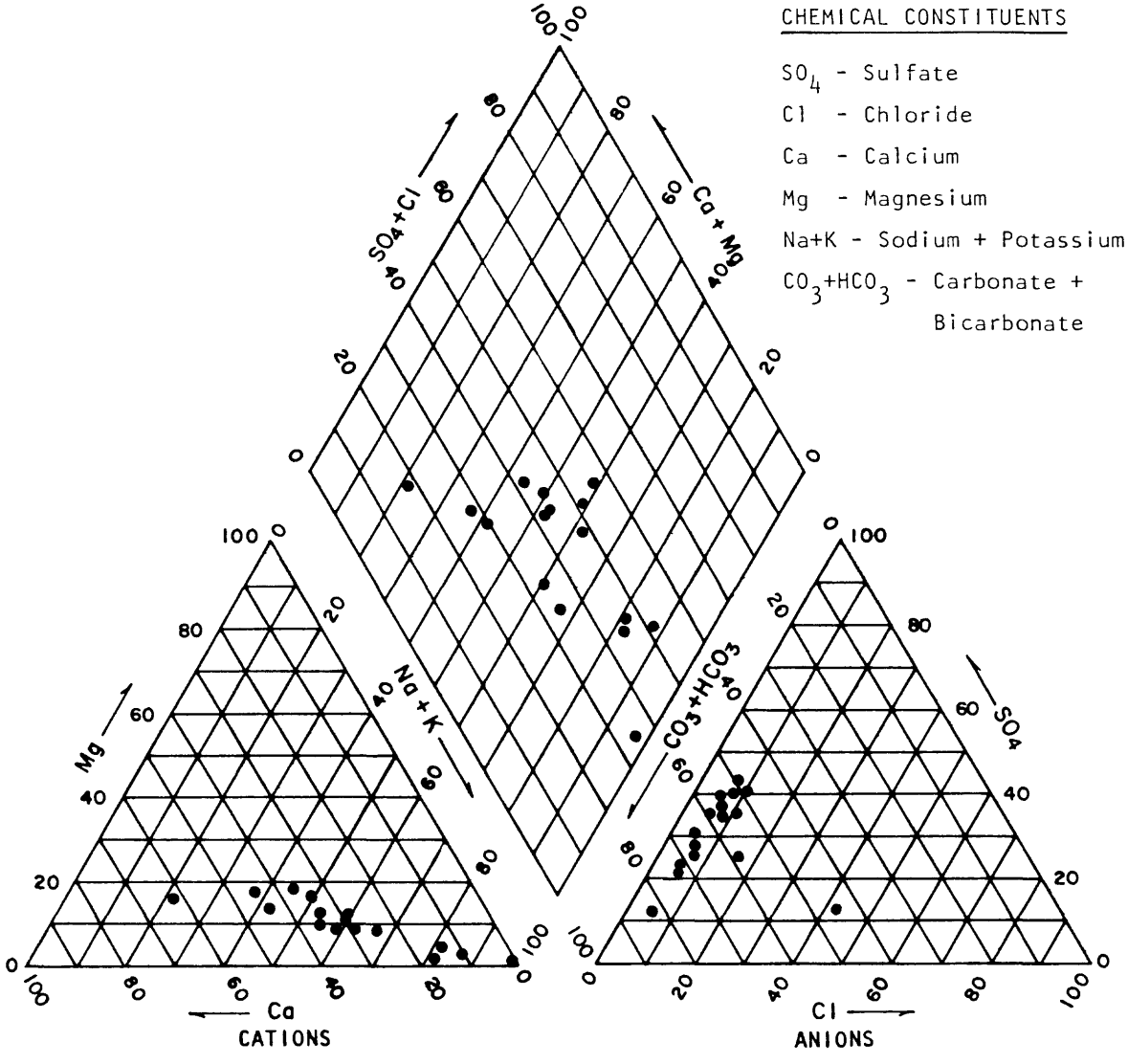

Figure 26.--Piper diagram of selected water analyses in the area west of Albuquerque where ion exchange is dominant.

EXPLANATION

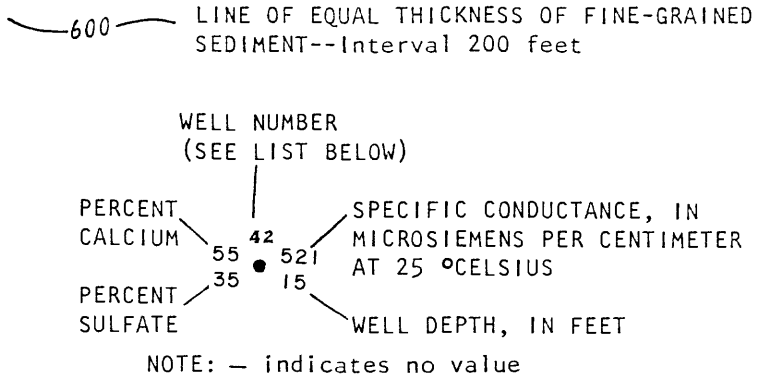

NOTE: — indicates no value

WELL NUMBER	LOCATION	WELL NUMBER	LOCATION
1	8N.1E.01.342	22	10N.3E.21.433
2	9N.2E.11.241	23	10N.3E.32.421
3	9N.2E.35.400	24	10N.3E.35.111
4	9N.3E.05.234	25	10N.3E.36.132
5	9N.3E.08.300	26	11N 1W.11.424
6	9N.3E.11.241	27	11N.1E.26.424
7	9N.3E.18.413	28	11N.2E.02.343
8	10N.1E.30.222	29	11N.2E.03.213
9	10N.2E.02.212	30	11N.2E.22.441
10	10N.2E.02.313	31	11N.3E.15.121
11	10N.2E.09.133	32	11N.3E.20.143
12	10N.2E.12.412	33	11N.3E.21.132
13	10N.2E.14.211	34	11N.3E.22.314
14	10N.2E.21.343	35	11N.3E.31.231
15	10N.2E.25.213	36	11N.3E.34.141
16	10N.2E.36.413	37	11N.3E.35.244
17	10N.3E.08.443	38	12N.2E.14.433
18	10N.3E.11.200	39	12N.3E.30.121
19	10N.3E.17.343	40	12N.3E.31.134
20	10N.3E.19.111	41	12N.3E.33.400
21	10N.3E.20.344	42	12N.3E.35.243

Figure 27.--Extent of the fine-grained sediments and ion-exchange area west of Albuquerque.

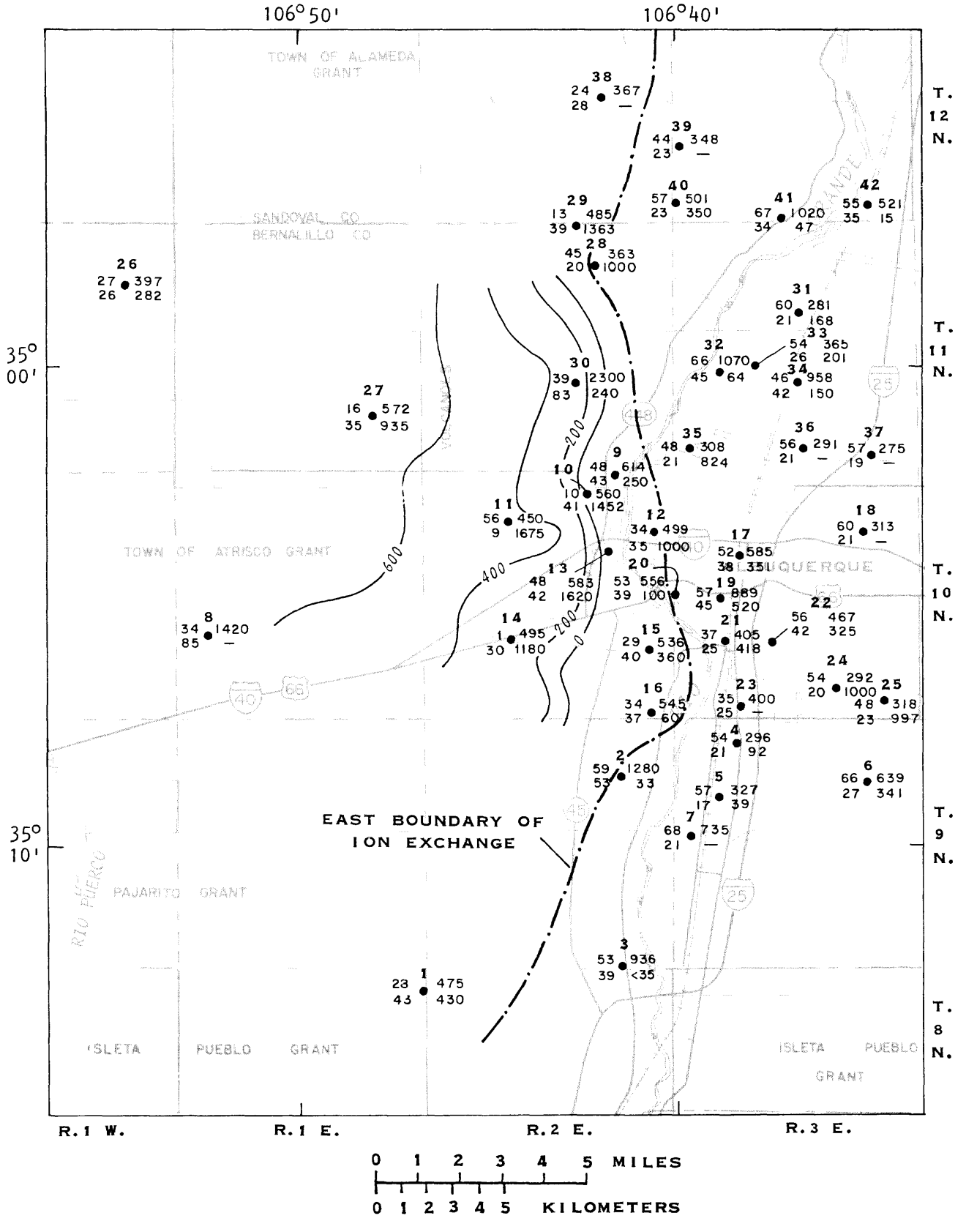
106°50'
106°40'
35° 00'
35° 10'
T. 12 N.
T. 11 N.
T. 10 N.
T. 9 N.
T. 8 N.
R. 1 W.
R. 1 E.
R. 2 E.
R. 3 E.
TOWN OF ALAMEDA GRANT
SANDOVAL CO
BERNALILLO CO
TOWN OF ATRISCO GRANT
PAJARITO GRANT
ISLETA PUEBLO GRANT
ISLETA PUEBLO GRANT
RIO PUERCO
ALBUQUERQUE
EAST BOUNDARY OF ION EXCHANGE
600
400
200
200
0
0 1 2 3 4 5 MILES
0 1 2 3 4 5 KILOMETERS

Water from the Rio Grande Valley

The chemical quality of ground water affected by irrigation practices in or adjacent to the Rio Grande valley varies considerably both vertically and laterally (table 10). The large variation in water quality is in part due to differences in the chemical quality of excess irrigation water that infiltrates and mixes with ground water. Differences in the chemical quality of excess irrigation water are due to differences in farming practices. For example, if the consumptive use of a specific crop is 2.0 acre-feet and a farmer applies 4.0 acre-feet, the excess irrigation water or recharge to the aquifer will be approximately 2.0 acre-feet. The percentage of applied water that is evaporated or transpired from plants generally is referred to as the irrigation efficiency and in this case is 50 percent. If the specific conductance of the applied irrigation water is 500 microsiemens, the recharge water will have a specific conductance of approximately 1,000 microsiemens because plants remove and transpire only water and assimilate little if any of the dissolved chemical constituents in the remaining water. The irrigation efficiencies of a particular farm or of specific areas of a field probably have a considerable range of values, thus there is a large variation in the chemical quality of the infiltrating water recharging the aquifer in the river valley. In the early 1900's, excess irrigation water caused ground-water levels to rise to the land surface in the river valley, resulting in evaporation from waterlogged fields and an increase of salt content in the soils and remaining water. Drains were constructed in the 1920's to drain these areas and to maintain water levels so that waterlogging would not again occur. At the present time (1985), the drains are a sink for the excess irrigation water, but mixing occurs between the excess irrigation water and ground water under the fields.

The chemical quality of ground water in the irrigated part of the river valley also is affected by infiltration of water from the irrigation canals and the Rio Grande. Water infiltrating from irrigation canals or the Rio Grande contains less dissolved solids than excess irrigation water. The localized ground-water flow system is substantially affected by the drains and infiltration of excess irrigation water, water from the Rio Grande, and leakage from irrigation canals. Ground-water pumpage from wells in the river valley results in the mixing of excess irrigation water, recharge water from irrigation canals and the Rio Grande, and local ground water. Deep wells in the river valley may cause this mixing to occur in deep parts of the aquifer. The flow system in the river valley can be complicated by all these factors, which creates complex chemical-quality distributions, both spacially and temporally, in ground water.

In the river valley, water quality varies with depth in the aquifer. The eastern edge of the area where ion-exchange is dominant can be defined by deep wells; however, shallow wells near this eastern edge do not always contain water with water-quality characteristics caused by ion exchange (table 13). The water derived from shallow wells generally has a large specific conductance and a calcium concentration greater than the sodium concentration (table 13). Chloride and sulfate concentrations also generally are larger in the water from these shallow wells than in water from the adjacent deeper wells (table 13). Usually calcium, bicarbonate, and sulfate are the dominant ions in water derived from shallow wells in the river valley and from wells east of the river valley. Water from deep wells usually has sodium and bicarbonate as the dominant ions and a specific conductance generally smaller than in water from nearby shallow wells.

Table 13. Water-quality data for adjacent wells of different depths near the east side of the ion-exchange area

[ft, feet; °C, degrees Celsius; mg/L, milligrams per liter]

Location	Well depth (ft)	Specific conductance (microsiemens per centimeter at 25 °C)	Calcium (mg/L)	Sodium plus potassium (mg/L)	Sulfate (mg/L)	Chloride (mg/L)
9N.2E.11.241A	33	1,280	172	90	370	68
10N.2E.36.413	60	545	39	65	100	14
10.N3E.20.344	418	405	30	41	48	22
10N.3E.21.433	323	467	53	21	94	30
10N.2E.24.233	336	454	33	56	78	15
10N.3E.19.111	100	556	63	38	110	16
10N.2E.12.412	1,000	499	36	62	87	12
10N.2E.14.211	162	583	58	45	120	20
10N.2E.2.313	1,452	560	10	101	99	18
10N.2E.2.212	250	614	61	38	130	26

Water from the Rio Grande Valley with Large Silica Concentrations

The silica concentrations of water from many wells in the Rio Grande valley are greater than 30 milligrams per liter (table 10). These are considered to be large silica concentrations, and they generally are greater than those in ground water in the Albuquerque-Belen Basin. The material-balance-model results indicate that, in many cases, there is a negative sodium concentration after the removal of silica (table 11). There also is a negative bicarbonate concentration after removal of silica, indicating that calcite has precipitated from solution. A positive bicarbonate concentration exists after removal of silica in ground water from the group of wells in the Rio Grande valley not having large silica concentrations (table 11), indicating calcite dissolution. This suggests that either there is a significant difference in the evolution of ground water in the Rio Grande valley or that the assumed model is not correct. The negative sodium and bicarbonate concentrations after the removal of silica in ground water from the Rio Grande valley having large silica concentrations probably indicate that the alteration of plagioclase to calcium montmorillonite assumed in the model is not correct. The large silica concentrations in ground water from the Rio Grande valley may be due to the dissolution of volcanic glass from sediments in the aquifer that were derived from the Jemez volcanic complex.

Conclusions

Calcium, bicarbonate, and sulfate are the dominant ions in ground water from the east that recharge the aquifer in the northern area. The specific conductance of this water generally is less than 500 microsiemens. Sodium is the dominant cation and sulfate is the dominant anion in ground-water recharge or inflow to the aquifer on the west side of the Albuquerque-Belen Basin. In the northern part of the area, ground-water inflow from the San Juan Basin to the aquifer contains large concentrations of sodium, sulfate, and chloride. Ground-water inflow from the Jemez geothermal reservoir generally mixes with local recharge water. Large concentrations of chloride and silica generally are indicators of ground water from the Jemez geothermal reservoir. Local recharge water from the Jemez volcanic complex is characterized by a specific conductance of less than 500 microsiemens. Bicarbonate generally is the dominant anion and sodium and calcium are the dominant cations in this local recharge water. Ground water from the geothermal reservoir mixes with local recharge water and flows into the aquifer along the northern boundary of the Albuquerque-Belen Basin.

Several wells along the east rift-boundary fault yield water that has relatively large chloride concentrations. These wells probably yield water that is leaking upward along the boundary fault. West of the Rio Grande, sodium is the dominant cation in the ground water from a large area. This area of relatively large sodium percentages corresponds to an area of generally fine grained sediments in the subsurface that was defined with the use of driller's and geophysical logs. The relatively large concentrations of sodium and small concentrations of calcium probably are due to calcium-for-sodium ion exchange on the clay and silt in the fine-grained sediments.

In the river valley, the chemical nature of ground water varies considerably. This is due to complex mixing patterns of infiltrating excess irrigation water with the ground water in the area. Various irrigation practices, pumpage of ground water from depth, and infiltration of water from the Rio Grande, irrigation canals, and drainage ditches create these complex mixing patterns.

SUMMARY

The Albuquerque-Belen Basin contains as much as 18,000 feet of basin-fill sediments in the Santa Fe Group that form the aquifer. The majority of ground-water inflow to the aquifer occurs as infiltration of surface water through river channels, infiltration of surface-water inflow from adjacent areas, infiltration of excess irrigation water, ground-water inflow from adjacent bedrock units, and ground-water inflow south from the Santo Domingo Basin.

In general, ground water flows from the basin margins toward the basin center and then southward toward the Socorro Basin. The axis of a ground-water trough coincides with the Rio Grande south of Belen, but north of Belen the axis of the trough is west of and parallel to the Rio Grande. Along the basin margins, the ground-water gradients are relatively steep and slope toward the ground-water trough. The major types of ground-water outflow from the Albuquerque-Belen Basin are evapotranspiration, ground-water pumpage, and ground-water outflow to the adjacent Socorro Basin to the south.

The average specific conductance of surface water from September 1969 to August 1982 from the Jemez River at Jemez Canyon Dam was 1,283 microsiemens. For the Rio Puerco near Bernardo, it was 2,047 microsiemens, and for the Rio Salado at San Acacia, it was 1,670 microsiemens. The average specific conductance of the Rio Grande for the same period was 358 microsiemens at San Felipe and 752 microsiemens at San Acacia. The increase in specific conductance downstream in the Rio Grande is due to solute concentration through evapotranspiration, tributary inflow of surface water with larger solute concentrations, and return of excess irrigation water with larger solute concentrations.

Ground-water quality in the Albuquerque-Belen Basin varies considerably. In the southeastern area, recharge or inflow to the aquifer is of two types. One type contains a large percentage of calcium and sulfate; the other type has a relatively small specific conductance and bicarbonate is the dominant anion. The specific conductance of most water in the aquifer in the southeastern area ranges from 1,000 to 1,200 microsiemens, and calcium and sulfate are the dominant ions. There also seems to be some upward movement of water with large chloride concentrations along the rift-boundary fault, as indicated by the quality of water from wells along the fault. The extent and volume of this upward-moving water probably are not large, as evidenced by the lack of a large plume of ground water having large chloride concentrations.

The ground-water quality along the east side of the basin is affected by recharge due to infiltration of runoff from the Manzano, Manzanita, and Sandia Mountains. In general, the specific conductance of ground water east of the Rio Grande valley is less than 400 microsiemens. Bicarbonate is the dominant anion and calcium generally is the dominant cation. Sodium is the dominant cation in several water samples, which may indicate cation exchange. The specific conductance of ground water in the Rio Grande valley from approximately Los Lunas to Bernardo ranges from 280 to 2,170 microsiemens and is larger than the specific conductance of ground water to the east. The increase in the specific conductance of ground water in the Rio Grande valley

in comparison to ground water to the east probably is due to the mixing of excess irrigation water and water in the aquifer. The specific conductance of ground water west of the Rio Grande valley and east of the ground-water trough south of Los Lunas ranges from approximately 500 to 900 microsiemens and, in general, is less than the specific conductance of ground water in the Rio Grande valley.

Along the western side of the southwestern area, sodium chloride brine enters the aquifer due to inflow from adjacent bedrock units. This brine flows south and eastward, mixing with ground water in the aquifer and with other ground-water recharge. The specific conductance of the mixed water varies considerably because of different mixing ratios of the brine and ground-water recharge or water in the aquifer. In general, the specific conductance of the mixed water gets smaller as it moves eastward because of dilution of the brine with less saline water. The mixed water in this area dissolves gypsum as it moves through the aquifer, as indicated by a general increase in percentages of sulfate and calcium in the mixed water in comparison to the percentages of calcium and sulfate in the brine. In the area of the basin near Bernardo and southwest, the water has large chloride concentrations, probably due to the upward movement of water in the aquifer. This upward movement is caused by a constriction to ground-water flow in the San Acacia area.

In the northern area of the Albuquerque-Belen Basin, ground-water inflow from the Jemez geothermal reservoir mixes with local recharge water and ground water in the aquifer. Large concentrations of silica and chloride generally are indicators of ground water from the Jemez geothermal area.

In a large area west of Albuquerque, sodium is the dominant cation in ground water. In this area, ion exchange of calcium and magnesium for sodium probably is a dominant process affecting the ground water. This area, where ion exchange seems to be a dominant process, is underlain by relatively fine grained sediments indicated on driller's and geophysical logs.

REFERENCES

Anderholm, S.K., 1985, Clay-size fraction and powdered whole-rock X-ray analyses of alluvial-basin deposits in central and southern New Mexico: U.S. Geological Survey Open-File Report 85-173, 18 p.

Baars, D.L., 1961, Permian strata of central New Mexico, in Northrop, S.A., ed., Guidebook to the Albuquerque Country: New Mexico Geological Society, 12th Field Conference, p. 113-120.

Bailey, R.A., Smith, R.L., and Ross, C.S., 1969, Stratigraphic nomenclature of volcanic rocks in the Jemez Mountains, New Mexico: U.S. Geological Survey Bulletin 1274P, p. P1-P9.

Baldwin, Brewster, 1956, The Santa Fe Group of north-central New Mexico, in Rosenzweig, A., ed., Guidebook to the southeastern Sangre de Cristo Mountains, New Mexico: New Mexico Geological Society, Seventh Field Conference, p. 115-121.

Bennett, G.D., 1979, Regional ground-water system analysis: Water Spectrum, Fall, p. 36-42.

Birch, Francis, 1980, Geophysical evaluation of basin hydrologic characteristics in the central Rio Grande; Pt. I, Gravity models of the Albuquerque-Belen Basin: Albuquerque, N. Mex., unpublished report prepared under U.S. Geological Survey contract no. 14-08-00001-17879, 30 p.

Bjorklund, L.J., and Maxwell, B.W., 1961, Availability of ground water in the Albuquerque area, Bernalillo and Sandoval Counties, New Mexico: New Mexico State Engineer Technical Report 21, 117 p.

Brown, L.D., Chapin, C.E., Sanford, A.R., Kaufman, S., and Oliver, J., 1980, Deep structure of the Rio Grande Rift from seismic reflection profiling: Journal of Geophysical Research, v. 85, no. B9, p. 4773-4800.

Bruning, J.E., 1973, Origin of the Popotosa Formation, north-central Socorro County, New Mexico: Socorro, New Mexico Institute of Mining and Technology, unpublished Ph.D. dissertation, 132 p.

Bryan, Kirk, 1909, Geology of the vicinity of Albuquerque: Albuquerque, University of New Mexico Bulletin 51, Geological Series 3, no. 1, 24 p.

_____1938, Geology and ground-water conditions of the Rio Grande depression in Colorado and New Mexico, in (U.S.) National Resources Committee, Regional Planning; Pt. VI, The Rio Grande joint investigation in the upper Rio Grande basin in Colorado, New Mexico, and Texas, 1936-37: U.S. Government Printing Office, v. 1, p. 197-225.

Bryan, Kirk, and McCann, F.T., 1936, Successive pediments and terraces of the upper Rio Puerco in New Mexico: Journal of Geology, v. 44, no. 2, pt. 1, p. 145-172.

REFERENCES - Continued

Bryan, Kirk, and McCann, F.T., 1937, The Ceja del Rio Puerco--A border feature of the Basin and Range Province in New Mexico; Pt. 1, Stratigraphy and structure: Journal of Geology, v. 45, no. 8, p. 801-828.

_____1938, The Ceja del Rio Puerco--A border feature of the Basin and Range Province in New Mexico; Pt. 2, Geomorphology: Journal of Geology, v. 46, no. 1, p. 1-16.

Callender, J.F., Grambling, J.A., and Wells, S.G., eds., 1982, Guidebook to Albuquerque Country II: New Mexico Geological Society, 33rd Field Conference, 370 p.

Callender, J.F., and Zilinski, R.E., Jr., 1976, Kinematics of Tertiary and Quaternary deformation along the eastern edge of the Lucero Uplift, central New Mexico, in Woodward, L.A., and Northrop, S.A., eds., Tectonics and mineral resources of southwestern North America, 1976: New Mexico Geological Society Special Publication 6, p. 53-61.

Chapin, C.E., Chamberlin, R.M., Osburn, G.R., White, D.W., and Sanford, A.R., 1978, Exploration framework of the Socorro geothermal area, New Mexico, in Chapin, C.E., Elston, W.E., and James, H.L., eds., Field guide to selected cauldrons and mining districts of the Datil-Mogollon Volcanic Field, New Mexico, 1978: New Mexico Geological Society Special Publication no. 7, p. 115-129.

Chapin, C.E., and Seager, W.R., 1975, Evolution of the Rio Grande rift in the Socorro and Las Cruces areas, in Las Cruces Country: New Mexico Geological Society, 26th Field Conference, p. 297-321.

Darton, N.H., 1922, Geologic structure of parts of New Mexico, in Contributions to economic geology: U.S. Geological Survey Bulletin 726, p. 173-275.

Denny, C.S., 1940, Tertiary geology of the San Acacia area, New Mexico: Journal of Geology, v. 48, no. 1, p. 73-106.

_____1941, Quaternary geology of the San Acacia area, New Mexico: Journal of Geology, v. 49, no. 3, p. 225-260.

Foster, R.W., 1957, Stratigraphy of west-central New Mexico, in Little, C.J., and Gill, J.J., eds., Guidebook to geology of the southwest San Juan Basin: Four Corners Geological Society, Second Field Conference, p. 62-72.

Freeze, R.A., and Cherry, J.A., 1979, Groundwater: Englewood Cliffs, N.J., Prentice-Hall Inc., 604 p.

Gabin, V.L., and Lesperance, L.E., 1977, New Mexico climatological data, precipitation, temperature, evaporation, and wind, monthly and annual means 1850-1975: Socorro, N. Mex., W.K. Summers and Associates, 436 p.

Galusha, Ted, 1966, The Zia Sand Formation, new early to medial Miocene beds in New Mexico: American Museum Novitates, no. 2271, 12 p.

Galusha, Ted, and Blick, J.C., 1971, Stratigraphy of the Santa Fe Group, New Mexico: American Museum of Natural History Bulletin, v. 144, pt. 1, 128 p.

Gardner, J.N., Goff, Fraser, Garcia, Sammy, and Hagan, R.C., 1986, Stratigraphic relations and lithologic variations in the Jemez Volcanic Field, New Mexico: Journal of Geophysical Research, v. 91, no. B2, p. 1763-1778.

Garrels, R.M., and MacKenzie, F.T., 1967, Origin of the chemical compositions of some springs and lakes: American Chemical Society, Equilibrium Concepts in Natural Water Systems, Advances in Chemistry Series 67, p. 222-242.

_____1971, Evolution of sedimentary rocks: New York, W.W. Norton and Company, Inc., 397 p.

Gawne, C.E., 1981, Sedimentology and stratigraphy of the Miocene Zia Sand of New Mexico--Summary: Geological Society of America Bulletin, v. 92, pt. 1, p. 999-1007.

Hawley, J.W., 1978, Correlation chart 1 and correlation chart 2, in Hawley, J.W., compiler, Guidebook to Rio Grande rift in New Mexico and Colorado: New Mexico Bureau of Mines and Mineral Resources Circular 163, p. 238-241.

Hayden, F.V., 1869, Preliminary field report of the U.S. Geological Survey of Colorado and New Mexico: U.S. Geological Survey third annual report, 155 p.

Hiss, W.L., Trainer, F.W., Black, B.A., and Posson, D.R., 1975, Chemical quality of ground water in the northern part of the Albuquerque-Belen Basin, Bernalillo and Sandoval Counties, New Mexico, in Seager, W.R., Clemons, R.E., and Callender, J.F., eds., Guidebook to Las Cruces Country: New Mexico Geological Society, 26th Field Conference, p. 219-236.

Kelley, V.C., 1952, Tectonics of the Rio Grande depression of central New Mexico, in Johnson, R.B., and Read, C.B., eds., Guidebook to Rio Grande Country, central New Mexico: New Mexico Geological Society, Third Field Conference, p. 92-105.

_____1974, Albuquerque, its mountains, valley, water, and volcanoes: New Mexico Bureau of Mines and Mineral Resources Scenic Trips to the Geologic Past 9 (rev. ed.), 106 p.

_____1977, Geology of Albuquerque Basin, New Mexico: New Mexico Bureau of Mines and Mineral Resources Memoir 33, 60 p.

Kelley, V.C., 1982, Diverse geology of the Hubbell Bench, Albuquerque Basin, in Callender, J.F., Grambling, J.A., and Wells, S.G., eds., Guidebook to Albuquerque Country II: New Mexico Geological Society, 33rd Field Conference, p. 159-160.

Kelley, V.C., and Northrop, S.A., 1975, Geology of Sandia Mountains and vicinity, New Mexico: New Mexico Bureau of Mines and Mineral Resources Memoir 29, 136 p.

Kelley, V.C., and Wood, G.H., Jr., 1946, Geology of the Lucero uplift, Valencia, Socorro, and Bernalillo Counties, New Mexico: U.S. Geological Survey Oil and Gas Investigations Preliminary Map OM-47, scale 1:62,500.

Kernodle, J.M., and Scott, W.B., 1986, Three-dimensional model simulation of steady-state ground-water flow in the Albuquerque-Belen Basin, New Mexico: U.S. Geological Survey Water-Resources Investigations Report 84-4353, 58 p.

Kottlowski, F.E., 1961, Pennsylvanian rocks in north-central New Mexico, in Northrop, S.A., ed., Guidebook to the Albuquerque Country: New Mexico Geological Society, 12th Field Conference, p. 97-104.

Lambert, P.W., 1968, Quaternary stratigraphy of the Albuquerque area, New Mexico: Albuquerque, University of New Mexico, unpublished Ph.D. dissertation, 329 p.

Lozinsky, R.P., 1986, The Gabaldon Badlands: New Mexico Geology, May 1986.

Lucas, S.G., 1982, Vertebrate paleontology, stratigraphy, and biostratigraphy of Eocene Galisteo Formation, north-central New Mexico: New Mexico Bureau of Mines and Mineral Resources Circular 186, 34 p.

Lucas, S.G., and Ingersoll, R.V., 1981, Cenozoic continental deposits of New Mexico--An overview: Geological Society of America Bulletin, v. 92, pt. 1, p. 917-932.

Lucas, S.G., Schoch, R.M., and Manning, E., 1981, The Eocene biostratigraphy of New Mexico: Geological Society of America Bulletin, v. 92, p. 951-967.

Machette, M.N., 1978a, Geologic map of the San Acacia quadrangle, Socorro County, New Mexico: U.S. Geological Survey Geologic Quadrangle Map GQ-1415, scale 1:24,000.

_____1978b, Preliminary geologic map of the Socorro 1° x 2° quadrangle, central New Mexico: U.S. Geological Survey Open-File Report 78-607, scale 1:250,000.

Moench, R.H., and Schleep, J.S., 1967, Geology and uranium deposits of the Laguna district, New Mexico: U.S. Geological Survey Professional Paper 519, 117 p.

Northrop, S.A., ed., 1961, Guidebook to the Albuquerque Country: New Mexico Geological Society, 12th Field Conference, 199 p.

Osburn, G.R., and Chapin, C.E., 1983, Nomenclature of Cenozoic rocks of northeast Mogollon-Datil volcanic field, New Mexico: New Mexico Bureau of Mines and Mineral Resources Statigraphic Chart 1.

Piper, A.M., 1944, A graphic procedure in the geochemical interpretation of water analyses: American Geophysical Union Transactions, v. 25, p. 914-923.

Plummer, L.N., Jones, B.F., and Truesdell, A.H., 1978, WATEQF--A Fortran IV version of WATEQ, a computer program for calculating chemical equilibrium of natural waters: U.S. Geological Survey Water-Resources Investigations 76-13, 63 p.

Read, C.B., Wilpot, R.H., Andrews, D.A., Summerson, C.H., and Wood, G.H., 1944, Geologic map and stratigraphic sections of Permian and Pennsylvanian rocks of parts of San Miguel, Santa Fe, Sandoval, Bernalillo, Torrance, and Valencia Counties, north-central New Mexico: U.S. Geological Survey Oil and Gas Investigations Preliminary Map OM-21.

Reeder, H.O., Bjorklund, L.J., and Dinwiddie, G.A., 1967, Quantitative analysis of the water resources in the Albuquerque area, New Mexico: New Mexico State Engineer Technical Report 33, 34 p.

Simonett, M.J., 1981, Irrigation return flow modeling at San Acacia, New Mexico: Socorro, New Mexico Institute of Mining and Technology, unpublished M.S. thesis, 112 p.

Slack, P.B., and Campbell, J.A., 1976, Structural geology of the Rio Puerco fault zone and its relationship to central New Mexico tectonics, in Woodward, L.A., and Northrop, S.A., eds., Tectonics and mineral resources of southwestern North America, 1976: New Mexico Geological Society Special Publication 6, p. 46-51.

Smith, C.T., 1961, Triassic and Jurassic rocks of the Albuquerque area, in Northrop, S.A., ed., Guidebook to the Albuquerque Country: New Mexico Geological Society, 12th Field Conference, p. 121-128.

Smith, R.L., Bailey, R.A., and Ross, C.S., 1970, Geologic map of the Jemez Mountains, New Mexico: U.S. Geological Survey Miscellaneous Geologic Investigations Map I-571, scale 1:125,000.

Spiegel, Zane, 1955, Geology and ground-water resources of northwestern Socorro County, New Mexico: New Mexico Bureau of Mines and Mineral Resources Ground-Water Report 4, 99 p.

Spiegel, Zane, and Baldwin, Brewster, 1963, Geology and water resources of the Santa Fe area, New Mexico: U.S. Geological Survey Water-Supply Paper 1525, 258 p.

Stearns, C.E., 1943, The Galisteo Formation of north-central New Mexico: Journal of Geology, v. 51, no. 5, p. 301-319.

Tedford, R.H., 1981, Mammalian biochronology of the late Cenozoic basins of New Mexico: Geological Society of America Bulletin, v. 92, pt. 1, p. 1008-1022.

_____1982, Neogene stratigraphy of the northwestern Albuquerque Basin, in Callender, J.F., Grambling, J.A., and Wells, S.G., eds., Guidebook to Albuquerque Country II: New Mexico Geological Society, 33rd Field Conference, p. 273-278.

Theis, C.V., 1938, Ground water in the middle Rio Grande valley, in (U.S.) National Resources Committee, Regional Planning; Pt. VI, The Rio Grande joint investigation in the upper Rio Grande basin in Colorado, New Mexico, and Texas, 1936-37: U.S. Government Printing Office, v. 1, p. 268-291.

Titus, F.B., Jr., 1961, Ground-water geology of the Rio Grande Trough in north-central New Mexico, with sections on the Jemez caldera and the Lucero Uplift, in Northrop, S.A., ed., Guidebook to the Albuquerque Country: New Mexico Geological Society, 12th Field Conference, p. 186-192.

_____1963, Geology and ground-water conditions in eastern Valencia County, New Mexico: New Mexico Bureau of Mines and Mineral Resources Ground-Water Report 7, 113 p.

Trainer, F.W., 1974, Ground water in the southwestern part of the Jemez Mountains volcanic region, New Mexico, in Siemers, C.T., Woodward, L.A., and Callender, J.F., eds., Guidebook to Ghost Ranch, central-northern New Mexico: New Mexico Geological Society, 25th Field Conference, p. 337-345.

U.S. Army Corps of Engineers, 1979, Albuquerque greater urban area water supply study: U.S. Army Corps of Engineers, Albuquerque District, Hydrologic Engineering Center, 8 sec., 255 p.

U.S. Department of Commerce, 1981, 1980 census of population and housing advance report: Washington, D.C., Bureau of the Census PHC80-v-33, p. 8.

U.S. National Resources Committee, 1938, Regional Planning; Pt. VI, The Rio Grande joint investigation in the upper Rio Grande basin in Colorado, New Mexico, and Texas, 1936-37: U.S. Government Printing Office, 566 p.

REFERENCES - Concluded

Wilkins, D.W., Scott, W.B., and Kaehler, C.A., 1980, Planning report of the Southwest Alluvial Basins (East) Regional Aquifer-Systems Analysis, parts of Colorado, New Mexico, and Texas: U.S. Geological Survey Open-File Report 80-564, 39 p.

Woodward, L.A., 1982, Tectonic framework of Albuquerque Country, in Callender, J.F., and Grambling, J.A., eds., Guidebook to Albuquerque Country II: New Mexico Geological Society, 33rd Field Conference, p. 141-145.

Wright, H.E., Jr., 1946, Tertiary and Quaternary geology of the lower Rio Puerco area, New Mexico: Geological Society of America Bulletin, v. 57, no. 5, 69 p.

☆ U.S. GOVERNMENT PRINTING OFFICE: 1988—576-702/85,005 REGION NO. 8